MEASUREMENT OF THE NONLINEARITY PARAMETER B/A IN BIOLOGICAL MATERIALS USING THE FINITE AMPLITUDE AND THERMODYNAMIC METHOD

BY

WING KONG LAW

B.S., University of Rochester, 1978
M.S., University of Illinois, 1980

THESIS

Submitted in partial fulfillment of the requirements
for the degree of Doctor of Philosophy in Electrical Engineering
in the Graduate College of the
University of Illinois at Urbana-Champaign, 1984

Urbana, Illinois

ABSTRACT

It is well-known that materials exhibit a decrease in compressibility when subjected to high compression. This decrease in compressibility may be described by the nonlinearity parameter B/A. Organic liquids have been shown to possess a wide variation of the parameter, ranging from 5 to 12. This thesis reports on the measurement of this parameter in biological materials, including tissue models and soft tissue. An acoustic method with the potential for in vivo measurements is developed for this purpose. The result of measurements is confirmed by a second method which determines the change of sound speed, and hence the compressibility, with changes in hydrostatic pressure and temperature. The measurements indicate that: (1) B/A increases approximately linearly with solute concentration for protein solutions; (2) B/A is relatively insensitive to the molecular weight of the solute for a fixed concentration; (3) B/A ranges from 6.5 to 11 for various soft tissues; and (4) B/A decreases when the cellular structure of a tissue is destroyed. It is felt that details of nonlinear ultrasonic propagation in living systems should contribute to the development of clinical diagnostic and therapeutic applications of ultrasound.

ACKNOWLEDGEMENTS

The author is indebted to his advisors, Professors Floyd Dunn and Leon A. Frizzell for suggesting the research topic and providing continuous guidance and support during the research. Their many helpful suggestions and criticisms are gratefully acknowledged.

Data in the numerical evaluation of harmonic generation was kindly provided by Dr. Michael E. Haran.

Appreciation is extended to Mrs. Wanda Elliott and Mr. Bob Cicone for assistance in manuscript preparation, Mr. Billy McNeill and Mr. Irv Franklin for machining the necessary equipment, and Mr. Joe Cobb for assistance in the electronic instrumentation.

This work was supported in part by a grant from the National Science Foundation and by a grant from the National Institutes of Health.

TABLE OF CONTENTS

CHAPTER 1

INTRODUCTION

Ultrasound has been used extensively in the diagnosis of diseases and in therapeutic applications. Because of the analytical complexity of dealing with nonlinear phenomena, it has long been considered useful and acceptable in the biomedical applications of ultrasound to treat acoustic propagation phenomena as following linear relationships [Kinsler et al., 1982]. However, experimental evidence is accumulating to indicate that such treatment may not always be appropriate. Carstensen et al. [1980] investigated experimentally nonlinear phenomena at clinically used frequencies and intensities in water and reported significant effects of nonlinearity upon the beam width and the power transfer from the source to a distant point, demonstrating the importance of nonlinear propagation in the area of diagnostic ultrasound. Muir et al. [1980] pointed out that, according to established theories of nonlinear acoustics, the intensity output of some commercial diagnostic instruments using focused beams is sufficient to cause significant nonlinear propagation. At the same time, Goss and Fry [1981] used focused ultrasound at 2 MHz in the hundred watts per square centimeter focal intensity region and reported intensity dependent absorption in animal tissues. Carstensen et al. [1981] also reported nonlinear effects on the threshold for lesion production in excised liver at intensities as low as 20 W/cm^2 using 4 MHz unfocused fields.

The nonlinearity in sound propagation is characterized by the dependence of propagation speed on the particle velocity u. The

nonlinear behavior stems from two sources. First, in the medium where the sound propagates, the fluid is not at rest but rather is moving with a velocity equal to the particle velocity at that particular point. Accordingly, the total propagation speed with respect to a fixed observer is the sum of the infinitesimal wave velocity c_o and the particle velocity u, i.e.,

$$dz/dt = u + c_o \quad . \tag{1.1}$$

The second source of nonlinearity arises from the properties of the medium. In a perfectly linear medium, the density varies linearly with the pressure applied. However, the pressure-density relation of a fluid is in general not linear. Fluids become increasingly more difficult to compress at ever higher pressures. Since the sound velocity depends on the compressibility of the medium, when the acoustic pressure is increasing, the medium becomes less compressible and the propagation speed is greater. Conversely, when the acoustic pressure is decreasing, the sound speed is lower. As a result, the local propagation speed is given by [Beyer, 1974]

$$c = c_o + 1/2(B/A)u \tag{1.2}$$

where B/A is a constant that characterizes the nonlinearity of the liquid; see Chapter 2 . B and A are, respectively, the coefficients of the second and first term in the equation of state which describes the pressure-density relationship of the medium.

Combining the effects of the two sources of nonlinearity, as described by Eqs. (1.1) and (1.2), assuming that the effects are

additive, one obtains

$$dz/dt = c_o + u + 1/2(B/A)u \tag{1.3}$$

Since u varies over the waveform, being positive at some points, and negative at others, part of the wave moves faster than the wave as a whole, and part of the wave is retarded. The immediate consequence of this nonuniform propagation speed is waveform distortion. Figure 1.1 shows a spatial plot of a finite amplitude wave, with the length of horizontal arrows indicating the propagation speed at various points on the waveform. It can be seen from the figure that the wave changes its shape as it travels. The peak tends to approach the zero crossover point, and the valley tends to be retarded.

As seen from the second term in Eq. (1.3), the deviation of the propagation speed from infinitesimal wave velocity, and consequently the amount of distortion of the wave, depends on the amount of nonlinearity of the medium and the magnitude of the particle velocity. The greater the wave amplitude, or the more nonlinear the medium, the more rapidly the wave is distorted. However, the amount of distortion also depends on the number of cycles of wave propagation to the position of observation, i.e., the effect of nonconstant propagation speed is cumulative. As a result, even a low amplitude wave will exhibit distortion if it is allowed to travel far enough. Alternatively, if the wave length is short, i.e., at high frequencies, the wave will be more rapidly distorted.

In the frequency domain, the distortion process implies that harmonics are generated. From the law of conservation of energy,

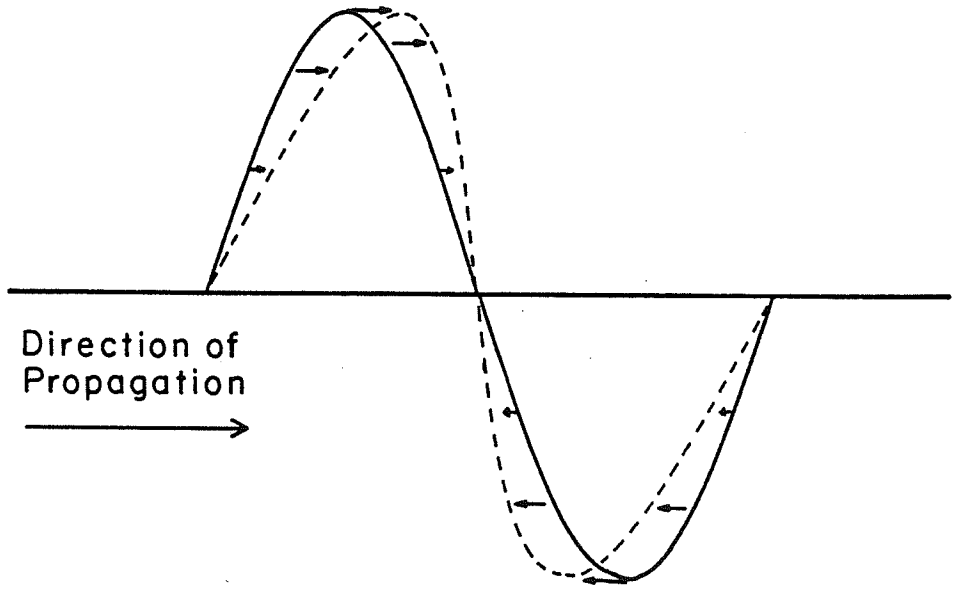

Figure 1.1. Illustration of the distortion process. Length of arrows indicates the local propagation speed at various points of the wave form.

the harmonics must be produced at the expense of the fundamental frequency component. The generation of harmonics, and the consequent depletion of the fundamental, may lead to the following phenomena.

A. Finite Amplitude Attenuation of the Fundamental

As the wave travels and distortion accumulates, more and more of the energy in the fundamental is transferred to harmonics. If one measures the magnitude of the fundamental component as a function of distance, an additional attenuation over that produced by the infinitesimal absorption of the medium will be obtained.

B. Saturation

The finite amplitude attenuation coefficient of the fundamental component increases with the increase in source intensity level. As a result, at a fixed point away from the source, the amount of energy in the fundamental rises less rapidly than the source level. Eventually, the finite amplitude loss becomes so severe that the received level approaches an upper limit which cannot be exceeded regardless of the acoustic power radiated by the source. This phenomenon is known as acoustic saturation.

C. Increase in Energy Absorption of the Acoustic Wave

Since the absorption of a medium is strongly frequency dependent, the energy absorption of a distorted wave, which includes the absorption of all frequency components, is greater than the absorption of an undistorted wave. The energy absorbed by the medium is converted into heat. The amount of heat

deposited by a finite amplitude wave, which undergoes a higher energy absorption, is, therefore, greater than that of an undistorted wave.

D. Change in Spectral Content of an Acoustic Pulse

The finite amplitude generation of harmonics, plus the depletion of the fundamental component, changes the spectral content of an acoustic pulse as a function of source intensity level, distance travelled, and characteristics of the medium.

In view of the phenomena described above, whether or not significant nonlinear propagation occurs in human tissue when using ultrasonic diagnostic and therapeutic instruments emerges as a worthwhile question. In the diagnostic use of ultrasound, understanding of nonlinear phenomena in mammalian tissue may lead to improved accuracy of the instruments and provide additional information on the state of the tissue. In the therapeutic area, the same understanding may lead to better control of the heat deposition of ultrasound. Furthermore, for both applications it is important to determine whether the nonlinear phenomena produce harmful effects to the patient.

The study of nonlinearity in tissue not only provides better understanding of and improvements in existing diagnostic procedures and therapeutic applications, but also offers new avenues for discovery and exploration in other areas. For example, Kompfner and Lemons [1976] have used the scanning acoustic microscope for visualizing nonlinear elastic behavior of biological tissues. The basic technique is to excite the specimen with an intense acoustic signal while detecting transmitted

acoustic signals at the harmonic frequencies. They found that images produced in such a manner revealed information not available by the regular monochromatic imaging method. Presumably the new information reflects the differential nonlinearity in the tissue components. It is, therefore, expected that the investigation concerning the nature and origin of the nonlinearity will reveal information useful to tissue characterization.

Investigation of nonlinearity in biological materials relies heavily on an accurate technique for determination of the nonlinearity parameter B/A. There are basically three methods of B/A determination [Coppens et al., 1965], viz., the static method, the finite amplitude method, and the thermodynamic method.

The static determination of B/A for a liquid requires a precise measurement of the density as a function of pressure at constant temperature. The method is equivalent to determining directly the equation of state to second order accuracy. The disadvantages and the difficulties of the method are in the extremely high pressure required for measuring the pressure-density relation to second order accuracy. Elaborate corrections must also be made for changes to the container under such pressures.

The finite amplitude determination of B/A generally involves studying the behavior and absolute magnitude of the distorted waveform or of one of its higher harmonics. Adler and Hiedemann [1962] investigated B/A by measuring the magnitude of the second harmonic component in water and m-xylene, and Zankel and Hiedemann [1959] investigated the distortion of finite amplitude waves using optical methods. However, both methods assume ideal plane waves,

which is not the case for radiation from a piston, as pointed out by Ingenito and Williams [1971] and Rogers [1965]. Law et al. [1981] and Dunn et al. [1981, 1982] reported the B/A value in tissues and tissue models using the finite amplitude method with corrections for diffraction and absorption. Cobb [1982] adopted and improved on the method of diffraction correction in an absorbing medium for piston sources suggested by Ingenito [1971] and measured the B/A value in animal tissues and protein solutions.

The finite amplitude method has the potential for in vivo measurement of the B/A values, and extremely small samples can be used if high frequency sound waves are utilized. The disadvantage of the method is the difficulty in calibrating the source and receiving transducers to the desired accuracy. The fact that the input/output characteristics of transducers are different for samples of different impedances makes the calibration problem even more complex. In general, one cannot expect an absolute accuracy of better than 5% due to uncertainties in the calibration of the transducers.

The thermodynamic method of B/A measurement involves studying directly the change of sound velocity with hydrostatic pressure and ambient temperature. Beyer [1960] and Coppens et al. [1965] used this method to measure successfully the B/A value for a number of liquids. The accuracy of this method can be very good since sound velocity, pressure, and temperature can all be measured to high degrees of accuracy. The disadvantage of the method lies in the need to apply high hydrostatic pressure to the sample in order to produce a sufficiently large change of sound

velocity, usually on the order of 10 atmospheres. The high pressure may alter the structural integrity of biological materials having differential compressibility in different components. Furthermore, in vivo measurement is not possible in such systems.

Of the above three methods, the finite amplitude method and the thermodynamic method do not require elaborate special equipment for measurement, but each has its own advantages and disadvantages. The finite amplitude method may be employed noninvasively, and therefore may possibly be suited for in vivo measurement in biological systems. But the necessity for transducer calibration limits its absolute accuracy. The thermodynamic method, on the other hand, can be extremely accurate, but lacks the versatility of the finite amplitude technique and has the potential for modifying the structure of the sample during the measurement procedure. The optimal solution to the problem is, therefore, to use the finite amplitude method for measurement in tissues and tissue models, and to use the thermodynamic method to confirm the accuracy of the finite amplitude techniques.

The purpose of this study is to determine(1) the nonlinearity parameter B/A in biological materials so that the amount of nonlinear acoustic distortion in these materials can be predicted and the consequences of such distortions can be estimated, and (2) the factors which can affect the values of B/A so that the origin of the nonlinearity in biological materials can be speculated upon. In order to make these measurements, an acoustic method of B/A measurement (finite amplitude technique) which takes into

account absorption and diffraction effects has been successfully developed. The results of this measurement technique compared favorably with a second independent method (thermodynamic technique), giving better than ± 1% agreement in liquid samples and better than ± 10% agreement in tissue samples when the same sample or samples from the same animal was used in a direct comparison.

Using the finite amplitude technique as the principal method of measurement, and using the thermodynamic technique for comparison, the B/A values of 15 different materials were measured. Using different tissues and models of tissue, the nonlinearity was investigated as a function of solute concentration, solute molecular weight, tissue type, and tissue structure.

The samples measured can be divided into three functional categories, viz., standard liquids, tissue models, and tissues. The standard liquids were employed to compare the measured values obtained by the finite amplitude technique with those obtained using the thermodynamic method in this laboratory and by workers elsewhere. The standard liquids have well characterized acoustic properties, and have impedance and absorption values similar to soft tissues.

The tissue models included protein solutions ranging in concentration up to 50%, covering the concentration range found in most animal tissues, thus allowing a comparison of the tissue models with tissues of comparable protein content. The two protein solutions used, viz., Bovine Serum Albumin (BSA) and hemoglobin, were chosen as tissue models because they produced

absorption and velocity values similar to that of soft tissues, over a wide frequency range. Furthermore, next to water, protein is the second largest constituent of soft tissues.

Dextrose, and its polymer, dextran, which are linear molecules, were studied at different concentrations to determine whether their B/A values are very different from solutions of globular protein, and whether the B/A value changes with concentration in a manner similar to that of protein solutions. Further, dextran is available over a large range of molecular weights in relatively pure form, so that the dependence of B/A on molecular weight could be investigated.

In order to investigate the importance of tissue structure in the nonlinearity of tissue, materials of progressively more complex organization were measured. The liquid tissue, blood, is structurally more complex than the solutions used as tissue models, and yet is homogeneous and isotropic. Its B/A value was compared with a hemoglobin solution of the same dry weight content. Whole liver was homogenized mechanically to destroy cellular structure, and the value of B/A in the homogenate compared with whole liver. Finally, various soft tissues were measured to determine their B/A values and to determine whether the B/A value changed from one tissue type to the other. The samples measured included liver, muscle, heart muscle, brain, and fat.

CHAPTER 2

THEORY

2.1. Origin of the Parameter B/A

If a fluid medium is perfectly linear, the relation between p, the pressure of the liquid, and ρ, the density, can be written as

$$p = p(\rho_o, s_o) + (\partial p/\partial \rho)_{p_o, \rho_o} (\rho - \rho_o) \tag{2.1}$$

where s_o is the entropy per unit mass of the undisturbed medium, ρ_o and p_o are, respectively, the equilibrium density and pressure. However, real media rarely, if ever, follow the linear relationship. A more realistic description of the medium is obtained by expressing p as a Taylor's series about the point ρ_o, s_o, (the equilibrium density and entropy), as

$$p = p(\rho_o, s_o) + (\partial p/\partial \rho)_{p_o, s_o} (\rho - \rho_o) + \tfrac{1}{2}(\partial^2 p/\partial \rho^2)_{\rho_o, s_o} (\rho - \rho_o)^2 + \tfrac{1}{6} (\partial^3 p/\partial \rho^3)_{\rho_o, s_o} (\rho - \rho_o)^3 + \ldots \tag{2.2}$$

It has been shown that, for liquids of the physical properties to be treated here, all terms beyond the quadratic in Eq. (2.2) are negligible [Goldberg, 1956]. Two constants, viz., A and B, which will be used to describe the degree of nonlinearity, are defined by rewriting Eq. (2.2) as

$$p = p(\rho_o, s_o) + A(\rho - \rho_o)/\rho_o + \tfrac{1}{2}B(\rho - \rho_o)^2/\rho_o^2 \tag{2.3}$$

where $A = \rho_o (\partial p/\partial \rho)_{\rho_o, s_o}$ and

$B = \rho_o^2 (\partial^2 p/\partial \rho_o^2)_{\rho_o, s_o}$.

A constant c can be defined by the equation

$$c^2 = (\partial p/\partial \rho)_{s_o} \tag{2.4}$$

which, when combined with Eq.(2.3), yields

$$c^2 = A/\rho_o \left[1 + (B/A)\ (\rho - \rho_o)/\rho_o\right] \tag{2.5}$$

For the case of very small changes of density, the second term is negligible and

$$c^2 = A/\rho_o \equiv c_o^2 \tag{2.6}$$

where c_o is by definition the well known sound speed for infinitesimal amplitude sound waves. However, from Eq. (2.5), it is obvious that for a finite amplitude wave, the sound velocity changes with the compression of the medium, and the amount of change is proportional to the parameter B/A.

2.2. B/A Expressed in Measurable Parameters

From the definitions of A and B and from Eq. (2.4), it is evident that

$$B/A = 2\rho_o c_o (\partial c/\partial p)_{\rho_o, s_o} \tag{2.7}$$

This ratio may be expressed in terms of parameters that can be obtained experimentally by considering c as a function of T and P, where T is the absolute temperature.

$$(\partial c/\partial p)_{\rho_o, s_o} = (\partial c/\partial p)_{T,s} + (\partial c/\partial T)_{p,s}\ (\partial T/\partial p)_{\rho_o, s_o} \tag{2.8}$$

where $(\partial c/\partial p)_{T,s}$ and $(\partial c/\partial T)_{p,s}$ are the measurable quantities.

The term $(\partial T/\partial p)_{\rho_o, s_o}$ can be transformed using Maxwell's thermodynamic relation

$$Tds = C_p dT - T(\partial V/\partial T)p dP \tag{2.9}$$

where s, V, and C_p are the entropy, volume, and heat capacity at constant pressure of the system. Since sound propagation in most fluids is to a first approximation an isentropic process, one may ignore entropy changes, i.e., ds is zero,

$$dT = (\partial V/\partial T)_{p,s}\ T\ dp/C_p \tag{2.10}$$

The term $(\partial V/\partial T)_p$ is equivalent to $\beta' V$, where β' is the coefficient of volume thermal expansion, so that the following relation holds

$$(\partial T/\partial p)_s = \beta' VT/C_p \tag{2.11}$$

Denoting the heat capacity per unit mass at constant pressure by c_p, and the mass of the total system by M, C_p equals $c_p M$ and V/C_p equals $1/\rho_o c_p$. Using this and Eqs.(2.11), (2.10), and (2.9), the following form for B/A is obtained

$$B/A = (\partial c/\partial p)_{T,s}\ (2\rho_o c_o) + (\partial c/\partial T)_{p,s}\ (2c_o T\beta'/c_p) \tag{2.12}$$

The propagation of acoustic waves with infinitesimal amplitude in liquids is, to a first approximation, adiabatic and reversible, and therefore an isentropic process. Therefore, measurements of the change of sound velocity with pressure and temperature, coupled with a knowledge of (1) the volume coefficient of expansion, (2) the heat capacity per unit mass at

constant pressure, (3) the density, and (4) the infinitesimal wave velocity, allow for the calculation of B/A by Eq.(2.12).

2.3. Plane Wave Theory, Nondissipative Medium

The equation of motion or the wave equation for acoustic phenomena is generally obtained by invoking three constitutive equations, viz., an equation of continuity, a dynamical equation, and an equation of state of the medium in which the propagation takes place. It is convenient to use Lagrangian coordinates (material coordinates), in which case one sees that in order for mass to be conserved, the equation of continuity would be $\rho = \rho_0 (1 + \partial\xi/\partial z)^{-1}$ where ξ is the particle displacement and z the axis along the direction of wave propagation. The dynamical equation in this coordinate system is $\rho\ddot{\xi} = -\partial p/\partial z$ where $\ddot{\xi}$ represents $\partial^2\xi/dt^2$. Finally, $c^2 = \partial p/\partial \rho$ is the equation of state. Combining these equations to eliminate all but the displacement ξ as the dependent variable leads to

$$\ddot{\xi} = [c^2/(1 + \partial\xi/\partial z)^2]\xi'' \qquad (2.13)$$

where $\ddot{\xi}''$ represents $\partial^2\xi''/\partial z^2$.

If a Hooke's Law type of relationship for the equation of state is employed, i.e., Eq.(2.1), the velocity of propagation c is a constant determined by the equilibrium density and pressure. If, in addition, the displacement amplitude of the wave is sufficiently small such that $\partial\xi/\partial z << 1$, Eq.(2.13) reduces to the ordinary lossless infinitesimal wave equation, viz., $\ddot{\xi} = c^2\xi''$.

Now consider the situation wherein the displacement amplitude is not negligible and the equation of state is more complex than

the simple Hooke's Law type of relationship. The equation of motion is, for the case where Eq.(2.3) is used as the equation of state,

$$\ddot{\varepsilon} = \frac{c_o^2}{(1 + \xi')^{2 + B/A}} \xi'' \qquad (2.14)$$

Here it is seen that for the situation where the wave amplitude is noninfinitesimal (finite), the parameter B/A becomes a measure of the nonlinearity of the propagating medium.

2.4. Fubini Solution--An Approximate Solution for Small Wave Amplitude

When the solution to Eq.(2.14) is expanded in a binomial series and only the first two terms retained, the resulting solution can be expanded as a Fourier series. If the amplitude of the wave is only moderate so that no discontinuity of the wave is produced, the solution, usually called the Fubini solution [Blackstock, 1966], expressed in terms of the acoustic pressure is,

$$p = p_1(o) \sum_{n=1}^{\infty} B_n \sin (\omega t - kz) \qquad (2.15)$$

where $B_n = 2I/nz\ J_n(nz/I)$

and $I = \rho_o c_o^3/(1 + B/2A)\ p_1(o)$,

ω is the angular frequency, p_1 is the amplitude of the fundamental component of the acoustic pressure, and J_n is the Bessel function of order n. Equation (2.15) indicates that, with propagation in a nonlinear medium and with finite wave amplitude,

an acoustic wave is distorted and the distortion is manifested by the presence of harmonic components. The magnitude of each harmonic component, $p_n(\sigma)$, can be written as

$$p_n(\sigma) = [2p_1(o)/n\sigma]\ J_n(n\sigma) \tag{2.16}$$

where $\sigma = z/l = \dfrac{(2 + B/a)\pi f p_1(o) z}{2\rho_o c_o^3}$.

This expression provides a relation between the parameter B/A and the pressure amplitude of the n^{th} harmonic component p_n.

It is possible, under the condition of small σ values, to simplify Eq. (2.16) to obtain a relation between B/A and the magnitude of the second harmonic component. By expanding the Bessel function J_n in a power series, and keeping only first and second order terms, one obtains

$$p_2(z) = Kz\ p_1^2(o) \tag{2.17}$$

where $K = \dfrac{(2 + B/A)\pi f}{2\rho_o c_o^3}$.

This approximation to the Bessel function is accurate to within 2% for σ values less than 1/4, and is more accurate for smaller σ values. Adler and Hiedemann [1962] used the relation of Eq. (2.17) as a basis for determining the B/A values of two liquids. They measured the parameter $P_2(z)/P_1^2(o)z$ at different distances from the source, and then extrapolated linearly to the origin (zero distance from the source) to obtain $p_2(z)/p_1^2(0)z \mid z \to 0$ from which K, and hence B/A, was obtained. These researchers pointed out that at the limit of zero distance from the sound source, the

effect of absorption should be negligible, and the Fubini solution, though derived only for the nondissipative case, could be applied to obtain the B/A value in an absorbing medium. However, there are two disadvantages to this method of B/A determination. First, $p_2(z)/p_1^2(o)z$ does not change linearly with distance in a dissipative medium. A linear extrapolation may lead to errors in determining $p_2(z)/p_1^2(o)z|z \to 0$. Second, the diffraction effects of a finite piston source were not included. Failure to correct for the effects due to diffraction may introduce errors in the computed B/A value. One method of B/A measurement used in this investigation is based on the Adler-Hiedemann method but with proper consideration of absorption and diffraction effects. These effects are now discussed in more detail.

2.5. Plane Wave, Dissipative Medium-Burgers' Equation

For materials with a known mechanism of absorption, the loss mechanism can be incorporated into the quadratic equation of state, resulting in a wave equation that describes the nonlinear behavior of the dissipative medium. For example, to describe a viscous absorbing medium, the Navier-Stokes equation [Kinsler et al., 1982]

$$\rho_o \ddot{\xi} = - p' + (4/3\eta + \eta')\dot{\xi}'' \qquad (2.18)$$

where $(4/3 + \eta'/\eta)$ is the viscous number, is combined with Eq. (2.3), the quadratic equation of state, to form a wave equation that includes both viscous effects and the nonlinearity of the medium. This equation, given as

$$\rho_o \xi_{tt} = A\xi_{xx} - 2A\beta\xi_x\xi_{xx} + (4/3\eta + \eta')\xi_{xxt} \qquad (2.19)$$

with $\beta = 1 + B/2A$,

when properly transformed and with higher order terms deleted, can be written in the form of Burgers' Equation [Mendousse, 1953]. The absorption coefficient, α, at the fundamental frequency is related to the viscosity coefficients by $\alpha = (1/2)(4/3\eta + \eta')(\omega^2/\rho_o c_o^3)$. This may be substituted into the Navier-Stokes equation to yield the Burgers' Equation, expressed in terms of the particle velocity u,

$$\frac{\partial u}{\partial z} = \frac{\beta\omega_o}{c_o^2} u \frac{\partial u}{\partial \tau} + \Gamma \frac{\partial^2 u}{\partial \tau^2} \qquad (2.20)$$

where $\tau = \omega_o t - kz$,

$\beta = 1 + B/2A$,

$\Gamma = 1/\alpha l$, $l = c_o^2/\beta u_o \omega$.

For small source pressures or in highly absorbing media ($\Gamma << 1$), the Burgers' Equation can be solved [Blackstock, 1964] to give the magnitude of the second harmonic in terms of the acoustic pressure as

$$\frac{p_2(z)}{p_1^2(o)} = k \frac{(e^{-2\alpha z} - e^{-4\alpha z})}{4\alpha} \qquad (2.21)$$

where K was defined previously (Eq. 2.17).

However, such inclusion of losses in the nonlinear wave equation is possible only when the mechanism of absorption is known, e.g., as viscous processes in the above example. For biological media, the origin of the high absorption and the near

linear relationship between absorption and frequency is not completely understood. Some researchers [Carstensen et al., 1953] suggested that a combination of relaxation mechanisms over distributions of relaxation frequencies may describe the observed absorption dependencies in biological materials. It is believed, however, that protein or possibly all large molecular species, are involved with the primary mechanisms such as proton exchange and conformational changes [O'Brien, 1970]. However, further investigations will be required to establish firmly the involved mechanisms. Due to this lack of knowledge of the absorption mechanisms, it is not possible to incorporate loss mechanisms into the wave equation to solve for the finite amplitude generation of harmonics.

2.6. Second Order Analysis with Correction for Attenuation

One possible way to solve for the harmonic generation without knowledge of the specific absorption mechansism(s) is to limit the number of harmonics being considered in the theory, and supply empirically determined absorption values for each of these harmonics. Since for small source signal amplitudes ($\sigma << 1$), the magnitude of the harmonics decreases rapidly with increasing frequency, this method is relatively accurate. By limiting the calculation to a few harmonics, within a small increment of distance, the attenuation of each of the harmonics can be considered individually, and the effect superimposed on the finite amplitude generation of harmonics. In the situation wherein one requires only information on the second harmonic amplitude, one may start with the Fubini solution $p_2(z) = Kz\ p_1^2(o)$, which can be

generalized as $dp_2(z)/dz = Kp_1^2(z)$, where $p_1(z)$ is the fundamental pressure at the distance z. This relation may be used to calculate the rate of generation of the second harmonic at z. The differential equation for the attenuation of the second harmonic components is

$$dp_2(z)/dz = -\alpha_2 p_2(z) \tag{2.22}$$

where α_2 is the attenuation coefficient of the second harmonic. Assume that the space rate of change of the amplitude of the second harmonic is the sum of the changes due to harmonic generation and to attenuation; the following approximate relation is obtained from Eq. (2.21) and Eq. (2.22)

$$dp_2(z)/dz = Kp_1^2(z) - \alpha_2 p_2(z) \tag{2.23}$$

Harmonics greater than the second are neglected in the above expression. Specifically, it is assumed that no energy is extracted from the second harmonic to generate higher harmonics.

If the source signal level is small, one may further assume that the energy lost from the fundamental in generating the second harmonic is negligible, and that the only loss results from absorption in the medium so that $p_1(z)$ is given by

$$p_1(z) \cong p_1(o)e^{-\alpha_1 z} \tag{2.24}$$

Combining Eq. (2.24) with Eq. (2.23) yields

$$\frac{dp_2(z)}{dz} = K\, p_1^2(o)\, e^{-2\alpha_1 z} - \alpha_2 p_2(z) \tag{2.25}$$

where α_1 and α_2 are, respectively, the attenuation coefficients for the fundamental and the second harmonic components.

The solution to Eq. (2.25) first derived by Thuras et al. [1935] is

$$P_2(z) = Kp_1^2(o) \frac{[e^{-\alpha_1 z} - e^{-2\alpha_1 z}]}{(2\alpha_1 - \alpha_2)} \tag{2.26}$$

an expression consistent with the fact that the second harmonic vanishes at z = o.

For a viscous absorbing medium, $\alpha_2 = 4\alpha_1$, and Eq. (2.26) becomes the same as Eq. (2.21) which is the small amplitude solution to the Burgers' Equation, thus giving some support to the assumption that within a small distance, the attenuation effect and the finite amplitude effect can be separately considered and superimposed on each other to account for the generation of harmonics in an absorbing medium. Equation (2.26) can be simplified further by making use of the mathematical relation

$$e^{ax} - e^{bx} = (a - b)x \exp [1/2(a + b)x] \sinh A/A \tag{2.27}$$

where A = (a - b)x/2. For small A values, (sinhA)/A approaches unity and Eq. (2.26) becomes

$$P_2(z) = Kz\, p_1^2(o) e^{-(\alpha_1 + \alpha_2/2)z} \tag{2.28}$$

This approximation introduces an error of about 1% when $(\alpha_2 - 2\alpha_1)z$ is 1/2. Due to the near linear relationship between attenuation and frequency in biological materials, $(\alpha_2 - 2\alpha_1)$ is usually small, on the order of 0.01 to 0.2 around 3 MHz [Goss et

al., 1978], and the simple exponential relationship in Eq. (2.28) provides a ± 1% description of the change of second harmonic amplitude with distance between the source to an observation point up to 3 cm away. In the Adler-Heidemann method of B/A determination, a logarithmic extrapolation of the parameter $p_2(z)/p_1^2(o)z$ can be used instead of a linear extrapolation. The exponential term in Eq. (2.28) approaches unity as z approaches zero, indicating that the Fubini Solution for the second harmonic can be applied regardless of absorption in the medium in the limit of z approaching zero. However, the effect of energy extraction by finite amplitude effect from the fundamental and the second harmonic waves, which is neglected in the above derivation, remains to be determined.

Since an applicable finite amplitude theory for biological materials does not exist, a numerical solution was undertaken, as described in the next section.

2.7. Numerical Method for Computing Generation of Harmonics

The second order analysis described in the previous section provides information on the second harmonic only and neglects the finite amplitude transfer of energy from the fundamental and the second harmonic. The numerical method for computing harmonic generation includes the effect of depletion and can be carried out for an arbitrary number of harmonics. The numerical method described by Haran [1983] uses the Burgers' Equation, Eq. (2.20), as a starting point. A continuous wave is represented in complex notation as

$$u = \sum_{n=-\infty}^{\infty} U_n \exp[in\tau] \tag{2.29}$$

where $\tau = (\omega_o t - kz)$ and u_n is the complex amplitude of the n^{th} harmonic. The differential change of the n^{th} harmonic is found by substituting Eq. (2.29) into Eq. (2.20) yielding

$$\frac{\partial u_n}{\partial z} = \frac{i\beta\omega_o}{c_o^2} \sum_{m=-\infty}^{\infty} (\eta - m)\, U_{n-m}\, U_m - \alpha_1 \eta^2\, U_n \tag{2.30}$$

The first term on the right side of Eq (2.30) represents the nonlinear interaction among the various spectral components. The second term represents losses having a quadratic dependence on frequency.

From linear theory, the decay of the n^{th} harmonic component is represented in differential form as $\partial U_n/\partial z = -\alpha(n)U_n$ where $\alpha(n)$ is the absorption coefficient for the n^{th} harmonic component [Kinsler et al., 1983]. For a viscous absorbing liquid $\alpha(n) = \alpha_1 n^2$, where α_1 is the absorption coefficient at the fundamental frequency.

For biological materials, the dependence is not quadratic with frequency but nearly linear and may be represented as $\alpha(n) = \alpha_1 n^b$, where b ranges from 1.0 to 1.2 [Wells, 1977]. To account for nonquadratic frequency dependent attenuation, Eq. (2.30) is rewritten as

$$\frac{\partial U_n}{\partial z} = \frac{i\beta\omega_o}{c_o^2} \sum_{m=-\infty}^{\infty} (\eta - m)\, U_n - m\, U_m - \alpha_1 n^b\, U_n \tag{2.31}$$

The summation term of Eq. (2.26) can be changed to facilitate calculation by computer. The final expression obtained is

$$\frac{\partial U_n}{\partial z} = \frac{i\beta\omega_o}{c_o^2} \left(\sum_{j=1}^{n-1} jU_j\, U_{n-j} + \sum_{j=\infty}^{\infty} jU_j^*\, U_{j-n} \right) - \alpha_o n^b\, U_n \qquad (2.32)$$

The terms within the bracket represent the combined effect of the generation of the n^{th} harmonic from the lower harmonics and the depletion of the n^{th} harmonic due to the generation of harmonics higher than the n^{th}. By using a truncated power series of the form

$$U_n(z + \Delta z) = U_n(z) + \partial U_n/\partial z \;\; \Delta z, \qquad (2.33)$$

the magnitude of the n^{th} harmonic at a distance z from the source is obtained numerically. Some results of the computation based on Eq. (2.32) [Haran, private communication], which considers the effects of 21 harmonics and uses a Δz of 0.1 cm and a fundamental frequency f_o of 3.4 MHz, are shown in Figs. 2.1, 2.2, and 2.3. A sound velocity of 1500 m/s and a density of 1 gm/cc are used in the computation. In order to compare the results of Eq. (2.32), which includes the effects of finite amplitude energy depletion, with the approximate solution of the previous section (Eq. 2.28), results of the computation in Eq. (2.32) are plotted as $\ln p_2(z)/p_1^2(o)z$ versus z. Figure 2.1 shows the second harmonic data for small source pressure (0.5 atm), but with different absorption values in the medium. The results when compared with Eq. (2.28) are found to agree to within $\pm$ 1% for distances less than 3 cm indicating that the effect of depletion is negligible for small source pressures. Moreover, the curves have the same intercept regardless of the absorption value in the medium. The intercept equals $(B/A + 2)\, \pi f/(2\rho_o c_o^3)$. Figure 2.2 shows the gradual deviation of the approximate solution from the more

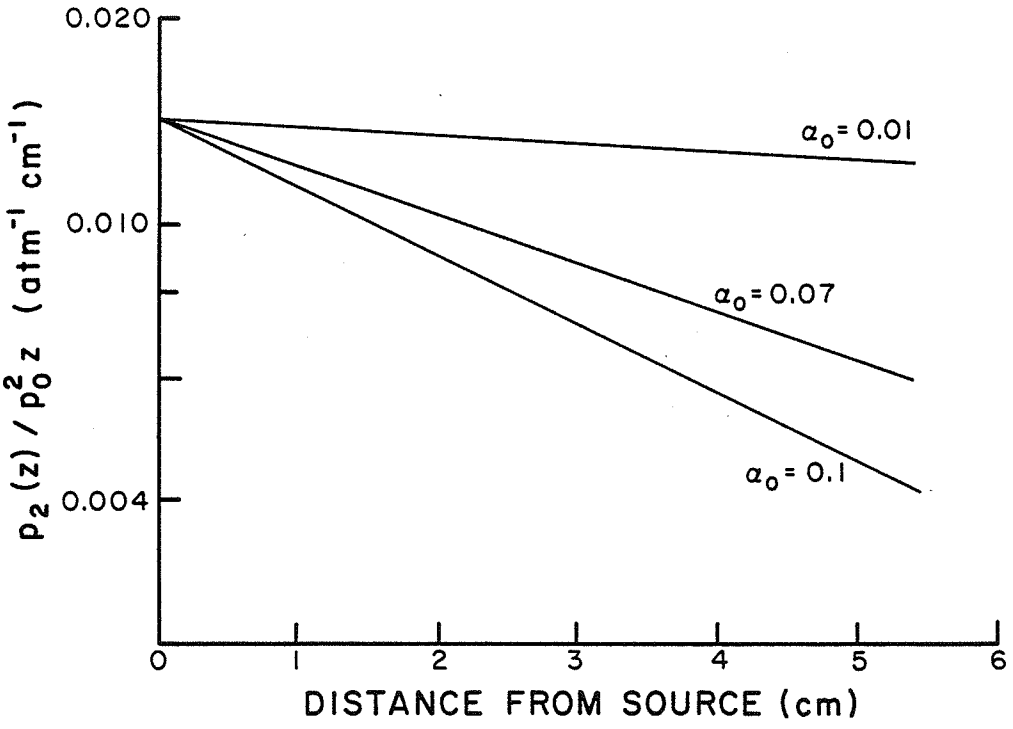

Figure 2.1. $p_2(z)/p_o^2 z$ at different distances from the source under small source pressure and different absorption in the medium.
$\alpha(f) = \alpha_o (f/f_o)^{1.3}$, B/A = 7, p_o = 0.5 atm.

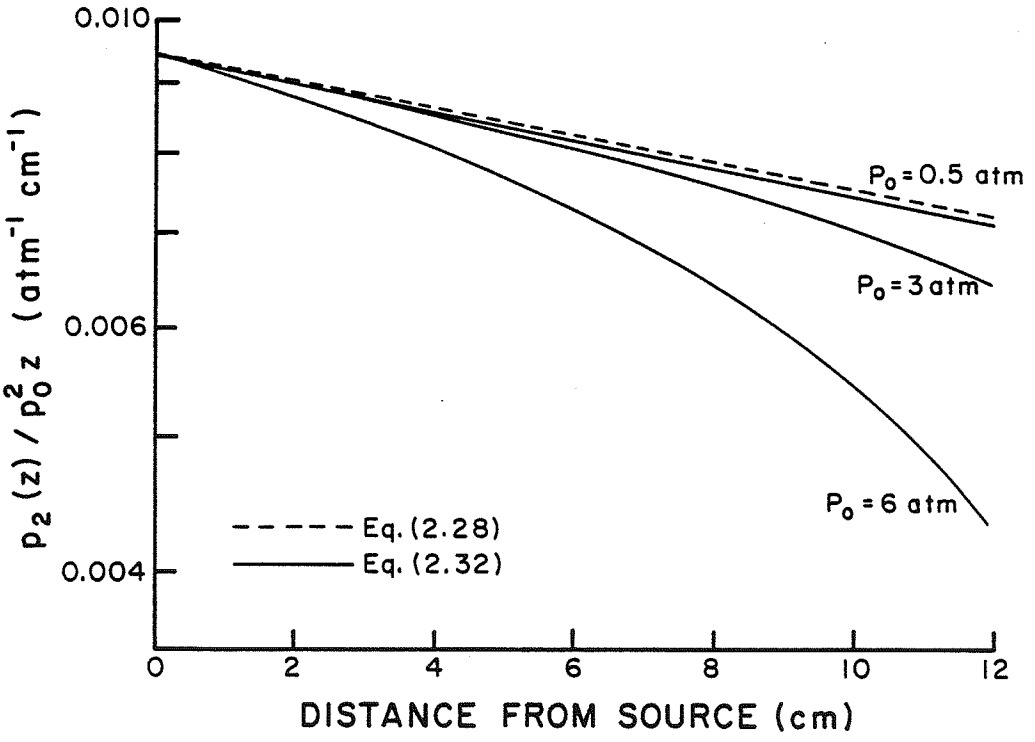

Figure 2.2. Comparison of the second order approximation (dotted line) with numerical computations (solid line) at different source pressures. $\alpha(f) = 0.01(f/f_o)^{1.3}$, B/A = 4.

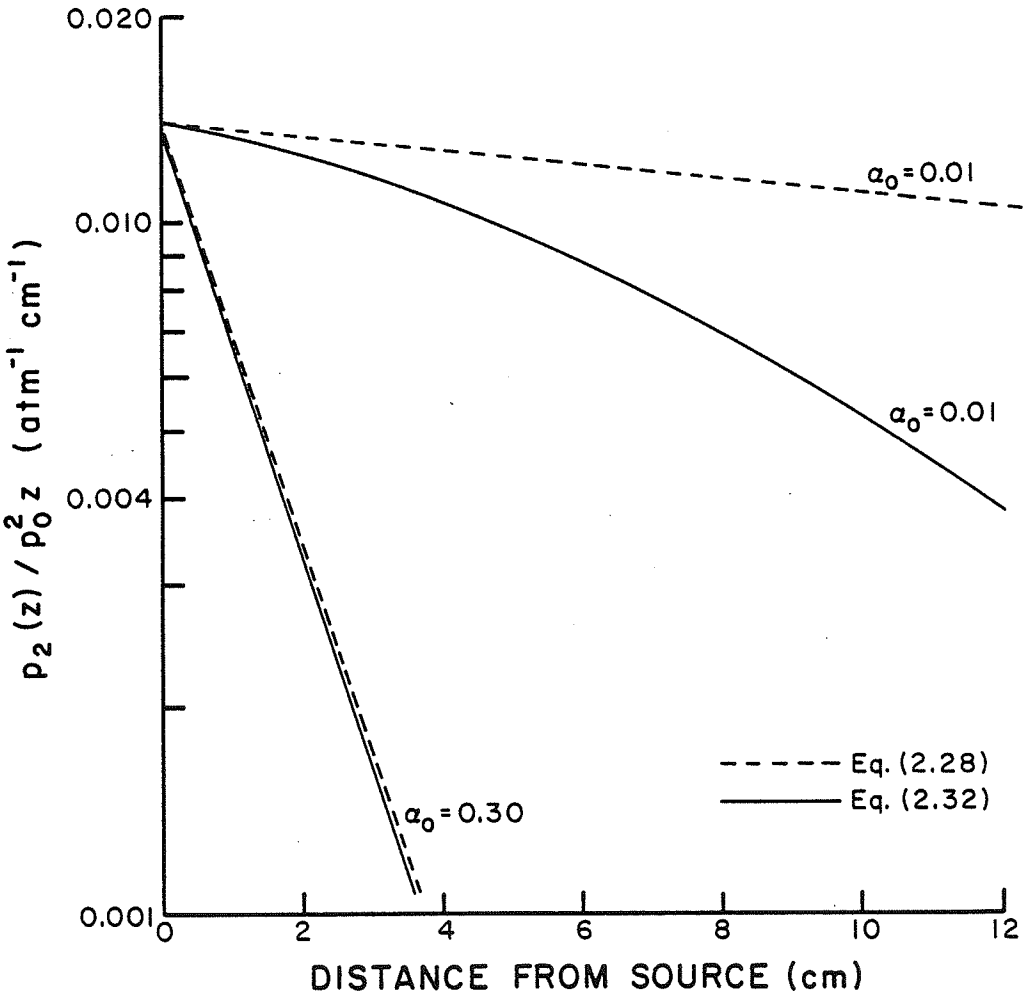

Figure 2.3. Comparison of the second order approximation (dotted line) with numerical computations (solid line) under high source pressure. (p_o = 6 atm). $\alpha(f) = \alpha_o (f/f_o)^{1.3}$, B/A = 7.

accurate numerical method at higher source pressures. The dotted line represents the approximate solution, Eq. (2.28), and the solid line represents the solution derived from the numerical method. Absorption values of $\alpha_n = 0.01(n)^{1.3}$ are used in these computations where n is the harmonic number. The solid lines represent solutions using $p_1(o)$ of 0.5, 3.0, and 6.0 atm respectively, as indicated in Fig. 2.2. The approximate solution deviates from the numerical solution when the source to receiver distance is large, or when the source pressure is high. For example, the deviation is 1% and 5% at 4 cm for source pressures of 3 and 6 atm, respectively.

Figure 2.3 shows the deviation of the approximate solution from the numerical method under high source pressure, with different absorption values in the medium. Again the dotted curves represent the approximate solution and the solid curves represent the solution derived from the numerical method. The absorption coefficients of the fundamental frequency component used for the computation are 0.01 and 0.3 Np/cm, as indicated in the figure. For the same source pressures and source to receiver distances, the difference between the two solutions is smaller for media of higher absorption values. For example, for a fairly high source pressure of 6 atm, the deviation is less than 1% at 3 cm when the absorption coefficient of the medium is 0.3 Np/cm at the fundamental frequency.

2.8. Diffraction Considerations

Since sound sources of sufficiently large size to produce the necessary acoustic fields are used in this investigation for

calibration of transducers, measurement of B/A, and measurement of absorption coefficients, the effects of diffraction on each of these measurements must be considered. In the calibration of transducers and absorption measurements, only the diffraction effect on the fundamental frequency component is involved. The diffraction theory of Bass [1958] is used to account for diffraction in these two cases. In the finite amplitude measurement of B/A, the source of the second harmonic is actually a column of the space between the source and the receiver, and the analysis is slightly more complicated than the case for the diffraction of the planar sound source. The theories of Ingenito [1971] and Rogers [1970] were used in this case.

2.8.1. Diffraction of the Fundamental Component

Two situations involving diffraction are of interest in this investigation. The first involves measuring the locations of pressure maxima and minima along the axis of the sound source using a small hydrophone probe. The second involves a receiver which was large enough to intercept virtually all of the beam and which therefore responded to the pressure amplitude averaged over its surface.

The first case has a well known theoretical solution for a plane, piston source [Kinsler et al., 1982]. If the distance, z, from the source in the near field is much greater than the radius of the source, a, the magnitude of the axial pressure, p_{ax} , at a distance z from the source, is given by

$$p_{ax} \cong 2p_o \left| \sin(ka^2/2z) \right| \qquad (2.34)$$

where p_o is the source pressure and k is the propagation $(2\pi/\lambda)$ constant of the acoustic wave. To find the positions of the maxima and minima, z_n, one sets the argument of the sine factor in Eq. (2.34) equal to $n\pi/2$. Then

$$z_n = 1/n\ ka^2/2\pi - n\ \pi/2k, \tag{2.35}$$

where odd integer values of n give the maxima, and even integer values of n give the minima. Equation (2.35) is the basis for experimentally determining an effective radius of the source, as described in detail in Chapter 3.

The second quantity of interest is the average complex pressure <p> over a circular disk of the same size as the source, in a plane parallel to it, centered on the same axis,

$$\langle p \rangle = 1/\pi a^2 \int_0^{2\pi} \int_0^{a} p(r,\theta)\ r dr d\theta \tag{2.36}$$

where $p(r, \theta)$ is the pressure at the field point (r, θ).

The magnitude of this quantity is, except for a phase factor, the pressure measured by a plane circular detector of the same radius as the source, and centered on its axis. The presence of the detector is assumed not to alter the acoustic field.

Equation (2.36) has been solved by several researchers. The solution by Bass [1958], which is accurate to $\pm$ 2% for $z > a$, is expressed in terms of the velocity potential $\langle \phi_1 \rangle$

$$\langle \phi_1 \rangle \cong \frac{i\rho_o}{k} e^{ikz} \{1 - (1 - \xi^2/2k^2a^2)\ [J_o(\xi) + iJ_1(\xi)]e^{i\xi} - \xi^2/2k^2a^2[J_1(\xi)/\xi]e^{ik\xi}\} \tag{2.37}$$

where $\xi = (k/2)[(z^2 + 4a^2)^{1/2} - z]$, and J_o and J_1, are the Bessel functions of the first kind with order zero and one, respectively. To express the solution in terms of acoustic pressure, the relation between pressure and velocity potential

$$p = \rho_o \omega \phi \tag{2.38}$$

can be used.

Equation (2.37) is used in this investigation to correct for effects of diffraction in calibrating the receiver and in the absorption measurements. Details of the application are described in Chapter 3. This equation is also used to determine the effect of diffraction on the finite amplitude generation of second harmonics, which is described in the next section.

2.8.2. Diffraction Effects on the Finite Amplitude Generation of the Second Harmonic

The mathematical analysis of the second harmonic generated by a piston source is more complex than the analysis of the fundamental component. The method used by Ingenito [1971] is outlined below.

Starting with the equation of motion,

$$\frac{\partial u}{\partial t} + (u \cdot \nabla)u = \frac{-\nabla p}{\rho} \tag{2.39}$$

the equation of continuity,

$$\frac{\partial \rho}{\partial t} + \nabla \cdot (\rho u) = 0 \tag{2.40}$$

and the equation of state,

$$p = p_o + A\left(\frac{\rho - \rho_o}{\rho_o}\right) + \frac{B}{2}\left(\frac{\rho - \rho_o}{\rho_o}\right)^2 \tag{2.41}$$

a second order wave equation is obtained by perturbation analysis. The field variables u, ρ, and p are expanded in series form,

$$u = \lambda u_1 + \lambda^2 u_2 + \ldots$$
$$\rho = \rho_o + \lambda \rho_1 + \lambda^2 \rho_2 + \ldots \qquad (2.42)$$
$$p = p_o + \lambda p_1 + \lambda^2 p_2 + \ldots$$

where λ is a mathematical parameter introduced for convenience, and the subscripts indicate the harmonic component. Equation (2.42) is substituted into Eqs. (2.39), (2.40), and (2.41), and like harmonic components are grouped together. From this set of equations, by assuming the wave amplitude to be small, a nonhomogeneous partial differential equation is obtained. When expressed in terms of the velocity potential, the equation is

$$\Box^2 \phi_2 = - \frac{1}{2c^2} \frac{\partial}{\partial t} \left[\Box^2 \phi_1^2 + \frac{\gamma + 1}{c^2} \left(\frac{\partial \phi_1}{\partial t} \right)^2 \right] \qquad (2.43)$$

where $\Box^2 = \nabla^2 - \frac{1}{c^2} \frac{\partial^2}{\partial t^2}$, $\gamma = 1 + \frac{B}{A}$.

ϕ_1 and ϕ_2 are, respectively, the velocity potentials of the fundamental and second harmonic components.

The inhomogeneous wave equation can be solved in terms of Green's function [Morse and Ingard, 1968] with the appropriate boundary conditions. The Green's function solution is equivalent to summing up all contributions from the sources of second harmonic which are distributed over the space between the source and the receiver. With the assumption that ka >> 1 so that the wave propagates mostly in the axial direction, the solution for the second harmonic potential is given by [Ingenito, 1971]

$$\phi_2(r,z) = -\frac{k^2(\gamma + 1)}{8c_o} \int_o^z e^{ik\zeta}\, \phi_1^2\, (r, z - \zeta/2)\, d\zeta \qquad (2.44)$$

where ζ is a dummy variable introduced for the purpose of integration.

The second harmonic potential averaged over the face of the receiver can be obtained by integrating over the area of the receiver,

$$\langle\phi_2\rangle = \frac{1}{\pi a^2} \int_o^a \int_o^{2\pi} r\phi_2(r,z)\, dr d\theta \qquad (2.45)$$

Combining Eq. (2.44) and Eq. (2.45), with the use of an appropriate expression for ϕ_1^2 in Eq. (2.44), and again assume small k, $\langle\phi_2\rangle$ can be expressed as

$$\langle\phi_2\rangle = -\frac{k^2(\gamma + 1)}{8c_o} \int_o^z e^{ik\zeta}\, [\langle\phi_1(z - \zeta/2)\rangle]^2\, d\zeta \qquad (2.46)$$

The term $\langle\phi_1\rangle$, which is the averaged velocity potential of the fundamental component, can be obtained by using Eq. (2.37). Through numerical integration, $\langle\phi_2\rangle$ can be obtained as a function of distance and used to correct for the effect of diffraction in a medium free of absorption. However, since most media cannot be considered absorption free, diffraction should be considered simultaneously with absorption. As discussed earlier in the plane wave case, the incorporation of the absorption mechanism in the wave equation is not possible due to insufficient knowledge of the absorption mechanism in biological materials. However, Cobb

[1983] gave an ad hoc solution to the problem by considering separately the attenuation of the fundamental and second harmonic component inside the integral of Eq. (2.46), which is discussed in the next section.

2.8.3. Diffraction in an Absorbing Medium

To interpret Eq. (2.46) physically, one may imagine a "source plane" located at a distance ζ away from the receiver and at a distance $(z - \zeta)$ away from the source. The fundamental frequency component travels from the source to this source plane, part of the energy is converted into harmonics, and the harmonic signal continues travelling from the source plane to the receiver. The integration in Eq. (2.46) sums all the contributions to the second harmonic component from $\zeta = o$ to $\zeta = z$. The attenuation of the fundamental from the sound source to the source plane is accounted for by multiplying the $<\phi_1>^2$ term within the integral of Eq. (2.46) by $\exp[-2\alpha_1(z - \zeta)]$. The attenuation of the second harmonic signal travelling from the source plane to the receiver is corrected by multiplying the integral by $\exp(-\alpha_2\zeta)$. The expression for the second harmonic component in an attenuating medium, with diffraction considered, is then

$$<\phi_2> = - \frac{k^2(\gamma + 1)}{8c_o} \int_o^z e^{ik\zeta} e^{-\alpha_2\zeta} e^{-2\alpha_1(z - \zeta)} [<\phi_1(z - \zeta/2)>]^2 \, d\zeta \quad . \tag{2.47}$$

In the case for a perfectly collimated wave, i.e., when $<\phi_1>$ is a constant,

$$<\phi_2(z)> = \frac{k^2(\gamma + 1)}{8c_o} \frac{(e^{-2\alpha_1 z} - e^{-\alpha_2 z})}{(\alpha_2 - 2\alpha_1)} e^{i2kz} \qquad (2.48)$$

an expression consistent with the solution for plane wave propagation, Eq. (2.26).

In the case where $\alpha_2 = 2\alpha_1$, a situation which is approximately true for most biological media, Eq. (2.47) becomes

$$<\phi_2> = - \frac{k^2(\gamma + 1)}{8c_o} e^{-2\alpha_1} \int_o^z e^{ik\zeta} [<\phi_1(z - \zeta/2)>]^2 \, d\zeta \quad . \qquad (2.49)$$

The second harmonic component is the product of a diffraction term, F(z), which is the integral on the right hand side of the equation, and an attenuation factor. The attenuation term $e^{-2\alpha_1}$ is the same as that obtained in the second order plane wave analysis, Eq. (2.28), under the condition $\alpha_2 = 2\alpha_1$. One may therefore consider the attenuation effect and the diffraction effect to be mutually independent and additive under the special situation of $\alpha_2 = 2\alpha_1$.

For a medium of near linear frequency dependence of absorption, one may approximate Eq. (2.47), expressed in acoustic pressure, as

$$p_2(z) = K \, p_1^2(o) \, e^{-(\alpha_1 + \frac{\alpha_2}{2})} F(z) \qquad (2.50)$$

where K is defined in Eq. (2.17). For $(\alpha_2 - 2\alpha_1)z < 1/2$, the approximation is accurate $\pm$ 2%, which is determined by a numerical evaluation of Eq. (2.47) and comparing the result with Eq. (2.50).

A plot of ln (F(z)/z) vs. z indicates that for 1 cm < z < 3.5 cm, one may approximate F(z) in the form cze^{-mz}, so that Eq. (2.50) becomes, for 1 cm < z < 3.5 cm,

$$p_2(z) = KC\, p_1^2(o)z\, e^{-(\alpha_1 + \frac{\alpha_2}{2} + m)z} \tag{2.51}$$

Taking the logarithm of Eq. (2.51), on may write

$$\ln \frac{p_2(z)}{p_1^2(o)z} = \ln (Kc) - (\alpha_1 + \frac{\alpha_2}{2} + m)z \tag{2.52}$$

Thus by measuring the parameter $p_2(z)/p_1^2(o)z$ as a function of z, plotting it in a semilog graph, and extrapolating to the point z = o to obtain the intercept, the value of KC can be determined. Since C is a constant obtainable through the diffraction correction term F(z), K, and hence B/A, is readily determined.

CHAPTER 3

INSTRUMENTATION AND PROCEDURE

Two experimental techniques were employed to determine the value of the nonlinearity parameter B/A. The finite amplitude method is described first, and then the thermodynamic method is discussed.

3.1. Finite Amplitude Method

As discussed in the theory section, the B/A value of a medium is related to the second harmonic generated in the medium. In a small amplitude approximation, for a medium with linear frequency dependence of absorption, the relationship can be written as

$$\frac{B}{A} + 2 = \frac{2\rho_o c_o^3}{\pi f} \frac{p_2(z)}{p_o^2 z} e^{(\alpha_1 + \frac{\alpha_2}{2})z} [F(z)]^{-1} \qquad (3.1)$$

where F(z) is a correction factor for diffraction determined by the radius of the source, the frequency of the fundamental, and the speed of propagation. In the finite amplitude method the value for $p_2(z)$ is determined at several distances, between 1 to 3.5 cm, and then the quantity $p_2(z)/p_o^2 z$ is extrapolated using a semilog plot to the point z = o, where Eq (3.1) no longer depends on the absorption of the medium, thus eliminating the necessity for absorption measurements and the errors associated with them. The diffraction correction factor, F(z), becomes a constant which is independent of attenuation in the medium when extrapolation is made to the point z = o, thus allowing convenient correction for the effect of diffraction. $F(z)|_{z \to o}$ equals 0.9 for the measurements reported herein.

As seen from the above expression, the finite amplitude determination of B/A requires the knowledge of

1. the second harmonic amplitude at several distances,
2. the effective radius of the sound source,
3. the amplitude of the source pressure,
4. the sound velocity in the sample, and
5. the density of the sample.

The following description will include instrumentation used in measuring the above quantities, the methods of transducer calibration, and the procedures for measurement of each of the above parameters. Methods of measurement of other parameters not listed above such as the absorption coefficient and concentration of solutions, are also described.

3.1.1. Equipment

Electronics - A block diagram of the electronic instrumentation used for the measurement of the second harmonic is shown in Fig. 3.1. The source transducer was driven by a pulse modulated RF signal with a carrier frequency of 3 MHz, with the carrier frequency monitored by an HP Model 314A frequency counter. The modulated signal was obtained by gating the output of a Ferris Model 22-A RF signal generator with a Model S-7 solid state switch from Watkins-Johnson. The solid state switch was controlled by a pulsing unit, which determined the on time and repetition rate of the pulses. The pulse modulated RF signal from the solid state switch was fed to an Amplifier Research Model 10LA wideband RF power amplifier which drove the source transducer. A low pass filter with a 3 MHz cut off frequency was placed between the power

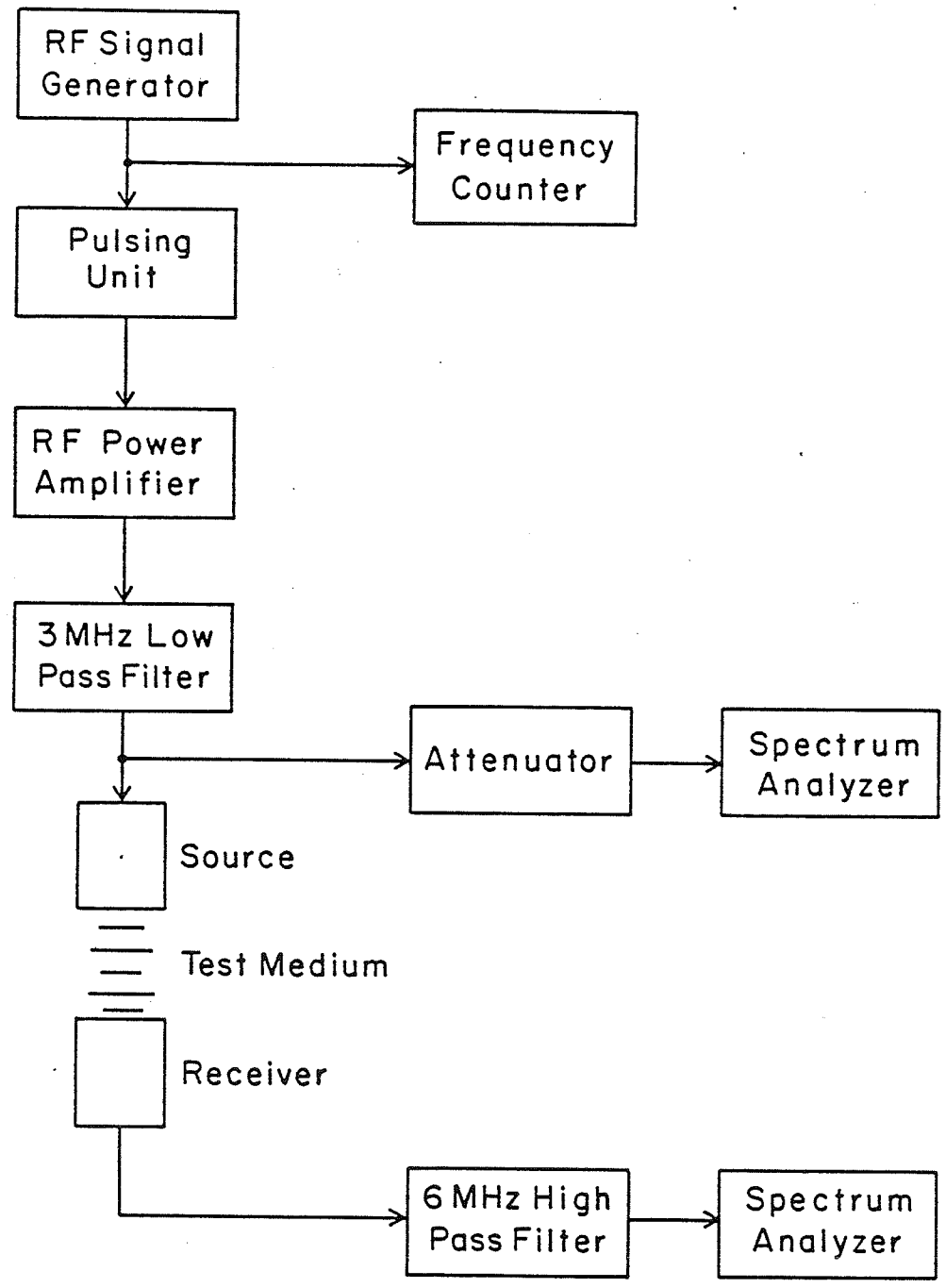

Figure 3.1. Schematic diagram of the electronic instrumentation for the finite amplitude measurement of B/A.

amplifier and the source transducer to remove higher harmonic components present at the output of the amplifier. The second harmonic component at the terminal of the source transducer was at least 60 dB below the fundamental. The driving voltage on the source transducer was monitored with an HP Model 8557A spectrum analyzer set in the zero frequency scan mode, i.e., the analyzer was used as a tuned amplifier. The same analyzer was also used to measure the second harmonic component on the receiving side. By using the same analyzer for measuring both P_2 and P_1, errors in the analyzer calibration partially cancelled each other. An attenuator between the source transducer and the analyzer reduced the voltage level so that the analyzer was not overloaded.

The duration of the RF pulses was chosen so that a pulse was long enough for the transducer output to reach steady state but short enough so that reflections from the receiver would not overlap with the signal. The repetition rate was chosen so that all reflections had time to decay to a negligible amplitude between successive excitations. An appropriate choice was 5 μs for the pulse on time with a repetition rate of 2,000 per second.

The finite amplitude acoustic pulse, after travelling a few centimeters in the sample, was detected by a wideband receiving transducer of the same size as the source. The received signal was first passed through a 6 MHz, 5 element, Butterworth high pass filter, then to an HP Model 8557A spectrum analyzer. The high pass filter was necessary to reduce the fundamental component to a level within the linear range of the analyzer, so that harmonics were not generated in the spectum analyzer.

Chamber for Acoustic Measurements - The acoustic chamber shown in Figure 3.2 was used for finite amplitude second harmonic measurements, for calibration of transducers, and also for velocity and absorption determinations. The waterjacket was basically a cylindrical chamber with the inner jacket also serving as a container for the sample and the coupling medium. The chamber was made of two concentric 1/8" wall thickness glass cylinders 3" and 4", respectively, in inside diameter. Water at a regulated temperature circulating between the two cylinders maintained the sample at a chosen temperature. The two cylinders were sealed at both ends with rubber gaskets to two end plates. The top plate was ring shaped, providing a 3" diameter access to the sample chamber. The bottom plate, made of anodized aluminum, had fixtures for mounting a transducer in the bottom of the sample chamber. The optically transparent chamber allowed visual inspection of transducer surfaces so that bubbles trapped in the sound path could be detected and removed.

The source transducer was mounted to radiate upwards, flush with the bottom of the sample cell. The chamber itself was mounted directly on a three point support. The support, consisting of three spring loaded legs which had provisions for adjusting their lengths, allowed the chamber, and hence the source transducer, to be tilted in two orthogonal planes, thus providing angular adjustment of the acoustic axis.

The receiver was mounted coaxially, and faced the source, in a 3-way positioner which provided for movement in three orthogonal directions transverse to and along the acoustic axis. The source-receiver alignment was made by an iterative process of

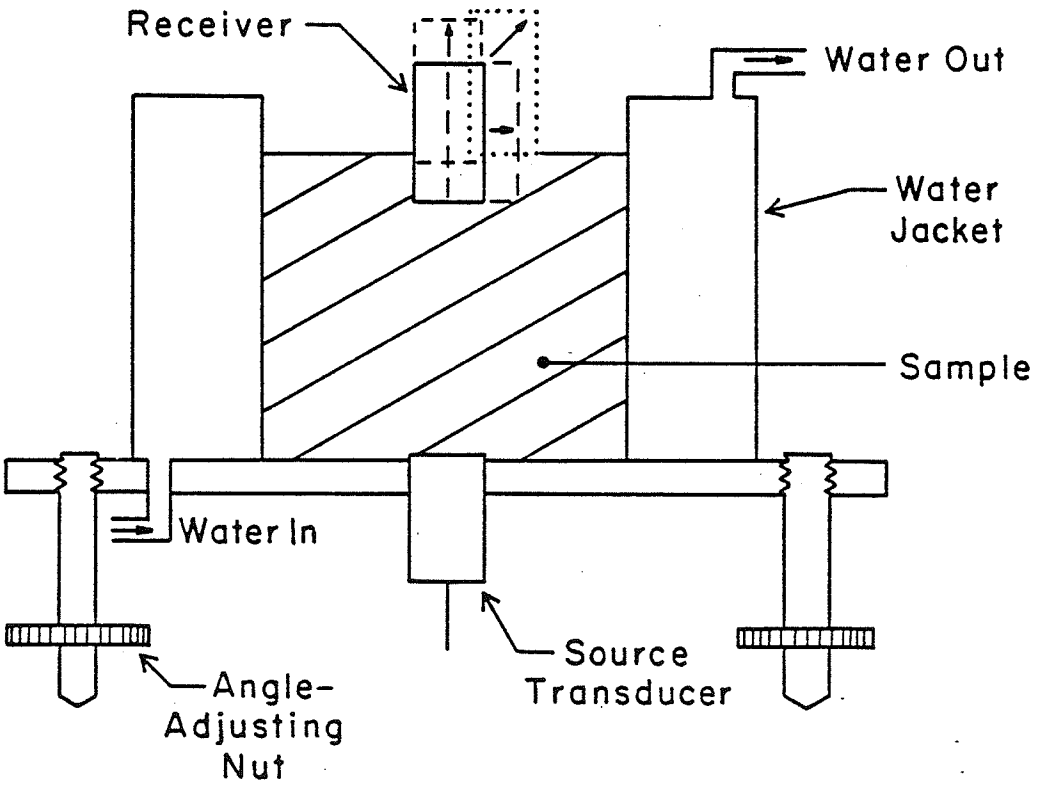

Figure 3.2. Schematic diagram of the acoustic chamber.

adjusting the three point support and the position of the receiver, using the maximum in received signals as an indication for alignment.

The receiver position could be read from a vernier scale attached to the positioner. The actual separation between the receiver and the source was determined using a 1 cm thick metal block as a thickness gauge to calibrate the z axis vernier scale on the positioner.

Transducers - The source transducer used in the B/A measurement system was a 1/2" diameter medium damped immersion transducer from K-B Aerotech. It was custom made to resonate at 3 MHz, and had a heavy duty 4 Watt tuning network to allow CW operation, which was necessary for the calibration by the radiation force technique. However, due to the high absorption of the backing material and the consequent generation of heat, the manufacturer did not recommend operation of the transducer in the CW mode for more than 5 seconds with 4 Watts input power. The stability of the transducer was tested by observing the sound pressure output of the transducer with a hydrophone before and immediately after a 5 sec, 4 Watts CW operation and the change in output was found to be less than 1%. Since only 2 Watts of input power were required for the radiation force calibration, the transducer was considered sufficiently stable for that purpose.

The receiving transducer was also a 1/2" diameter medium damped immersion transducer from K-B Aerotech, though the resonating frequency was 5 MHz. Since the receiver had a 30% -3dB bandwidth, the sensitivity was sufficient for measurement at 6 MHz.

For calibration purposes, a 6 MHz, 1/2" diameter sound source calibrated with the radiation force technique was used as a secondary standard. Such a transducer was constructed from a 6 MHz, 1/2" diameter PZT4 ceramic disc from Channel Industries and mounted in an appropriate housing.

3.1.2. Calibration

Effective Radius of the Source - The calibration of the transducer, as well as the analysis of diffraction effects, require knowledge of the radius of the sound source. Because of edge effects, the effective radius of a transducer is slightly different from that of the geometric radius. Here, effective radius refers to the radius of an ideal piston source which would produce a sound field resembling that of the real transducer. An acceptable method for the determination of the effective radius [Khimunin, 1978], is to compare the theoretical and experimental values of the positions of the near field extrema on the acoustic axis of the transducer. The effective radius is the radius of the ideal piston which gives an axial field distribution that best matches the positions of experimentally observed extrema.

A small hydrophone, [Law, 1978] made of a 2 mm diameter thickness mode ceramic element resonant at 20 MHz was used as a sound detector for determining the axial extrema. The source transducer was mounted on the acoustic chamber, as described in the previous section, and the hydrophone was supported by an angular positioner, which was in turn mounted on a 3-way (x, y, z) positioner. The source transducer was aligned so that its axis

was parallel with the z axis (vertical axis) of the x, y, z positioner, using a bubble inclinometer. The hydrophone was then moved to the end of the near field, where the sound distribution had a well defined maximum. Alignment of the hydrophone was achieved by adjusting its angle and lateral position to achieve a maximum in the received signal. After alignment, the hydrophone was then moved along the axis of the transducer to locate the positions of the extrema.

Table 3.1 lists the positions of the last six extrema measured for the 3 MHz source. Also in the table are theoretical values for the positions of extrema for piston sources 0.635 cm (1/4") and 0.59 cm in radius. The second radius (0.59 cm) was chosen amongst other possible values because it gave the smallest total error when comparing the experimentally determined positions of extrema with those generated theoretically. As seen in the table, for the distances used in B/A measurements, 1 - 3 cm, the positions of measured extrema agree well with those predicted for a 0.59 cm radius piston source. However, the match was not perfect, probably expressing the difference between an ideal piston source with uniform sound distribution and a real source with some nonuniformity in the distribution around the edge. The average deviation of the measured positions of extrema from theory using a 0.59 cm radius reflects a $\pm$ 2% uncertainty in the effective radius of the transducer.

Determination of Source Acoustic Pressure- The average source acoustic pressure p_o was determined by measuring the total power output of the source transducer, dividing it by the effective area

Table 3.1. Positions of the axial extrema (in cm) as measured experimentally and computed theoretically using a_o = 0.635 cm and a_o = 0.59 cm.

Positions of axial extrema (experiment)	7.1	3.80	2.37	1.65	1.32	1.08
Positions of axial extrema (theory, a_o = 0.635 cm)	8.0	3.99	2.64	1.96	1.54	1.26
Positions of axial extrema (theory, a_o = 0.59	6.91	3.44	2.27	1.68	1.32	1.08

to obtain the average acoustic intensity, and then converting to acoustic pressure using the plane wave relationship between intensity and pressure, viz., $I = p_o/2\rho_o c$. The total acoustic power was determined by a radiation force balance, schematically shown in Fig. 3.3. The radiation force target, made of sound absorbing rubber, was machined so that the sound was incident at a 45^o angle to one face. A copper weight at the bottom of the target served to maintain the orientation of the target relative to the sound source. Since the radiation force generated by an absorbing target or a reflecting target is the same when the sound is incident at 45^o, this arrangement eliminated errors due to reflection resulting from impedance mismatch between the medium and the target. The accuracy of the alignment between the transducer and the target was estimated to be about $\pm 3^o$, measured with a protractor. Since the radiation force is independent of the angle of incidence for a totally absorbing target, and only a small amount of energy was reflected from the target-medium interface, the alignment was judged adequate.

The radiation force target was suspended with a single steel wire 0.01" in diameter to a Mettler Model H15 balance. The thin wire minimized the surface tension force at the interface between the coupling medium and the wire. The balance had an accuracy of $\pm$ 0.05 mg and a resolution of 0.1 mg. The radiation force balance assembly was calibrated by adding known weights on top of the submersed rubber target and comparing the buoyancy corrected weight with the readout on the balance. Results of the comparison indicated agreement within 1% for weights between 10 mg and 100

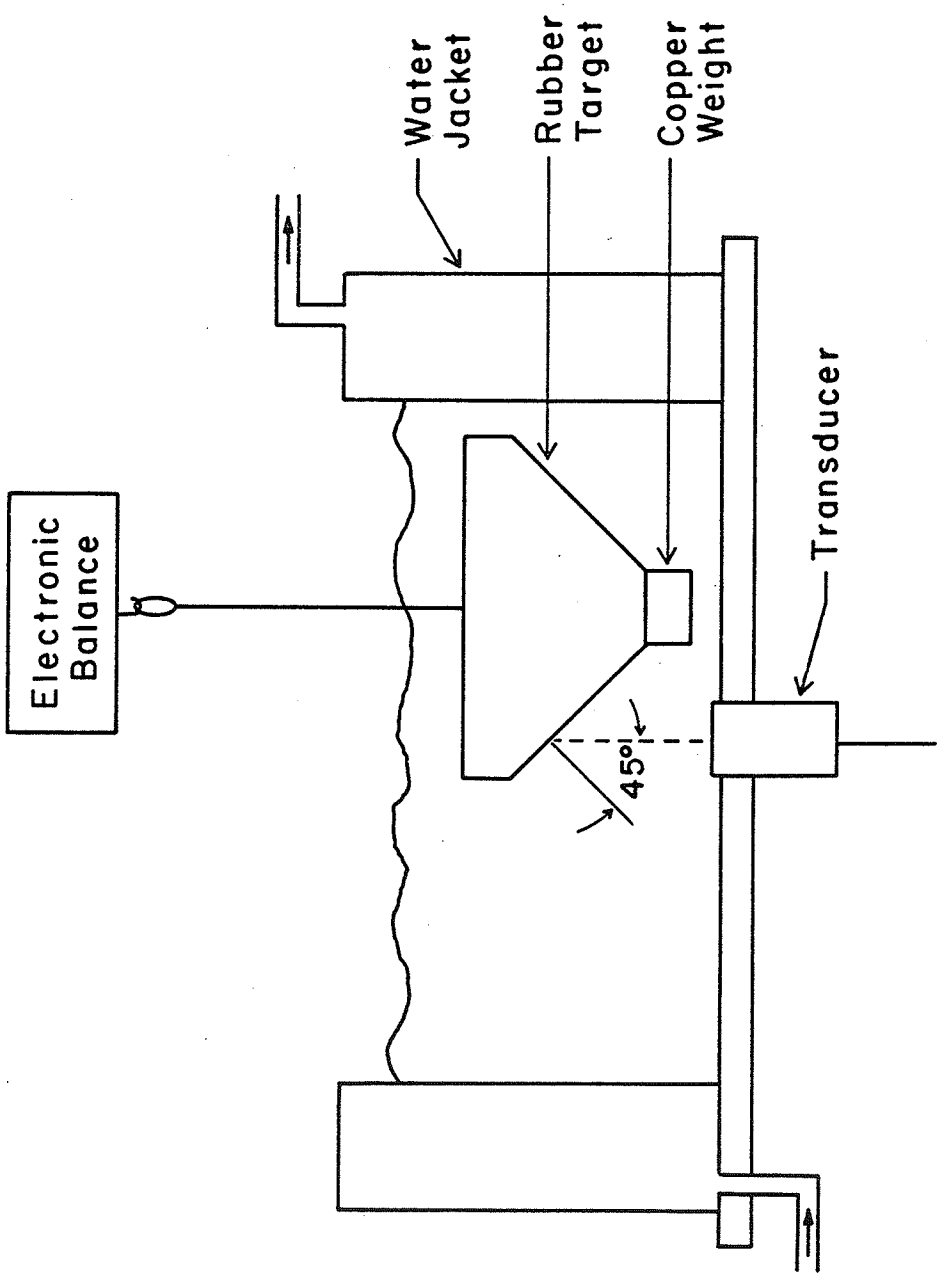

Figure 3.3. Schematic diagram of the radiation force balance.

mg. Thus the error due to surface tension was insignificant for radiation force measurements within this range.

The sound receiving face of the radiation force target was placed approximately 2 cm from the center of the transducer, 2 cm being the minimum separation possible without the copper weight on the target touching the tank. The face of the target, which was 2.5 cm by 5 cm, was large enough to intercept most of the sound beam. The absorption of sound in the 2 cm path length was insignificant for all the calibrating media used in this investigation, except for the 30% solution of sodium chloride which required a correction of about 2%. Temperature of the chamber was maintained at $30^{\circ}C$, $\pm$ $0.2^{\circ}C$ for all calibrations.

The radiation force readings were taken at the end of a 5 sec "on period," and 5 sec after the sound was turned off; 5 sec being the time required for the target to equilibrate at its new position. Since the target was sound absorbing, it was heated slightly during the 5 sec of irradiations, resulting in a slight increase in buoyancy. The buoyancy change due to heating of the target was observed to be about 4% of the radiation force for every 5 sec of irradiation. However, the heat loss from the target is a much slower process. By observing the change in weight with time, the buoyancy change in the first 10 sec after the sound was turned off was estimated to be less than 2% of the radiation force. For this reason, reading of the balance was made at the end of the irradiation period, and after the sound was turned off, rather than at the beginning of the irradiation period. The error due to buoyancy change of the target was therefore estimated to be less than 2%.

Error was also caused by thermal disturbance in the coupling medium and mechanical vibrations in the room, which caused the acoustic target to oscillate randomly during measurements. Three or four readings of the radiation force were usually taken to obtain the average value. The standard deviation of the readings was about $\pm$ 2% of the radiation force. The error due to the random oscillation of the target is therefore estimated to be $\pm$ 2%.

In the finite amplitude method of B/A measurement, the transducers were in direct contact with the sample being measured, resulting in a change of load impedance to the transducers when samples of different impedances were measured. The output of the source transducer was therefore calibrated at different load impedances to account for different impedances in the samples. For the purpose of calibration, impedances greater than water were provided by sodium chloride solutions of various concentrations, while impedances less than water were provided by methanol-water mixtures. These solutions and mixtures had the advantage of possessing low absorptions, so that energy loss between the transducer and the target is insignificant. Table 3.2 gives the densities and sound velocities in these calibrating media at 30^{o}C. Velocities were determined by a continuous wave moving transducer method, and densities were determined by a volumetric method. Both of these methods are described in the following sections.

Figure 3.4 shows the average source pressure of the 3 MHz transducer as a function of impedance of the radiated medium, indicating that for the 6 MHz source, constructed from a channel cermanic disc, the output pressure can change as much as 40% for

Table 3.2. Density, velocity, and impedance of the media used for transducer calibrations (30°C).

Media	Velocity $x10^{-5}$ (cm/s)	Density (gm/cc)	Impedance $x10^{-5}$ ($gms^{-1}cm^{-1}$)
50% Methanol-water	1.483	0.915	1.36
Water	1.509	0.996	1.51
5% Saline	1.55	1.02	1.58
10% Saline	1.59	1.05	1.67
15% Saline	1.64	1.08	1.77
20% Saline	1.68	1.11	1.87
25% Saline	1.73	1.14	1.97
30% Saline	1.77	1.17	2.07

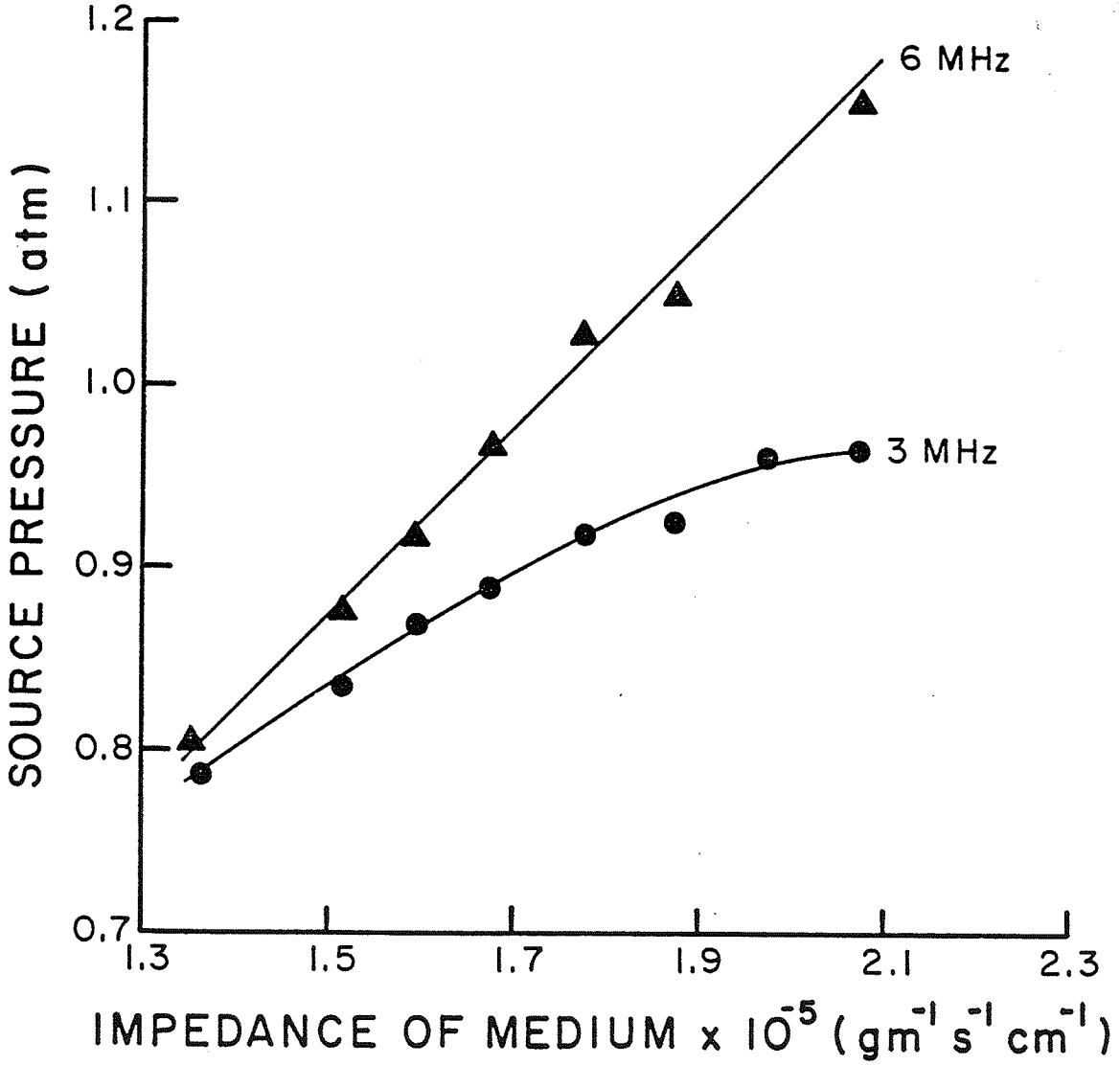

Figure 3.4. Average source pressure output of the 3 MHz and 6 MHz transducers as a function of the impedance of the medium under a constant driving voltage.

a 50% change in impedance loading. On the other hand, the output of the 3 MHz wideband transducer changed only 20% for the same change in load impedance. However, in both cases, the change of source pressure with load impedance was significant.

Calibration of Receiver - The calibration procedure for the ultrasound receiver involved first calibrating a 6 MHz, 1/2" sound source using the same procedures as described for the 3 MHz source transducer, and then placing the receiver parallel and coaxial with the calibrated sound source and recording the output voltage of the receiver. Due to diffraction effects, the sound beam from a piston source diverges and has a nonuniform phase front. As a result, the average pressure at the receiver is smaller than the average pressure at the source, because the receiver does not intercept the entire diverging sound beam and because some phase cancellation occurs in the plane of the receiver. Diffraction theory for a phase sensitive receiver the same size as the source, and placed parallel and coaxial with it, is well established [Bass, 1958]. The ratio p_{av}/p_o, where p_{av} is the spatial average pressure at the receiver, and p_o is the source pressure, can be determined accurately from Eq. (2.37) in the theory section. This ratio, plotted as a function of source-receiver separation, is shown in Fig. 3.5 for a 6 MHz, 1/2" diameter source. At 3 cm from the source, the distance at which the receiver was calibrated, p_{av}/p_o is 0.9. The receiver calibration was corrected for diffraction by dividing the receiver output voltage by this factor of 0.9.

The procedure for calibrating the receiver involved the same

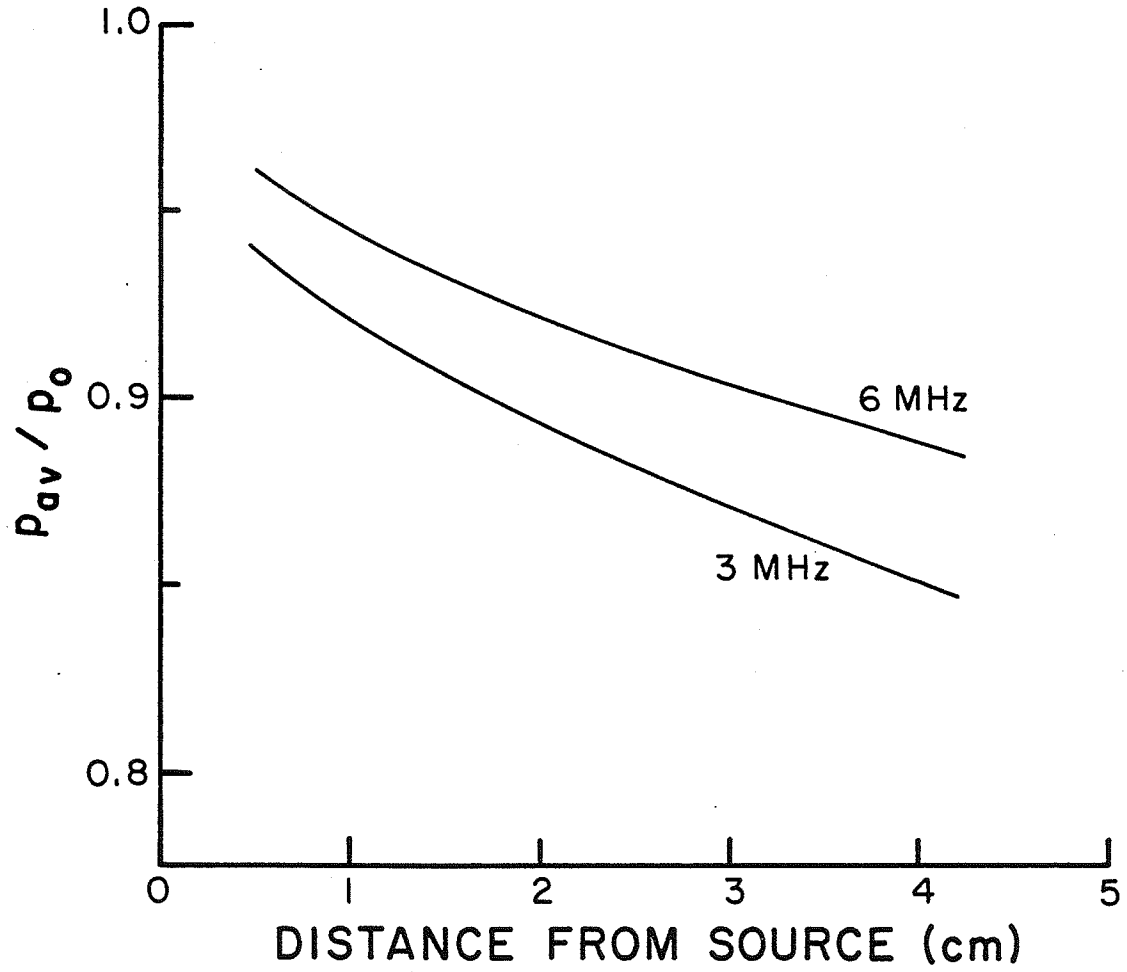

Figure 3.5. p_{av}/p_o at different distances from the source, as predicted by diffraction theory.

equipment for transducer mounting as in the B/A measurements. Transducers were also aligned in a similar fashion as in the B/A measurement, i.e., by adjusting the angle of the source transducer and the x, y position of the receiver alternately until a maximum in received voltage was obtained. The sound source was driven with RF pulses of 5 μs duration, the duration used in actual B/A measurements. Aqueous solutions of sodium chloride and methanol-water mixtures, temperature regulated to $30^{o}C \pm 0.2^{o}C$ were again used as media to obtain calibration values for media of various acoustic impedances. Results of the receiver calibration, plotted as sensitivity (volt/atm) vs. impedance of the medium, are shown in Fig. 3.6. The sensitivity was found to decrease with increasing impedance of the medium. The calibration of the receiver as a function of load impedance is therefore necessary in order to measure accurately the B/A values in samples of different impedances.

3.1.3. Determination of Attenuation Coefficients

Although attenuation coefficient values were not necessary to the determination of B/A by the finite amplitude method employed in this investigtion, they were useful in comparing the measured second harmonic amplitude with the theoretical predictions thus supporting the correctness of the theory and hence the validity of this method. The attenuation coefficient was obtained by taking the negative logarithm of the slope of the p(z) vs. z curve and correcting for diffraction [O'Brien, 1968]. The apparatus for attenuation measurements was set up in the same way as in B/A measurements. The wideband transducer used in the B/A measurement

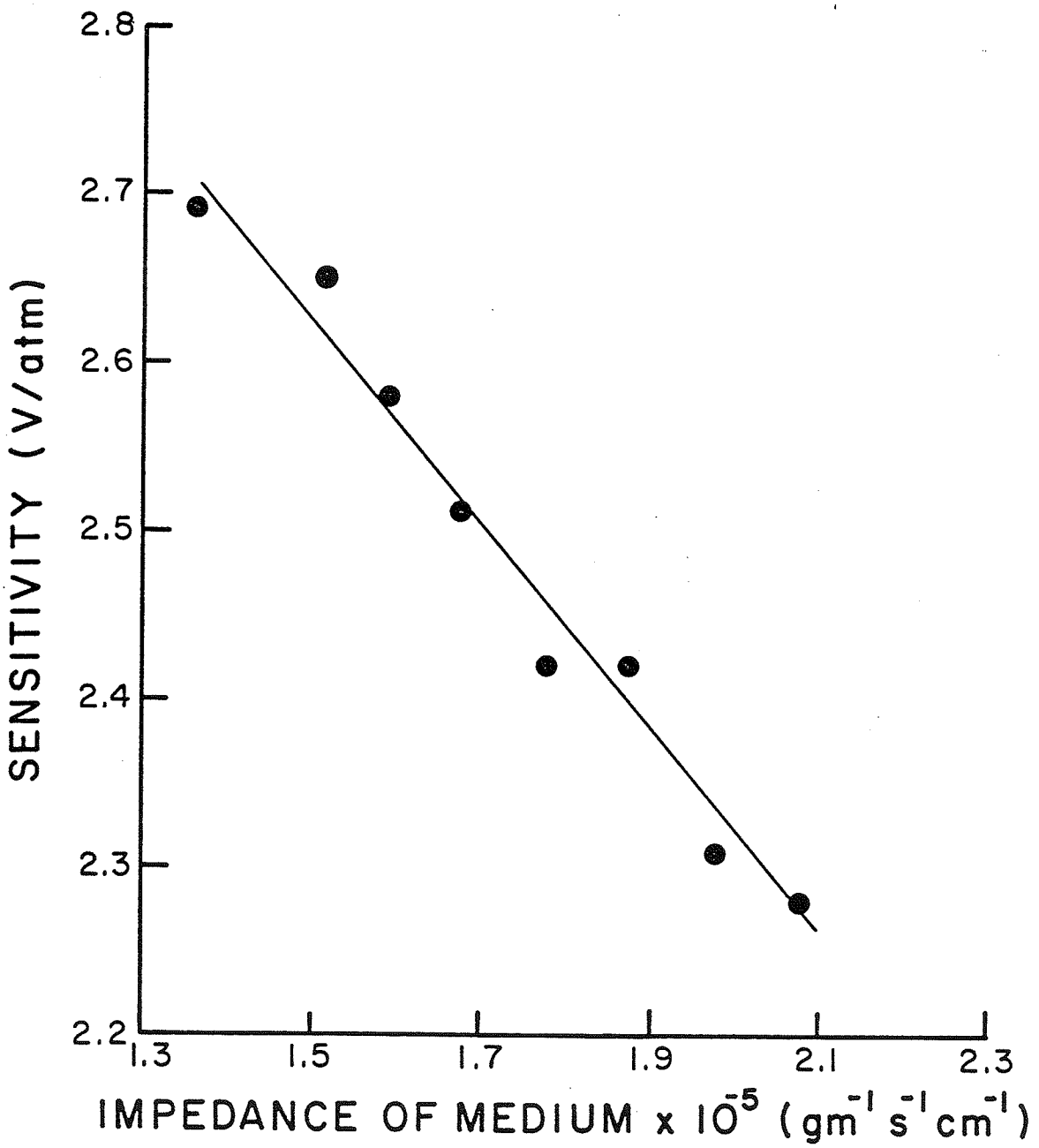

Figure 3.6. Sensitivity of the acoustic receiver at 6 MHz as a function of impedance in the medium.

system had wide enough bandwidth to cover both 3 and 6 MHz. By switching the frequency of the driving voltage applied to the source from 3 to 6 MHz, the attenuation at either frequency could be measured by the same system. A low amplitude for the driving voltage was used to minimize finite amplitude effects on the attenuation measurements. For liquid samples the source-receiver separation was changed in 2 mm steps and the acoustic pressure p(z) at each position recorded. For tissue samples, starting with a suitable length of the specimen, sections of the samples several millimeter thick were subsequently cut away from the ends of the sample, and the transmitted acoustic pressure was measured for each sample thickness, with the source and the receiver in direct contact with the sample. The p(z) at each distance z was corrected for diffraction, using the diffraction computation of Eq. (2.37). Curves for diffraction correction at 3 and 6 MHz are shown in Fig. 3.5, generated according to Eq. (2.37). A least squares fit to the diffraction corrected ln p(z) vs. z data then yielded the slope, which in turn gave the attenuation coefficient.

The standard deviation in the attenuation coefficient measurements was estimated to be 2% for liquid samples, and about 5% for tissues. In the latter case, the major contribution to the uncertainty was probably the error associated with measurement of the sample length. Due to the careful choice of tissue samples which were free of large blood vessels, the effect of phase cancellationshould be minimal.

3.1.4. Determination of Speed of Sound

Two methods for speed of sound determination were used,

depending on the type of sample studied, viz., a continuous wave, moving transducer method [McSkimin, 1964] was used for liquid samples, and a time-of-flight method, with correction for system delay [Wells, 1977], was used for solid tissue samples. The temperature of all samples was maintained at $30^{o}C \pm 1^{o}C$.

The moving transducer method used the same apparatus as in the B/A measurement, except that the source transducer was driven by a 3 MHz CW signal, establishing a standing wave pattern between the source and the receiver. The receiver was then moved through a fixed number of consecutive nodes, and the total displacement of the receiver recorded. The wavelength, and hence the velocity, was obtained by dividing the total displacement of the transducer by the number of nodes. The accuracy of the method was estimated to be better than $\pm$ 1/2%.

For solid tissue samples, the velocity was obtained by measuring the time for a 3 MHz pulse to travel from the source to the receiver, with the tissue sample in direct contact with both transducers. The same apparatus, as used for B/A measurement, was used for the velocity measurement, except that the receiver was connected to an oscilloscope with digital Δ time measurement capability (Tektronics model 465B) which has an accuracy of 1%. The driving voltage applied to the source transducer was connected to the second channel of the oscilloscope to provide the reference for the beginning of the pulse travel. The seventh zero crossing in the electrical signal driving the source, and the same zero crossing in the received signal, were used as time marks for measuring the time-of-flight (Δt). To correct for time delays in the transducer and in the electronics, the system was calibrated

using the known velocity of water as a standard. The system delay was subsequently subtracted from individual time - of - flight measurements to yield the true transit time of the acoustic signal through the sample. The uncertainty of this method was estimated to be about 1%.

3.1.5. Determination of Density

The density of samples was determined by volumetric methods. Picnometers with calibrated capillary seals were used. For liquid samples the bottle was first weighed, then filled with the liquid, the seal was inserted, and the bottle carefully wiped clean. The capillary seal was calibrated by the manufacturer so that the bottle together with the seal would have a known volume when the liquid was filled to the top of the capillary seal. Care was taken to avoid trapping bubbles inside the picnometer. The liquid filled bottle was then weighed again. The difference in weight between the liquid filled bottle and the empty bottle was then the weight of liquid, which, when divided by the volume of the bottle, gave the density of the liquid specimen. Inaccuracy in filling and in cleaning of the bottle was a major cause of the uncertainty in this method. Repeated measurements indicated that the uncertainty was about 0.5%.

For tissue samples, a long, roughly cylindrical piece was cut and weighed. This piece was then submerged completely into a measuring cylinder containing isotonic saline. Bubbles were carefully removed from the surface of the sample by moving it up and down the cylinder. The change in the level of the saline solution inside the cylinder then indicated the volume of the

tissue sample, and the density of the sample was taken as the weight divided by the volume. Tissue samples without major blood vessels were chosen for measurements to avoid errors due to trapped air inside the blood vessel. The major error in the measurement came from inaccuracy in reading the volume and was estimated to be about 1%.

3.1.6. Preparation of Samples

Liquid Samples - Bovine serum albumin (BSA) was obtained in dehydrated powder form from Sigma Chemicals. These fraction v crystals were specified by the manufacturer to be 96.99% pure. Aqueous solutions of BSA were obtained by dissolving an appropriate amount of the powder into degassed distilled water. The water was first heated to 40°C, and the powder added slowly, with constant stirring of the solution. A solution of about 40% (gm solute/100 cc solution) was first prepared and solutions of lesser concentration were obtained by dilution. Air bubbles that were created during the stirring process were removed by centrifugation.

Solutions of dextrose and dextran were prepared by a procedure similar to that used to prepare the BSA solutions. Dextran in powder form was obtained from Pharmacia Fine Chemicals in molecular weights of 1.5×10^5 and 2×10^6 Da. Dextrose has a molecular weight of 180 Da. Since the objective in measuring dextran was to observe the effect of molecular weight on the value of B/A, these solutions were each made to approximately the same concentration (weight/volume). Once prepared, the BSA and dextran solutions were stored in a refrigerator at 5°C until use.

Porcine whole blood was obtained from freshly slaughtered pigs; 4 grams of sodium citrate was mixed with each 100 cc of blood to prevent coagulation. A measured amount of sodium citrate was first placed in a container of known volume, which was placed directly under the incision at the throat of the slaughter animal so that it bled into the container. The blood was stirred constantly during collection to disperse the sodium citrate throughout the blood volume. The container was removed when the blood reached a predetermined level. These samples were used within 5 hr after collection.

Hemoglobin solutions were obtained directly from porcine red blood cells. Whole blood was centrifuged to separate the serum from the red cells. The tightly packed red cells were collected and lysed with toluene at $5^{o}C$ over a 24 hr period, the excess toluene was removed, and the mixture was centrifuged, after which the cellular debris was readily separated from the liquid hemoglobin solution. The hemoglobin solutions so obtained had a concentration of about 50%. Solutions of lesser concentration were obtained by dilution with degassed, distilled water.

Tissue Samples - Tissue samples of bovine liver, porcine muscle, and porcine fatty tissue were obtained from freshly slaughtered animals within 2 hr after death. The liver samples were taken from around the edge of the liver, where large blood vessels were less numerous. The muscle samples were taken from the shoulder, where thickest. Fatty tissue samples were also taken in this region, between the skin and the muscle. Unlike liver, the muscle and fatty tissue samples were usually free of large blood vessels. Tissue samples were usually used within 24

hr of slaughter. Rectangular sections of tissue about 6 cm on a side and 5 cm thick were removed from a larger section of tissue using a disposable microtone knife, with special attention given to avoid portions with blood vessels larger than 1 mm in diameter. For liver, the exterior surface, which is an elastic supportive membrane, was always removed from the sample. For muscle, the sample was cut with the length parallel to the fibers. These samples were then massaged in isotonic saline solution to remove bubbles clinging to the surface.

Before a tissue sample was put into the B/A measurement chamber, the thickness was measured with a rule on four edges of the sample. Although the cuts were made freehand, the relatively wide blade of the microtone knife helped to maintain a smooth cut and the thickness was usually uniform to within 2 mm on the four sides. However, when the sample was placed in the measurement chamber and held between the two transducers, a slight pressure was applied which smoothed out this nonuniformity. In order to provide this gentle pressure, the transducer separation was set so that it was 1 mm less than the minimum thickness of the sample. The separation of the transducers was used as the thickness of the sample in the computation of B/A. Due to the nonrigid and deformable nature of the tissue, the tissue sample sometimes may slip sideways, causing an uneven surface. To correct for the slip, the tissue sample was manipulated slightly by hand laterally before each measurement, using the maximum in fundamental components of the received signal as the indication of alignment.

Several measurements of the second harmonic magnitude at different sample lengths were required to determine the B/A value

using the finite amplitude method. These samples of different lengths were obtained by consecutively removing thin slices, between 0.6 cm and 1 cm thick, from the just measured sample. The slicing and mounting of the samples of new lengths between transducers followed the same procedure as described above. Measurements were always made at approximately the same site as for the previous measurements, though due to the deformability of the tissue it was difficult to pinpoint exactly the same location in every measurement. The inability to follow the same sound path in measurements of different sample lengths may be a source of significant error if the sample is sufficiently inhomogeneous. However, when a tissue sample was free of large blood vessels, the tissue homogeneity was found to be satisfactory, and the necessity for having duplicated exactly the sound path was reduced. The tissue homogeneity was demonstrated by an experiment by Cobb [1982], in which an ultrasound transmission scan across a 1 cm thick piece of liver was made to determine the absorption coefficients at different sites of the liver. The result indicated that the attenuation coefficient across the liver was uniform to $\pm$ 5%.

The second harmonic data obtained in this investigation also suggested that the homogeneity of the tissue samples was acceptable. When $\ln p_2(z)/z$ was plotted against z, the data points were found to scatter only slightly from a straight line. Not more than 10% fluctuation was observed for each of the various thicknesses measured. The average deviation of the data points from a least squares straight line fit was less than 3%.

Liver Homogenate - Liver homogenates were prepared by removing the exterior surface from beef liver, not more than three hours after excision, and cutting the liver into pieces about 1" square. Blood vessels larger than 1 mm in diameter were removed and the pieces were placed in a Waring model 10 blender, with speed set to "liquify," and processed for 1 min. To remove the bubbles created during this liquification process, the liver homogenate was subjected to a gentle vacuum (70 cm Hg) until bubble evolution at the surface ceased. The liver homogenate was then measured as the other liquid samples.

3.1.7. Determination of Solution Concentration

The concentration (dry weight content) for solutions was determined by measuring the amount of residue left when a known volume of the solution was completely dried. A volume of 10 cc of the solution was measured with a pipette, and delivered to a petri dish. The solution was then placed in a decsicator and subjected to a vacuum of about 60 cm Hg for 24 hr. The difference in weight between the empty Petri dish and the one with residue provided the amount of solute in the solution. The concentation (in %) of the solution was defined as the amount of solute (in grams) per 100 cc of the solution.

3.2. Thermodynamic Measuremnt of B/A

The thermodynamic method comprises the measurement of sound velocity as a function of pressure and temperature. The velocimeter, or delay line, consisted of a hollow cylinder with a transmitting quartz crystal transducer attached to one end and a

receiving transducer at the other. The two transducers faced each other, with the acoustic axes aligned along the length of the cylinder. The sample to be tested was contained within the bore of the cylinder and constituted the sound path through which acoustic pulses propagated from the source transducer to the receiver. The source transducer was driven by a pulse modulated RF signal with a carrier frequency of 3 MHz. Each pulse caused the transmitting crystal to send out a wave packet which propagated through the sample to the receiver. The propagation time was measured by comparing the received signal directly with precision time markers. The received acoustic signal, together with the electromagnetic pick-up of the electrical driving signal of the source, was displayed on one channel of an oscilloscope. The second channel displayed a series of time markers which were synchronous with the driving signal applied to the source. The interval between time marks was adjustable and measured to ± 0.001% with a digital counter. By using the delayed sweep option of the oscilloscope, which allowed the "expanded" display of a small portion of the wave form, the time marker could be aligned to a fixed point of the wave packet to the accuracy of 1/100 of a cycle. The delay time between the electromagnetic pick-up signal and the corresponding received acoustic signal was the propagation time of the acoustic wave packet. Dividing the length of the sound path by the propagation time gave the velocity of the sound wave in the intervening sample.

The velocimeter was enclosed in a pressure vessel to allow for measurement of velocity at different hydrostatic pressures. The pressure vessel, with the velocimeter enclosed, was placed in

a temperature controlled water bath, so that velocity could be measured as a function of temperature.

3.2.1 Equipment

Crystals - The transducers were X-cut quartz disks 3/4" in diameter with a resonance frequency of 3 MHz. Both faces of the crystals were fine-ground, with complete gold on chrome plating on the ground side and gold on chrome plating over a circle 1/2" diameter on the other side. A thin wire was soldered to the center of the smaller electrode for electrical input. The completely plated side was the ground. The crystals were held against the ends of the sample chamber by clamping on the edges. When assembled, the completely plated face of the crystal was in electrical contact with the sample chamber, providing good grounding.

Sample Chamber - Figure 3.7 shows the sample chamber, made of 304 stainless steel, the transducer housings, and the mounting of the crystals. The sample chamber consisted of two hollow cylinders of unequal lengths, joined together by seven screws. The design allowed the placement of soft tissue samples inside the sample chamber without disassembling the transducer mounting. A rubber diaphragm sample chamber allowed the pressure inside the sample chamber to equalize with the pressure outside. When liquid samples were measured, the liquid was introduced through a fill hole opposite the rubber diaphragm. The fill hole was sealed with a screw and O-ring when the sample chamber was completely filled with the liquid. An important requirement in filling the sample chamber was to allow as little air as possible in the

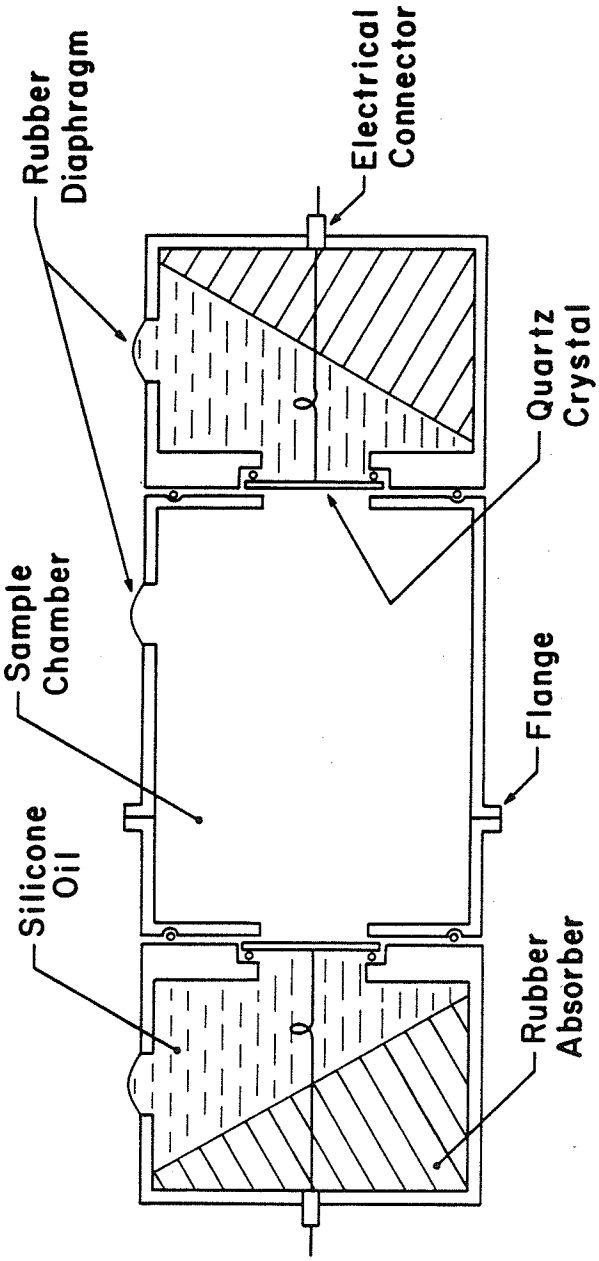

Figure 3.7. Schematic diagram of the velocimeter.

system. After the sample chamber was filled, it was placed horizontally and the presence of bubbles was determined by inspection through the semi-transparent rubber diaphragm. The complete velocimeter assembly, consisting of the sample chamber and the transducer housings, was surrounded by degassed water in the pressure vessel.

The length of the sample chamber was 3" $\pm$ 0.001" at 25°C. The thermal expansion coefficient of the 304 stainless steel used for the sample chamber was 17.3×10^{-6} $(^{\circ}C)^{-1}$. From this data, the length of the sample chamber at various temperatures could be computed. The bulk modulus was not available from the manufacturer but was obtained from the values of the elastic tension moduli and the Poisson's ratio, which were respectively, 28×10^{6} lb/in^2 and 0.29.

The crystals were sealed to the sample chamber by a recessed O-ring, as shown in Fig. 3.7. Pressure was applied on the edge of the crystal by the transducer housing so that the O-ring was compressed and a direct metal to crystal contact was formed.

The sample chamber was 2" in diameter, large enough to avoid wave guide effects. In a wave guide, for propagation in a certain mode, the group and the phase velocities are different, and only at the lowest modes will they approach, asymtotically, the same value, which corresponds to the "free" speed of sound. The 2" diameter cylinder is much larger than the wave length, and the wave guide effect was assumed to be insignificant. Furthermore, in a cylinder of smaller diameter, viscous losses at the walls may introduce additional damping in the propagated signal and consequently affect the speed of propagation. The large diameter

used in the sample chamber greatly reduced the importance of this viscous effect.

The sample chamber narrows to 3/5" in diameter immediately in front of the crystals. When measuring soft tissues, the samples were shaped to conform with the shape of the sample chamber, or a small piece of the tissue 1/4" thick and 3/5" in diameter was used to fill the space inside the narrow neck immediately in front of the crystals.

Transducer Housing - The two transducer housings were made of 304 stainless steel. Each was attached to the end of the sample chamber with the quartz crystal clamped at the edge. Rubber diaphragms covering openings to the sample chamber and the transducer housings transmitted the hydrostratic pressure from outside the velocimeter to the inside and also equalized the hydrostatic pressure in front of and behind the crystals to eliminate stress on the crystals from the applied pressure. The housings were filled with Dow Corning 710 silicone oil to facilitate equalization of hydrostatic pressure and lined with rubber absorbers with a 45^{o} angle to the axis of the crystals to eliminate reflections at the back face of the crystals.

Pressure Vessel - The pressure vessel was made of 304 stainless steel, with a wall thickness of 1/4". Two threaded end caps closed the pressure vessel. A bellows was connected to one endcap and transmitted the hydrostatic pressure from the hydraulic pressure generation system to the inside of the pressure vessel. The other end cap contained the electrical feed through connectors for the source and receiver. The velocimeter was also attached to

this cap so that the cap and the sample chamber could be removed as a complete assembly. The cap was tapered conically at the center fill-hole, so that when oriented vertically, air bubbles would collect at the fill hole and escape when the cap was screwed into the pressure vessel. The fill-hole was plugged by a small screw and O-ring after the cap was put in position.

It was very important to allow as little air as possible inside the pressure vessel, otherwise the bellows could be extended beyond its elastic limit when the system was pressurized. Before the end cap was completely tightened, the pressure vessel was tilted in three orthogonal planes repetitively so that bubbles trapped at the corners inside the vessel could rise to the fill hole at the center of the end cap.

Bellows - The bellows, which was used to transmit pressure from the oil filled hydraulic system to the water filled pressure vessel, was able to accommodate the change in volume of the contents inside the pressure vessel when it was subjected to increased hydrostatic pressure and temperature changes. The maximum change in volume, Δv, that the bellows might encounter was computed to be 7 ml. The computation assumed a maximum pressure of 2000 psi and a temperature change of not more than $10^{o}C$.

A bellows that could accomodate the Δv requirement was supplied by Servometer (Cedar Grove, NJ). The bellows was made of nickel with a 0.0001" copper lamina, and had an effective area of 4.45 in^2, a spring rate of 80 lbs/in $\pm$ 30%, and a maximum allowable volume change of 20 ml.

Pressure System - A schematic diagram of the pressure system is shown in Fig. 3.8. Other components of the thermodynamic system are also shown in the same figure. The pressure generator was a Blackhawk hand pump maufactured by Porta-power. The pump was connected via a stop valve to the pressure vessel and a pressure gauge. The Heise-bourdon gauge was a model CM-40385TC manufactured by Heise with a range of 0 - 3000 psi. (Throughout this thesis, the pressure will be given as gauge pressure, i.e., the pressure in excess of atmospheric pressure.) The pressure gauge was equipped with a protecting link to avoid damage due to abrupt changes in pressure. The full scale accuracy of the gauge as specified by the manufacturer was $\pm$ 0.1%. The pressure system was filled with hydraulic oil supplied by Enerpac, as were all connecting rubber coated nylon hydraulic hoses.

The hand pump was used to increase the pressure of the system. When the pressure reached the desired level, the valve between the hand pump and the vessel was closed to prevent leakage from the hand pump. To release the pressure, this valve, and a valve at the hand pump, had to be released to allow oil to flow back into the reservoir inside the pump.

Temperature Controlled Bath - The temperature bath, shown in Fig. 3.8 with the other components of the thermodynamic system, consisted of a 24" long by 16" deep by 14" wide plexiglass tank, with an electric stirrer, a heating coil, and a thermistor temperature sensor for the temperature controller. The temperature was controlled by a TSI model 72 proportional temperature controller, which had a temperature control bandwidth

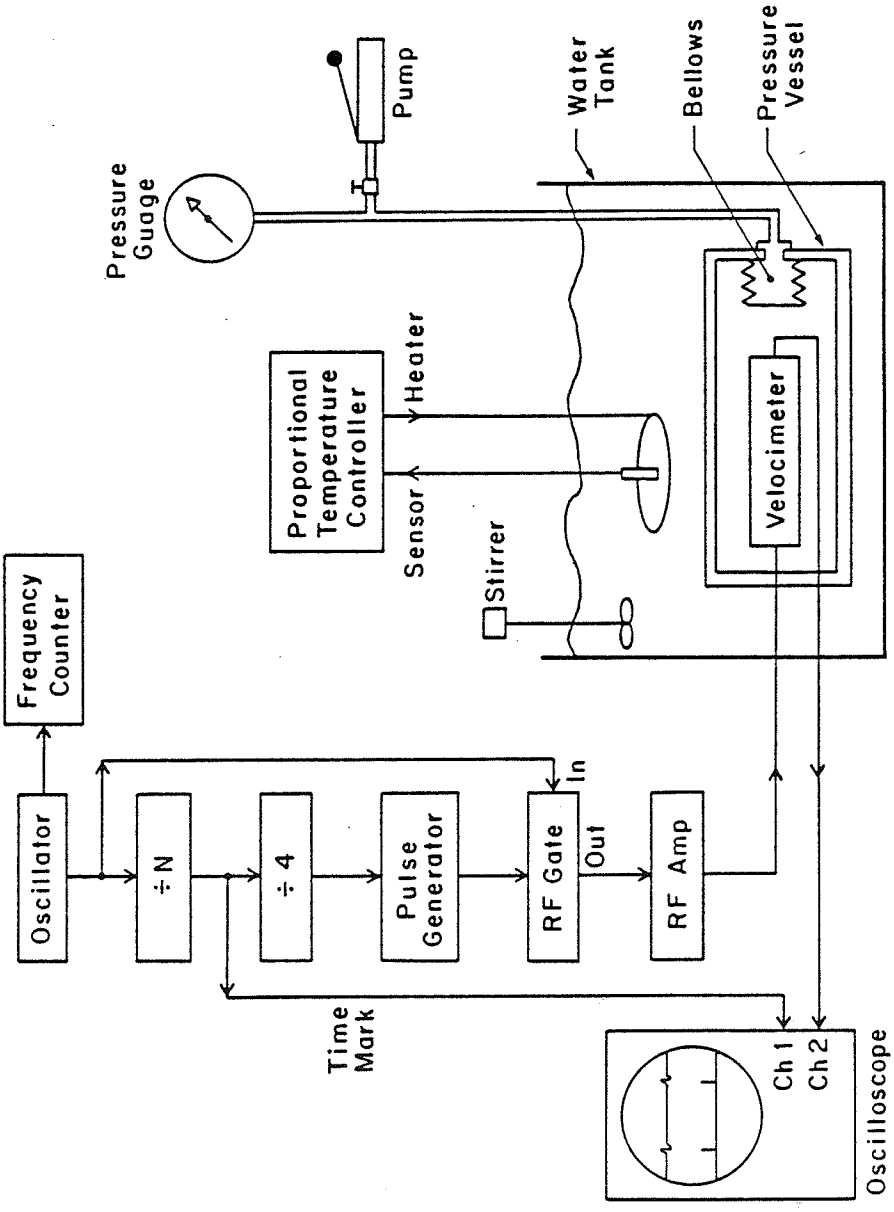

Figure 3.8. Schematic diagram of the thermodynamic system for B/A measurement.

of $0.1^{o}C$. Since all measurements were made above room temperature, no special cooling was applied to the tank.

Figure 3.9 shows a typical record of the temperature fluctuation inside the bath during a 6 hr period. The temperature deviated not more than $0.02^{o}C$ from the average temperature. Since the test sample was enclosed by the sample chamber and pressure vessel, which constituted a large thermal mass, the attendant thermal lag probably reduced the temperature variation of the sample to much less than $0.02^{o}C$.

The temperature of the bath was measured by a platinum resistance thermometer, model 9535 from Guild Line Instruments, which had a resolution of $0.001^{o}C$ and an accuracy of $\pm$ $0.01^{o}C$, according to the manufacturer.

Electronics- A block diagram of the electronic equipment is shown in Fig. 3.6. An RF oscillator, Ferris model 22-A, generated sine waves of adjustable frequency around 3 MHz. The signal was fed to a Berkeley Nucleonics Corporation model 7010 digital divider which divided the RF signal by a selectable integer n and produced short pulses at a repetition frequency of f/n, where f is the frequency of the RF oscillator. These short pulses were used as time markers in the time-of-flight measurements. The exact interval between pulses, n/f, was obtained by measuring the frequency of the RF oscillator with an HP model 5314A frequency counter, which had an accuracy of $\pm$ 40 Hz at 3 MHz. The output pulse of the n divider was further divided by 4 with a TTL divider to produce pulses about 200 μs apart. These pulses were used to trigger a monostable pulse generator

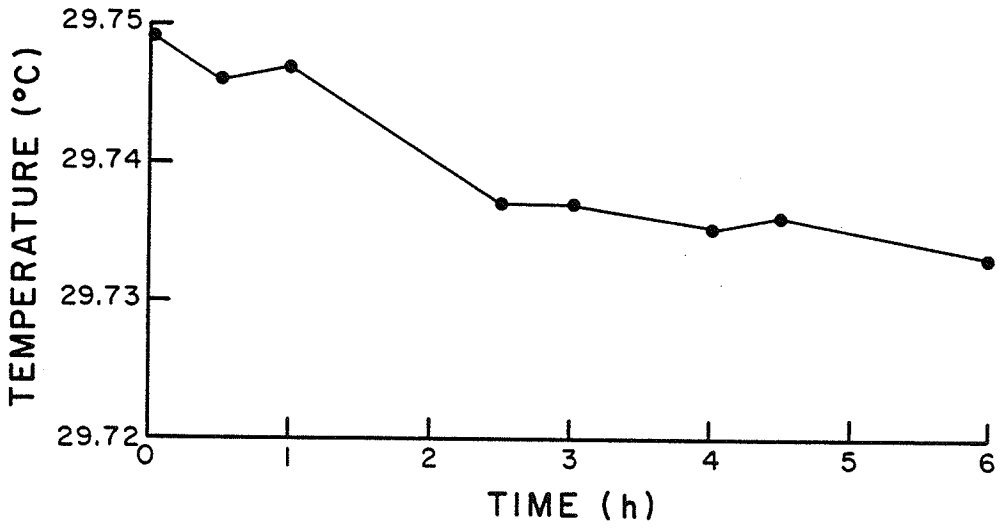

Figure 3.9. Temperature fluctuation in the waterbath in a 6 hr period.

which then produced pulses about 5 μs in duration with 200 μs separation. These pulses were used to control a solid state RF switch, model S7 from Watkins-Johnson, which gated the 3 MHz RF signal to produce RF bursts with a carrier frequency of 3 MHz. These RF pulses drove an RF power amplifier, model 10LA from Amplifier Research. The amplified signal was then applied to the source transducer. The 200 μs interval between pulses allowed the multiple reflections between the transducers to decay to a negligible amplitude before the start of a new pulse.

The acoustic pulse was converted into electrical signals when reaching the receiving crystal. The signal was fed directly to a Tektronix 465B oscilloscope. The second channel of the scope displayed the time marks generated by the selectable frequency divider. The scope was triggered, through a voltage attenuator, by the driving voltage of the source transducer.

The first time mark was positioned 0.25 μs before the beginning of excitation to the source transducer due to the delay in the electronic circuit. The position of the second time mark could be adjusted by either changing the setting on the n-divider, or by changing the frequency of the RF oscillator. The second time marker was always positioned at the seventh zero crossing of the received signal, which served as a convenient point of reference to keep track of the change of velocity as a function of pressure and temperature. The positioning was accomplished by first adjusting the setting on the n-divider so that the time mark was closest to the point of reference, and then adjusting the frequency of the oscillator to move the time mark to the exact position. Thus, the frequency of the signal driving the source

transducer was always maintained within a narrow range, approximately 3 MHz $\pm$ 20 kHz, and frequency dependent errors within the system were minimized.

The resolution of this method was primarily limited by the jitter in the oscilloscope display, which was approximately 1/100 of a cycle or 4^{o}, corresponding to $\pm$ 8 parts in 10^5. The frequency counter had an accuracy of $\pm$ 40 Hz at MHz, corresponding to $\pm$ 1.3 parts in 10^5. The resolution of the time measurement was therefore 1 part in 10^4.

3.2.2. Correction for Pressure and Temperature Effects

Since very small changes in sound speed were measured, the thermodynamic system had to be corrected for errors caused by the change of hydrostatic pressure and temperature on the sample chamber. These included the change in length of the sample chamber as a function of pressure and temperature, and the pressure differential across the extended bellows when hydrostatic pressure was applied to the system.

Corrections For Delay Line - The length of the sample chamber was measured at 25^{o}C and atmospheric pressure. At other temperatures and pressures, the length of the sample chamber is given by

$$L = L_{o}[1 + \gamma P + \alpha(T - 25)] \qquad (3.2)$$

where L_o is the length at 25^{o}C and atmospheric pressure, γ is related to the bulk modulus E_B by the equation $1/E_B = -3\gamma$, α is the coefficient of thermal expansion, which is given by the

manufacturer as 17.3×10^{-6} $(^{o}C)^{-1}$, T the temperature in ^{o}C, and P the pressure in psi.

To obtain the bulk modulus from the modulus of elasticity E_Y and Poisson's ratio ρ', which were available from the manufacturer, one may use the formula

$$E_B = E_Y/3(1 - 2\rho') \tag{3.3}$$

For 304 stainles steel, $E_Y = 28 \times 10^6$ lb/in^2, $\rho' = 0.29$; therefore, the value for γ was -1.5×10^{-8} lb/in^2, and the length of the sample chamber at various temperatures and pressures was

$$L = 3" \left[1 - 1.5 \times 10^{-8}\ p + 17.3 \times 10^{-6}(T - 25)\right] \tag{3.4}$$

Correction for Bellows - It was necessary to determine the pressure differential across the bellows, i.e., between the oil and the contents inside the pressure vessel, since the bellows had a finite spring constant. The pressure increment Δp across the bellows resulting from an extension Δl of the bellows is given by $\Delta p = k' \Delta l/A$, where k' is the spring constant and A the effective area of the bellows. Also $\Delta l = \Delta V/A$, where ΔV is the change in volume, given by $\Delta V/V = BP$, B is the isothermal compressibility, p is the applied pressure, and V is the volume of liquid in the vessel. At 2000 psi, the change in volume was approximately 7 ml. The computed pressure differential across the bellows was about 2 lb/in^2, which is 0.1% of the applied pressure.

Correction for Time Delay in Electronics - In order to measure the absolute velocity accurately, the velocimeter was calibrated using distilled, degassed water as a reference. In the

time-of-flight measurements, the time delay in the transducers and associated electronics, together with an ambiguity in defining the arrival of the sound pulse, often introduce errors to the absolute velocity measurements. However, by calibrating the velocimeter against a medium of known velocity, the time delay can be determined and subtracted from subsequent measurements. Furthermore, by using a zero crossing in the stabilized portion of the wave packet instead of the ill-defined rising edge of the received signal as the point of reference, the position of the pulse is better defined. In the experiments reported herein, the time-of-flight was defined as the time between the seventh zero crossing in the excitation signal and the same zero crossing in the received signal, subtracting a small time delay in the transducers, as determined in calibrations using water as the reference liquid.

To determine the accuracy of the velocimeter under applied hydrostatic pressure and temperature change, the measured data of $(\partial c/\partial P)_T$ and $(\partial c/\partial t)_P$ in water and glycerol were compared with literature values [Coppens, 1964]. The agreement was within $\pm$ 2%.

CHAPTER 4

RESULTS AND DISCUSSION

4.1. Finite Amplitude Method

The nonlinearity parameter B/A was measured for 15 different materials, including several organic liquids, aqueous protein solutions, and homogenized and whole tissues, at 3 MHz and 30°C, which can be divided into three categories. The first includes those liquids for which the physical and acoustical properties, and most importantly, the B/A value, have been previously reported. The second category is biological fluids, including solutions of proteins, solutions of linear polysacharids, blood, and homogenized liver, all homogeneous and isotropic on a macroscopic scale. The third category comprises tissues:beef liver, beef heart muscle, beef brain, pig muscle, and subcutaneous pig fat.

4.1.1. Measurement of Standard Liquids

Water is one of the most important biological constituents, and is also probably one of the most extensively studied liquids. Figure 4.1 shows an actual measurement of second harmonic data in water, plotted as $\ln p_2(z)/p_o^2 z$ vs. z. Measurements start at z = 0.8 cm since multiple reflections interfere with measurements at shorter distances. A theoretical line, based on Eq. (2.47) and using the literature value of the absorption coefficient, speed of sound, and density, but with a B/A value adjusted to fit the extrapolated intercept of the experimental data is also plotted in Fig. 4.1 for comparison. The theoretical curve between z = o to

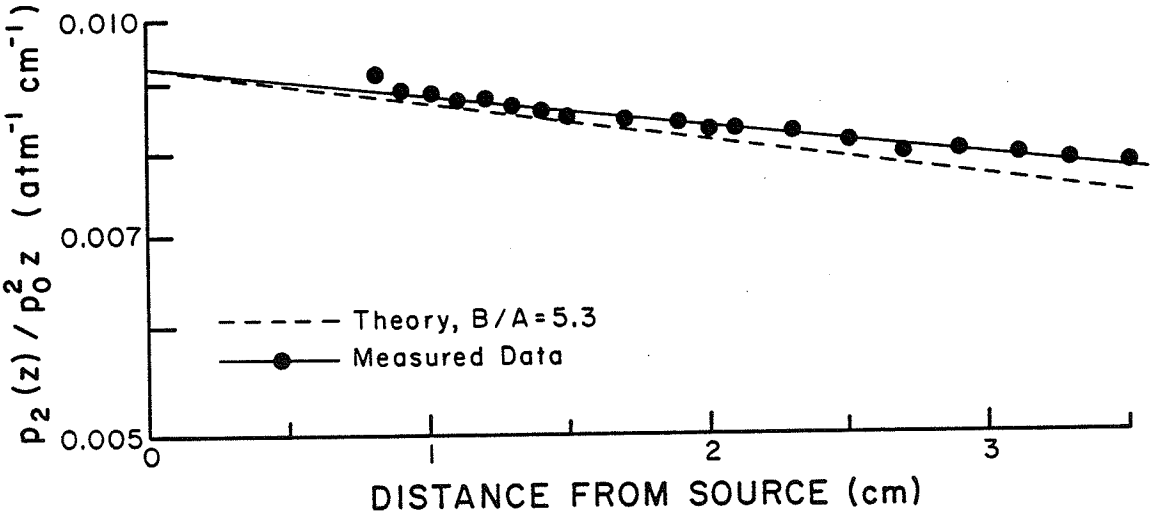

Figure 4.1. Comparison of measured second harmonic data with theory in degassed water.

z = 1 cm is also an extrapolation since the theory is no longer valid in this region. This portion of the curve is shown as a lightly dotted line. The published reports of the B/A of water, determined by the thermodynamic technique, give a value of 5.2 [Beyer, 1960]. The data of Fig. 4.1 yields a B/A value of 5.3. A least square linear regression fit to the experimental data results in a curve with a slightly less negative slope compared to the theoretical curve. If the experimental data were fitted to a straight line with the same slope as the theoretical line, the resulting B/A value would be 2% greater. Since the effect of absorption in water was negligibly small when compared to the effect of diffraction, the error can be the result of either an inadequacy in the diffraction theory or a departure of the sound source from a perfect piston operation. Since the accuracy of the theory has been verified experimentally [Ingenito, 1971; Cobb, 1982], it appears that the error was most likely caused by the sound source which produced diffraction effects slightly less than those of a perfect piston source.

The value of B/A for water measured with the finite amplitude method varied considerably during the two years of measurements in this project. The average of seven measurements in two years produced an average B/A of 5.5 for water, with a standard deviation of $\pm$ 0.3. However, more recent measurements gave a B/A value of 5.3 consistently. To investigate the possible effect of the quality of water on the B/A value, tap water was used in a B/A measurement and found to be 2% less than that of degassed water. However, the 2% difference was well within the margin of error of the finite amplitude measurement system. The difference between

the earlier measurements and the more recent ones was attributed to calibration of transducers which had an uncertainty of ± 10%. There were three separate calibrations throughout the two years of measurement. Each of the calibrations resulted in a slightly different calibration number due to unavoidable variations in experimental conditions, uncertainties in instrument readings, and perhaps to a lesser extent, change of transducer properties with time.

The agreement between the finite amplitude method and literature values of B/A was good for the other liquids tested. Figures 4.2 and 4.3 show the second harmonic data for a 50% methanol-water mixture and ethylene glycol, respectively, plotted as $\ln p_2(z)/p_o^2 z$ vs. z. A theoretical curve based on the literature value of B/A is included in each graph for comparison (see Table 4.1 for the parameters used).

The absorption coefficient for the methanol-water mixture was too low to be measured accuarately by the method used in this investigation, so the value was taken to be that of water. The actual absorption was probably slightly higher. The B/A value determined was 8.5, approximately 2% greater than the literature value. For ethylene glycol, the absorption coefficient, density, and velocity were measured according to the method described previously in Sections 3.1.3, 3.1.4, and 3.1.5. The measured B/A value was 3% greater than the literature value. However, there is again a slight discrepancy between the slopes of the experimental and theoretical curves, similar to that observed for water.

The absorption coefficient for glycerol was comparable to that of tissue at the fundamental frequency, but much higher at

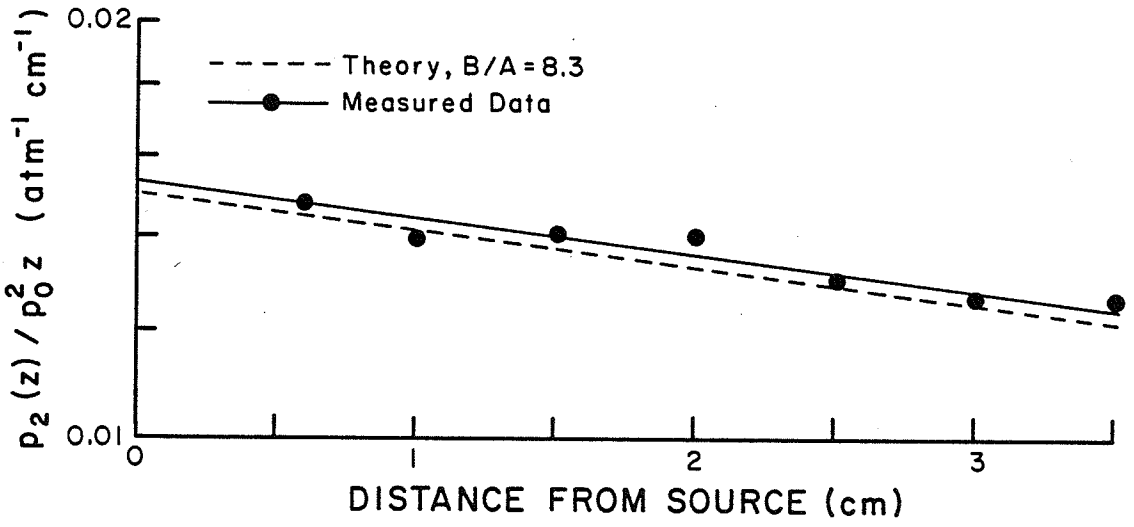

Figure 4.2. Comparison of measured second harmonic data with theory in 50% methanol-water mixture.

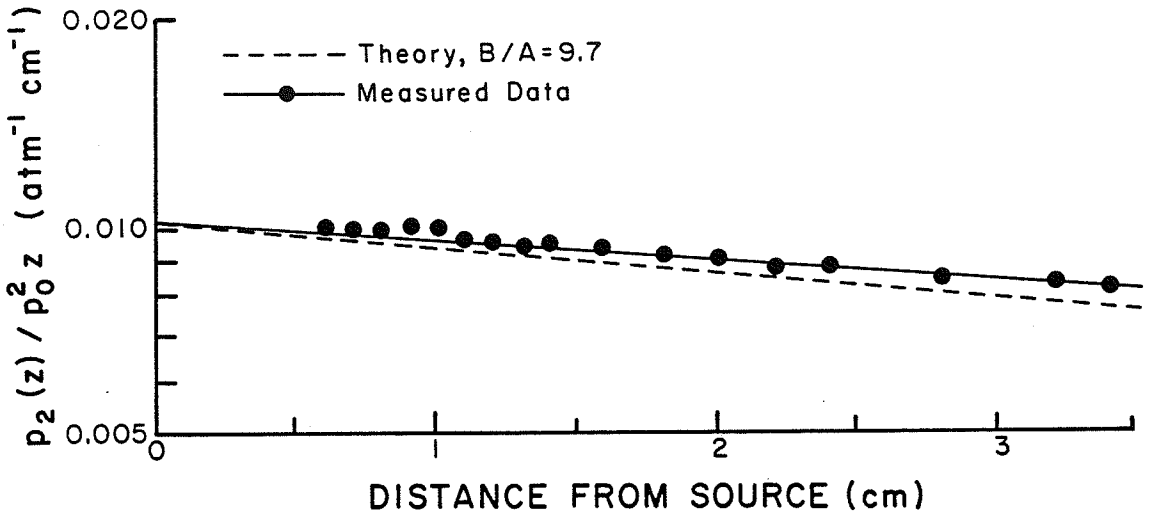

Figure 4.3. Comparison of measured second harmonic data with theory in ethylene glycol.

Table 4.1. Values of B/A in standard liquids measured by finite amplitude method.

Material	Velocity (cm/sec)	Density (gm/cc)	α_1 (Np/cm)	α_2 (Np/cm)	B/A	Literature B/A[1]
water	1.509×10^5	1.00	0.002	0.008	5.5±0.3	5.2
50% methanol water mixture	1.483×10^5	0.915	0.002	0.008	8.5	8.3
ethylene glycol	1.644×10^5	1.11	0.009	0.031	9.93	9.7
glycerol	1.87×10^5	1.26	-----	-----	9.4	9.0

[1]From Beyer, 1974

the second harmonic, due to the frequency squared dependence. The B/A value for glycerol, measured by the finite amplitude method, was found to be 9.4, 4% greater than the literature value of 9.0.

The measurement of B/A values of the standard liquids is consistently 2 to 4% greater than the B/A values reported in the lieterature, indicating the possibility of a systematic error in the transducer calibrations. However, the discrepancies are within the error of ± 10% for the calibration.

4.1.2. Measurements of Biological Fluids

The B/A value for aqueous bovine serum albumin (BSA) solutions of 8% to 40% concentration are shown in Fig. 4.4. The B/A value for water is included as the 0% concentration value. The error bar on the water datum point indicates the standard deviation of the seven measurements. Each of the other points represents the result of one measurement. The méasured velocity and density of the solutions, as a function of concentration, are shown in Figs. 4.5 and 4.6, respectively. The solutions were very viscous and exhibited a strong tendency to stick to the container walls or to trap small air bubbles, at the higher concentrations employed, making accurate determination of density difficult. This is the likely explanation for increased scatter of the density data at high concentrations.

The measurements for BSA were repeatd approximately two years after the initial measurements. For both sets of measurements, the values of B/A were found to increase approximately linearly with concentration. However, the values of B/A in the more recent measurements were below those of the earlier measurements. The

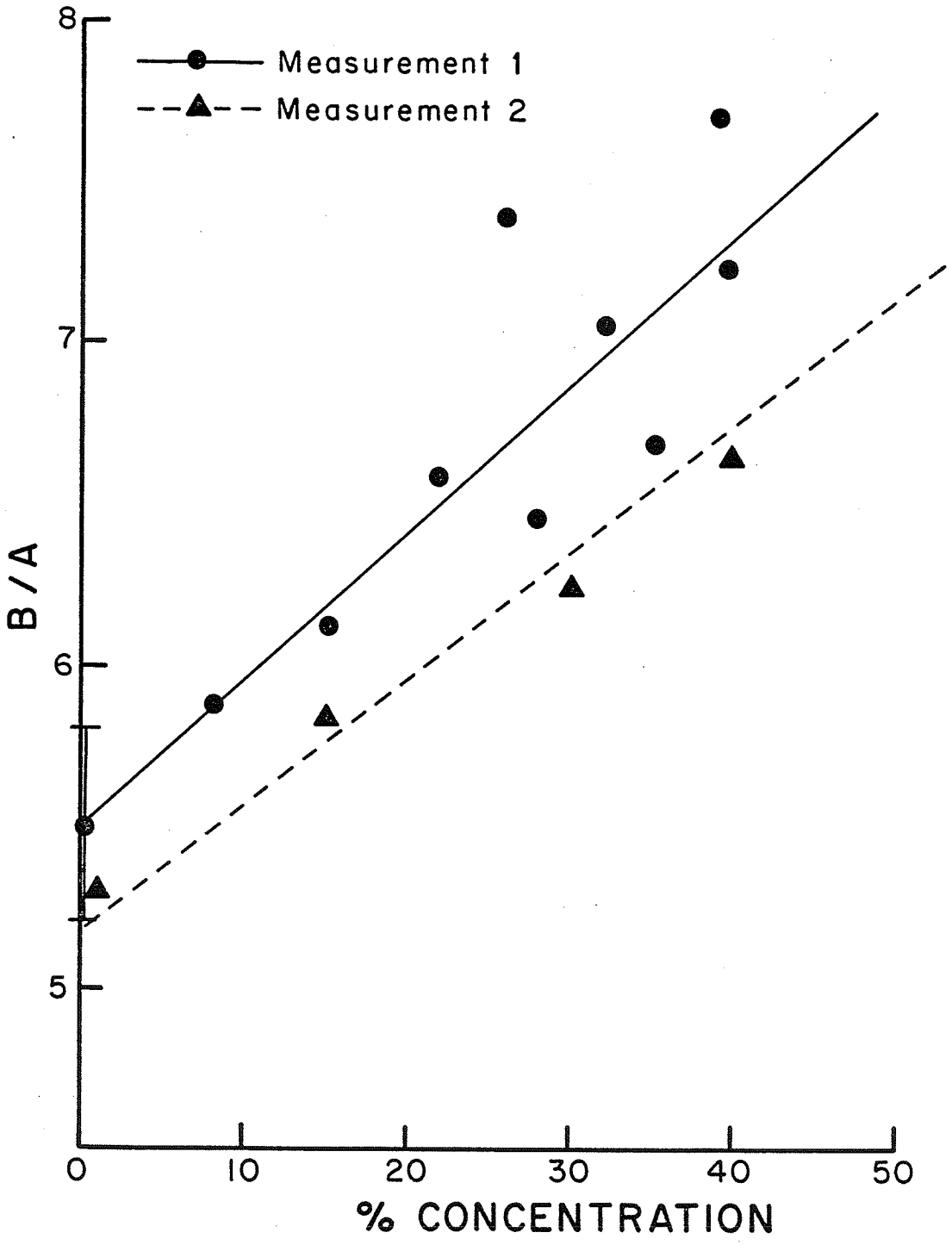

Figure 4.4. B/A as a function of concentration measured by the finite amplitude method in BSA solutions.

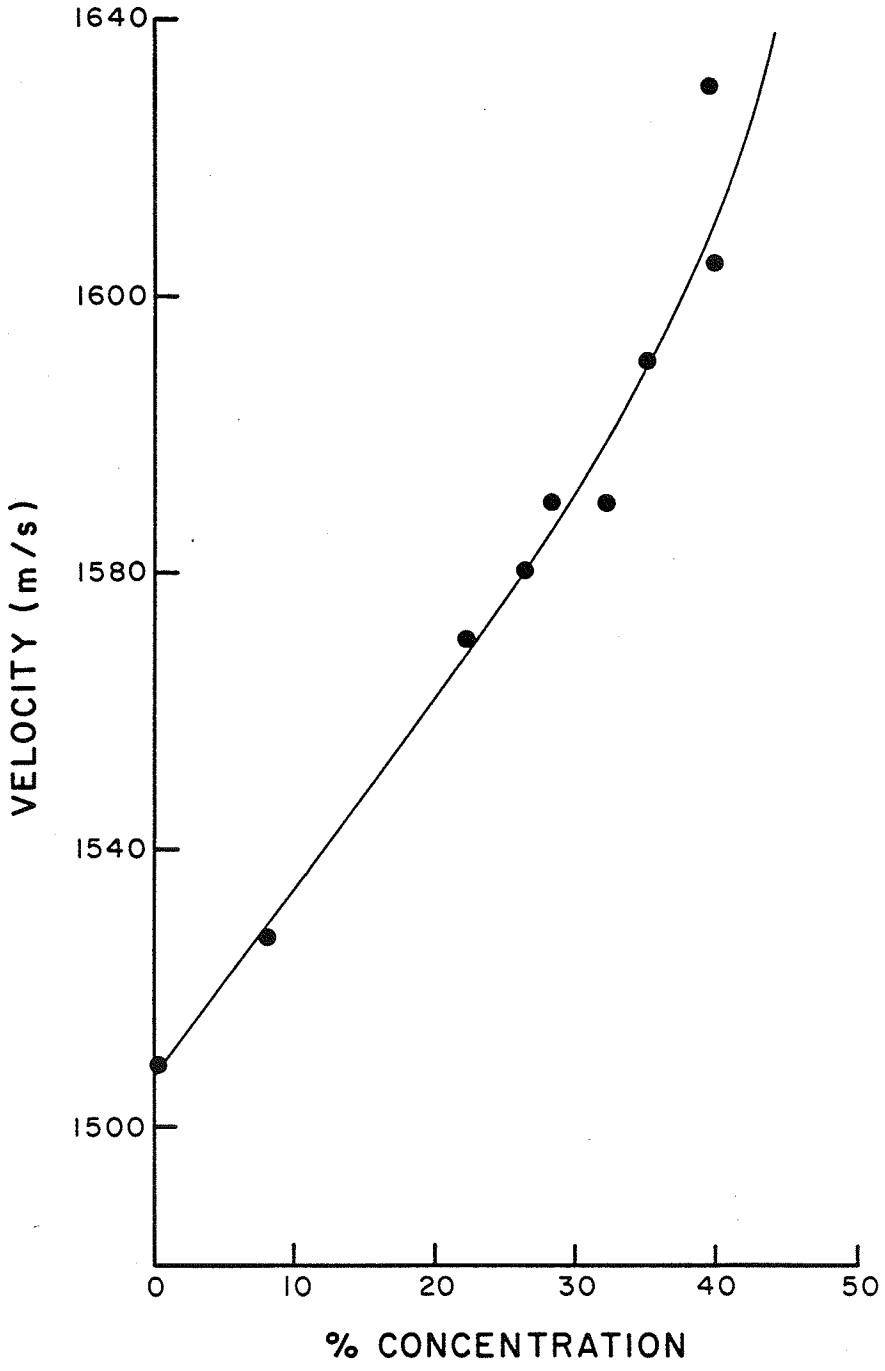

Figure 4.5. Velocity of BSA solutions as a function of concentration.

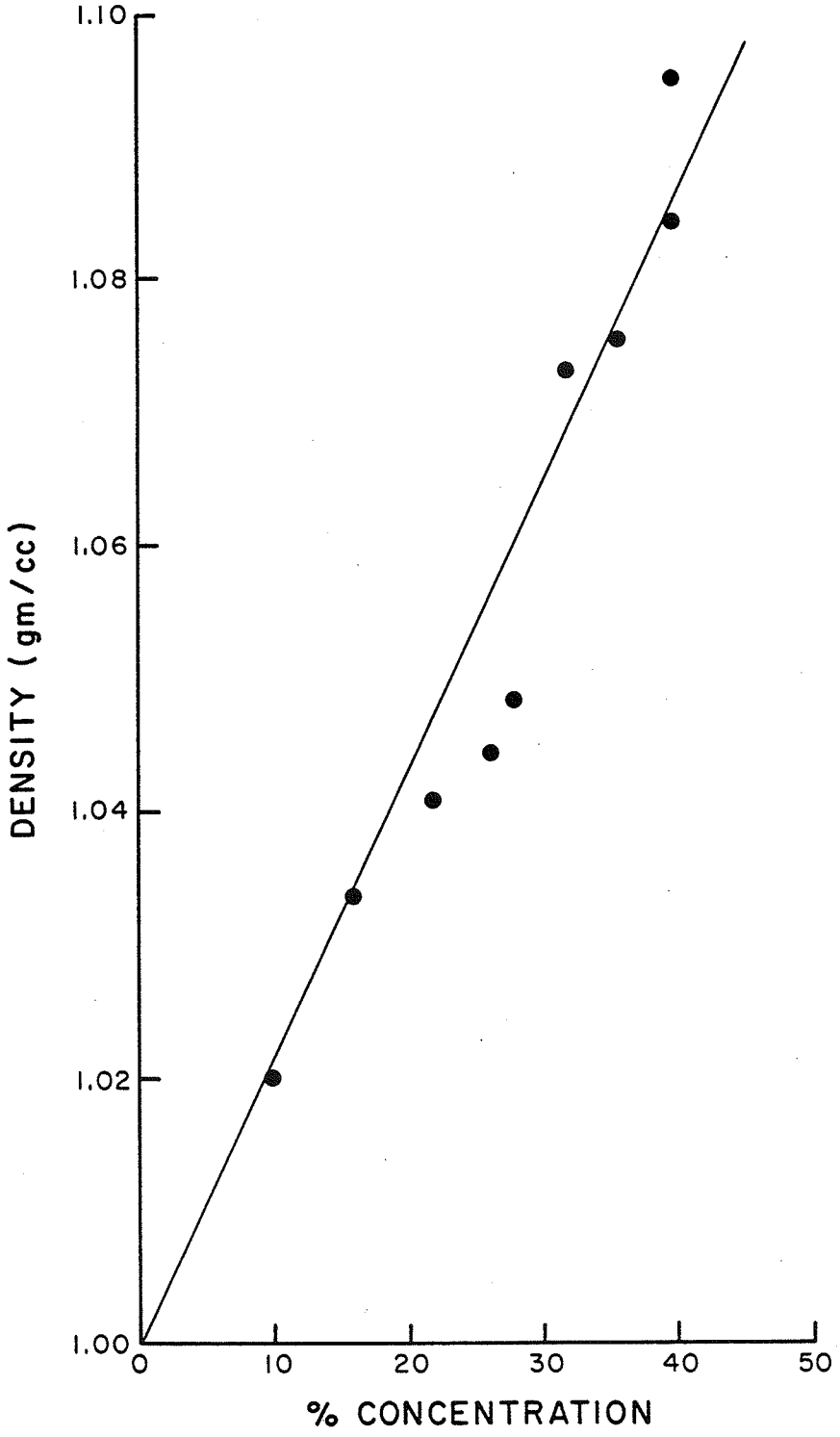

Figure 4.6. Density as a function of concentration in BSA solutions.

two sets of measurements had similar slopes, but the earlier values were greater by approximately 10% and the data points were more scattered. The discrepancy is probably due to a combination of two factors. First, there may have been differences in the calibrations among the two sets of measurements, as is exemplified in the different values of B/A obtained for water. Second, a drift was observed in the output of the internal calibrator of the spectrum analyzer with room temperature, by as much as $\pm$ 10% on an especially hot day during spring and summer when the air conditioning system of the building failed. (The observed drift with temperature was within the manufacturer's specification and was not due to malfunctioning of the unit.) Since some of the data of BSA was obtained during that time of the year, the drift could have affected the measurements. The problem had been corrected later by calibrating the spectrum analyzer against a high precision RF voltmeter and better control of the room temperature. The decreased amount of scatter in data points, as is evident in the more recent measurements in BSA, indicates that the problem has been corrected effectively.

Another source of variation may be associated with measurements of biological materials themselves. To minimize the effects of sample variation, a direct comparison between the finite amplitude method and the thermodynamic method was made on the same sample of BSA solution and is discussed in a later section. (The comparison indicated that the more recent finite amplitude measurements agreed very well with the thermodynamic measurements).

Measurements of B/A were made on a second protein solution, hemoglobin, and are shown in Fig. 4.7. The associated velocity and density data are shown in Figs. 4.8 and 4.9, respectively. Again, a greater variation in measured density is exhibited at the greater concentrations. For both BSA and hemoglobin solutions, the velocity was found to increase more than linearly with concentration at the higher concentrations, a result in agreement with that previously reported [Goss, 1974]. The B/A values for both BSA and hemoglobin solutions were found to increase approximately linearly with solution concentration.

The B/A value for Dextran T2000 (M_W = 1.56 x 10^5 Da) is shown in Fig. 4.10 to increase approximately linearly with concentration, though the rate of increase is less than that for the BSA or homoglobin solutions. Table 4.2 lists the B/A values for solutions of Dextran T2000, T150 and dextrose. Their B/A values are nearly the same when normalized to the same concentration by assuming that dextrose and dextran solutions have a linear relationship between B/A and concentration. Thus the B/A value in dextran solutions appears to be relatively insensitive to molecular weight over four orders of magnitude of molecular weight.

Whole blood is more structured, by virtue of its cellular constituents, than a protein solution but can be considered homogeneous and isotropic. Table 4.3 shows the results of two samples of porcine whole blood measurement, together with velocity and density data. The dry weight content of the whole blood was determined to be 22.3%. The B/A value of whole blood is seen to

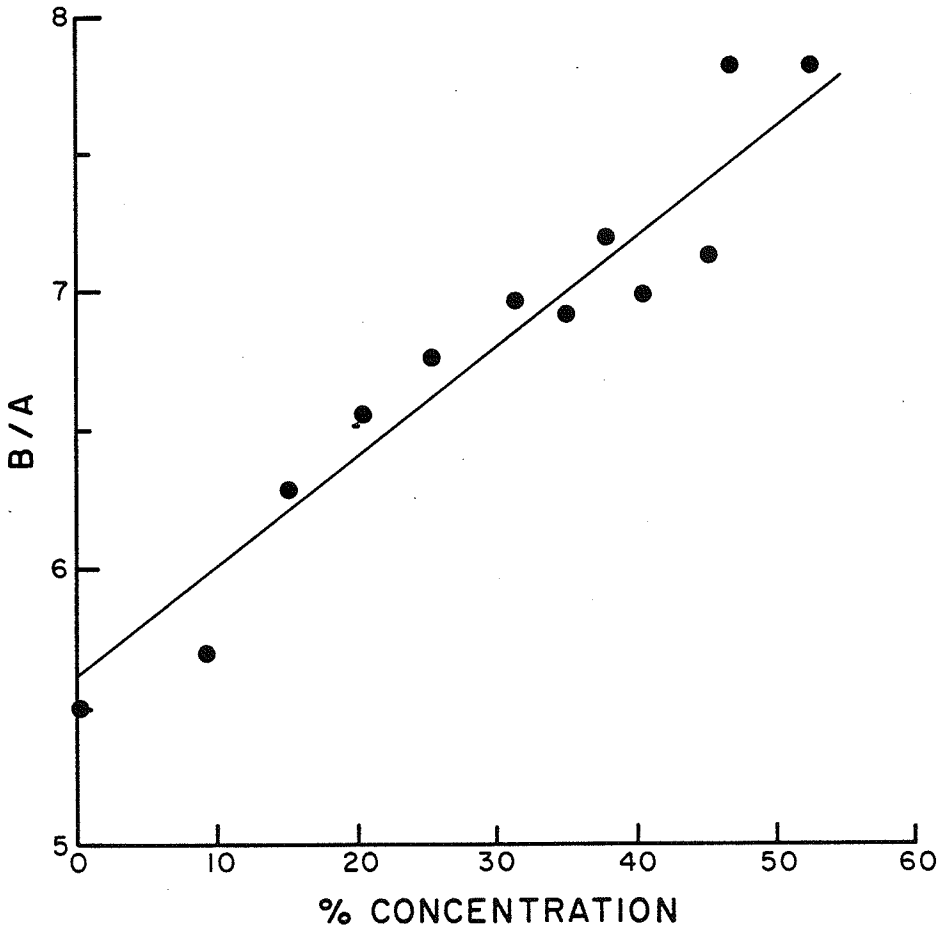

Figure 4.7. B/A as a function of concentration in hemoglobin solutions.

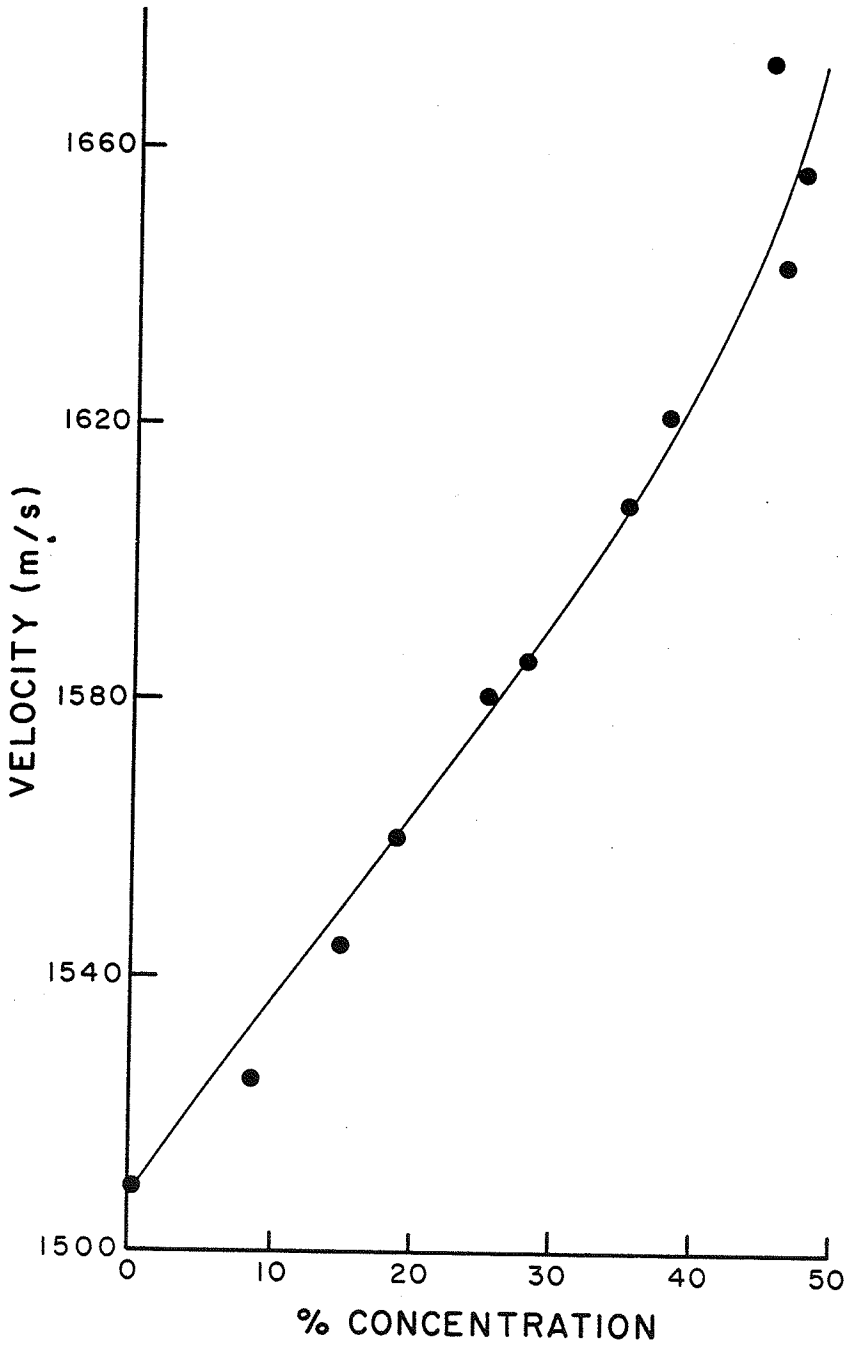

Figure 4.8. Velocity as a function of concentration in hemoglobin solutions.

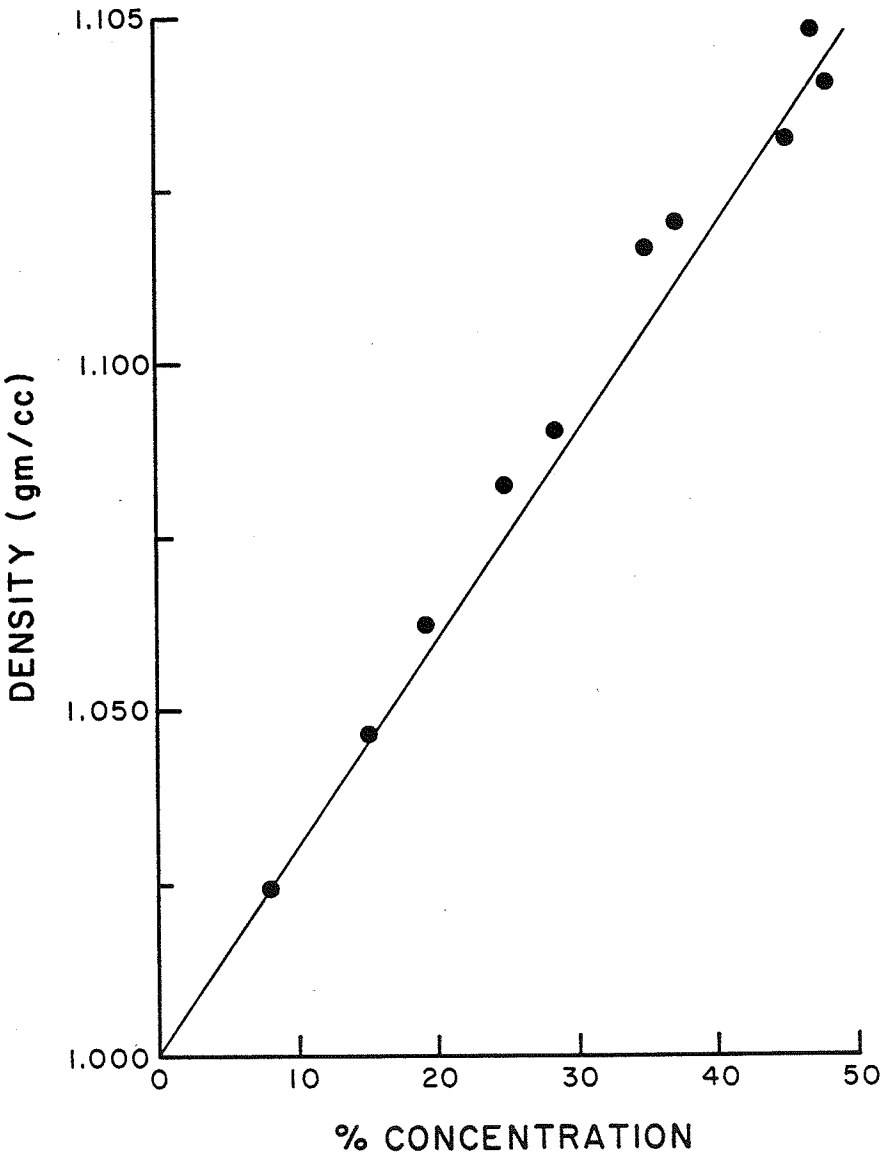

Figure 4.9. Density as a function of concentration in hemoglobin solutions.

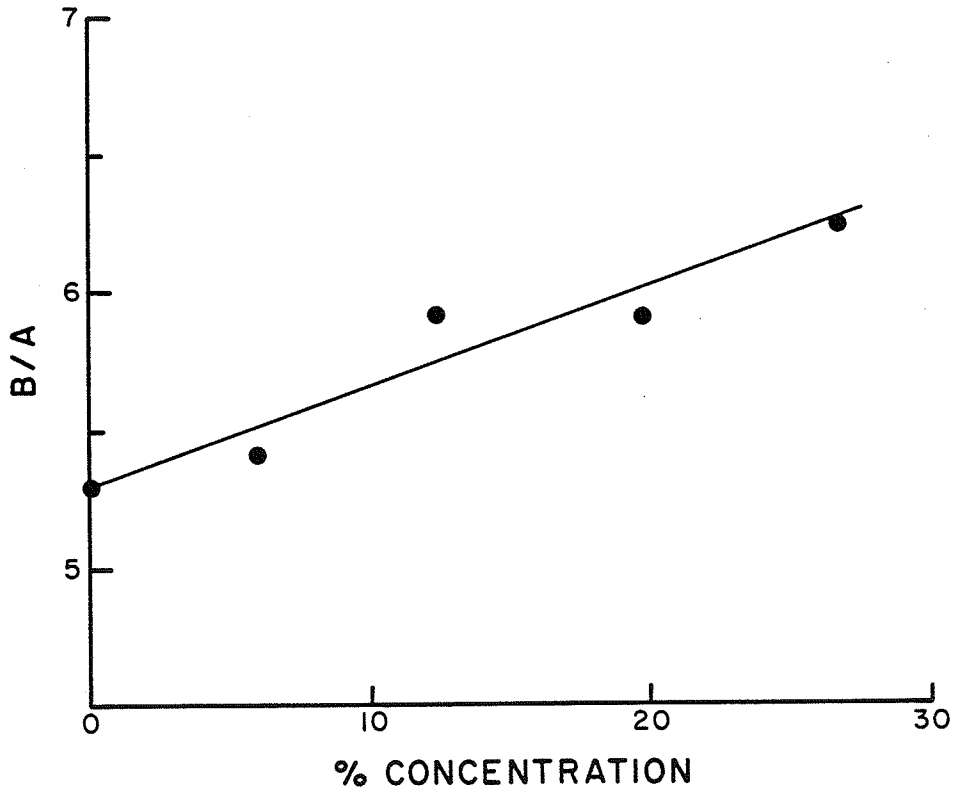

Figure 4.10. B/A value of Dextran T2000 as a function of concentration.

Table 4.2. Value of B/A in dextran solutions of different solute molecular weights, finite amplitude method.

Material	Mw (Daltons)	Concentration (gm/100 cc)	Velocity (cm/sec)	Density (gm/cc)	B/A
Dextrose	180	28.9	1.61×10^5	1.10	6.04
Dextran T150	1.5×10^5	24	1.57×10^5	1.08	5.94
Dextran T2000	2×10^6	26.4	1.56×10^5	1.08	6.2

Table 4.3. Value of B/A in liquid tissues, finite amplitude method.

Material	Velocity	Density	B/A
Porcine Blood	1.59×10^5	1.02	6.4, 6.22
Homogenized Bovine Liver	1.59×10^5	1.05	7.2,6.7

be similar to or slightly greater than that of a hemoglobin solution of the same dry weight content.

Table 4.3 also shows the results of B/A determination of two samples of homogenized beef liver having a dry weight content of approximately 27%. The B/A value is seen to be greater than that of whole blood and a protein solution of similar dry weight content.

4.1.3. Measurements of Soft Tissues

Six samples of beef liver, two samples of beef heart muscle, one sample of beef brain, two samples of pig muscle, and two samples of pig subcutaneous fat were measured. Three of the six samples of liver came from the same animal. The results of B/A measurements of these tissues, together with velocity and density data, are listed in Table 4.4. For some of the tissue samples, the absorption coefficients at the fundamental and second harmonic frequencies were measured. When available, the absorption coefficients are also listed in the table. When attenuation values are available, theoretical calculations of the second harmonic signal level are made using Eq. (2.47), using the B/A value obtained with the finite amplitude technique.

The theoretical predictions, together with the measured data, are plotted as $p_2(z)/p_o{}^2 z$ vs. z, in Figs. 4.11 and 4.12, for beef brain and pig fat, respectively. The agreement is seen to be excellent for beef brain. However, a discrepancy in slope was observed for pig fat, though within the error margin in the determination of the absorption values.

The beef liver had an average B/A value of aproximately 7.7,

Table 4.4. Values of B/A in Soft Tissues.

MATERIAL	VELOCITY (cm/sec)	DENSITY (gm/cc)	α_1 (Np/cm)	α_2 (Np/cm)	B/A
Beef Liver*	1.588×10^5	1.05			8.0
Beef Liver*	1.599×10^5	1.05			7.5
Beef Liver	1.596×10^5	1.05			7.5
Beef Liver+	1.610×10^5	1.05			8.9
Beef Liver+	1.632×10^5	1.05			6.2
Beef Liver+	1.620×10^5	1.05			7.9
Beef Brain	1.548×10^5	1.03	0.213	0.483	7.6
Beef Heart	1.566×10^5	1.05			6.8
Beef Heart	1.570×10^5	1.05			7.4
Pig Muscle	1.593×10^5	1.07			7.5
Pig Muscle	1.607×10^5	1.07			8.1
Pig Fatty Tissue	1.439×10^5	0.98	0.209	0.662	11.0
Pig Fatty Tissue	1.455×10^5	0.93	0.236	0.718	11.3

* Measured at $23^{\circ}C$.

+ Samples obtained from the same animal.

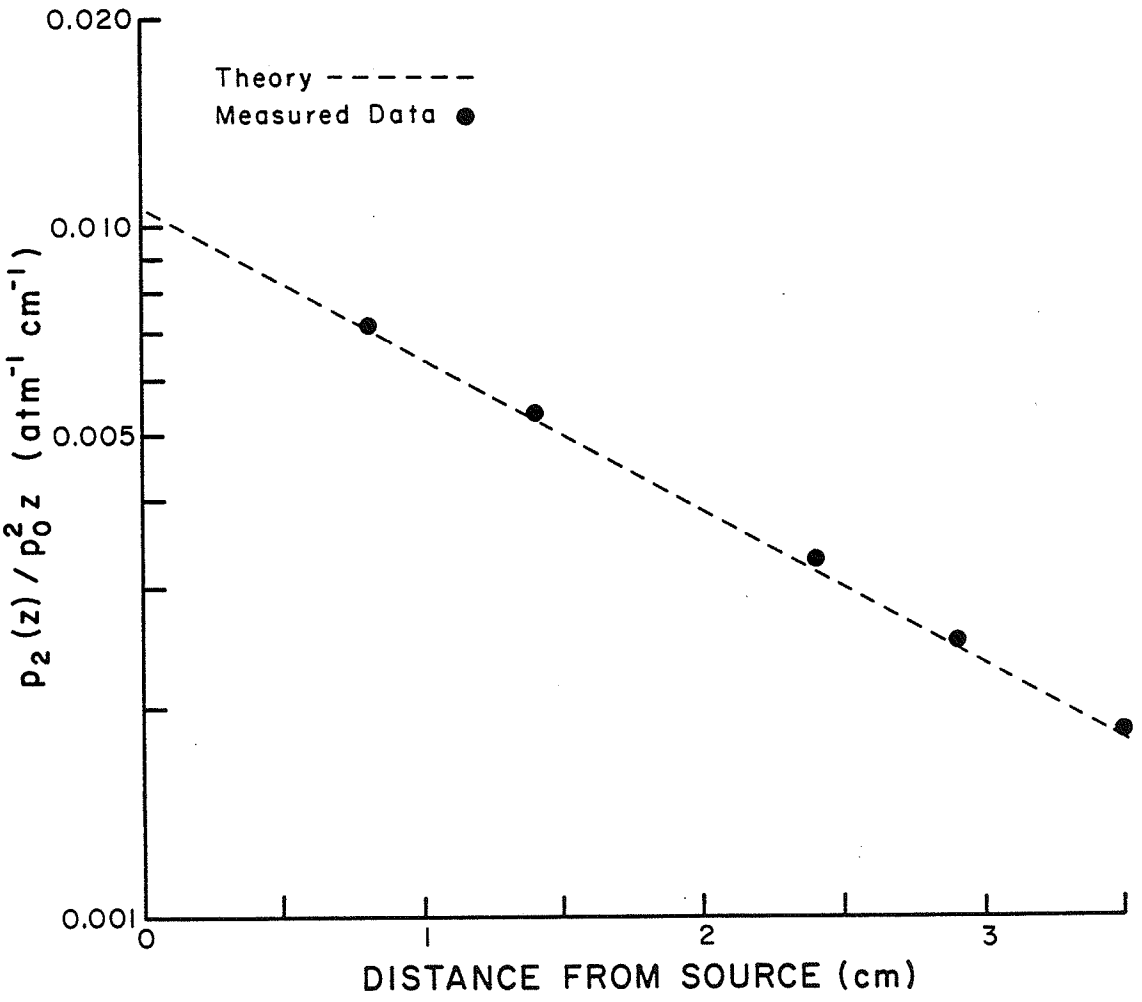

Figure 4.11. Comparison of measured second harmonic data with theory in beef heart muscle.
α_1 = 0.213 Np/cm, α_2 = 0.483 Np/cm,
ρ = 1.03 gm/cc, c = 1548 m/s.

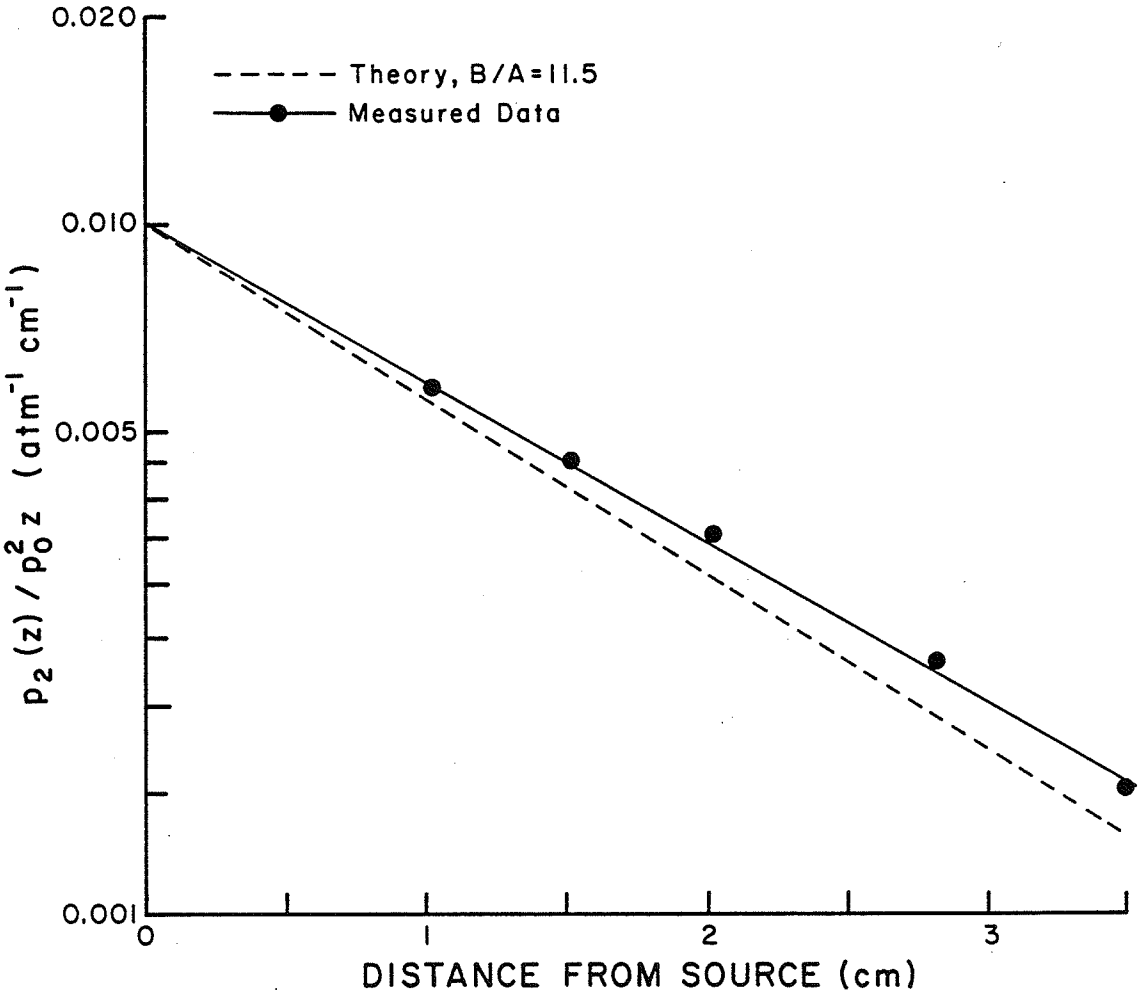

Figure 4.12. Comparison of measured second harmonic data with theory in pig fatty tissue.

with a standard deviation of 0.9. It is not clear at this time whether this standard deviation is a result of the variation in individual samples or uncertanties in the experimental technique. However, of the six samples of liver, the two samples that deviated the most from the average B/A value and from each other came from the same animal. Thus, if the variation is due to differences in samples, the B/A actually varies within the liver. Alternatively, if it is assumed that the B/A value is approximately the same in different parts of a liver, the variation would be attributed to experimental technique.

Beef liver, beef heart, beef brain, and pig muscle all have B/A values between 6.8 and 8.1. However, pig fat has a much greater B/A value, viz., around 11. The greater B/A value possibly reflects the high fat content in fatty tissues, which may reach 75% of the total weight [Wells, 1977].

4.2. Error Analysis for the Finite Amplitude Method

The errors in the finite amplitude measurements of B/A arise mostly in the calibration procedure, which involves the absolute calibration of a source transducer, a similar calibration of another transducer which serves as a secondary standard, and the calibration of a receiver using the secondary standard as a reference. The estimated errors of this procedure are itemized as follows:

1. Determination of Average Source Pressure:
   - $\pm$ 2% random error in setting the source driving voltage
   - $\pm$ 3% random error in the radiation force balance due to mechanical and thermal disturbances

± 2% systematic error due to the change of buoyancy in the acoustic target from ultrasonic heating

± 2% systematic error due to the uncertainty in the effective area of the transducer

2. Calibration of the Receiver:

± 3.6% RMS random error and ± 4% systematic error in the absolute calibration of the secondary standard, as described in the previous paragraph

± 2% random error in measuring the output voltage of the receiver

± 1% error in the alignment of the source and receiver.

In the actual determination of the nonlinearity parameter, there are also errors in alignment, in reading the second harmonic amplitude, in measuring the density and the sound velocity, and in the deviation of the source transducer from a perfect piston source. These errors are itemized below for measurements of liquid samples and in tissues. The errors are greater for tissue than for liquids due to their inhomogeneous, semi-solid, and deformable nature. The estimated errors are, therefore, listed separately for the two different types of materials.

3. Measurements of Liquid Samples:

± 1/2% random error in density

± 1/2% random error in sound velocity

± 2% random error in measuring the amplitude of the second harmonic component

± 2% systematic error due to deviation of the transducer from an ideal piston source.

4. Measurements in Tissues:

± 1% random error in the density

± 1% random error in the sound velocity

± 2% random error in measuring the amplitude of the second harmonic component

± 2% random error in measuring the thickness of the samples

± 2% systematic error due to deviation of the transducer from an ideal piston source.

The nonlinearity parameter is given by Eq. (3.1)

$$B/A + 2 = \frac{2\rho_o c_o^3}{\pi f} \left. \frac{p_2(z)}{p_o^2} \right|_{z\to o} \left. F^{-1}(z) \right|_{z\to o} \qquad (4.1)$$

Assuming that all the random errors are independent of each other, the root mean square (RMS) error in (B/A + 2) is computed to be ± 6.6% for liquid samples, and ± 7.1% for tissues. The total systematic error is ± 8% for liquid or tissue samples.

4.3. Results of Thermodynamic Measurements

Results of the thermodynamic measurements and the parameters used for computations are summarized in Table 4.5, all at 30°C. A major purpose of these measurements is to confirm the results of the finite amplitude measurements of B/A and to use the superior accuracy of the thermodynamic method to resolve small differences in the values of B/A of dextran solutions of different solute molecular weights. Measurements were made of degassed and distilled water, BSA solutions, dextrose and dextran solutions, whole and homogenized beef liver, and pig fat.

Table 4.5. Results of thermodynamic measurements.

MATERIAL	ρ gm/cc	c m/s	β'^{-1} °C	C_p J/(gm-°C)	$(\partial c/\partial p)_T$ m/(s-psi)	$(\partial c/\partial T)_p$	B/A'	B/A"	B/A
Water	0.996	1509	3.67×10^{-4}	4.18	0.0119	1.748	5.17	0.14	5.31
BSA (38.8%)	1.094	1615	3.67×10^{-4}	4.18	0.0130	1.115	6.58	0.10	6.68
Dextrose (25%)	1.092	1602	3.67×10^{-4}	4.18	0.0115	1.345	5.84	0.12	5.96
Dextran T150 (24%)	1.088	1567	3.67×10^{-4}	4.18	0.0119	1.676	5.91	0.14	6.05
Dextran T2000 (26%)	1.090	1574	3.67×10^{-4}	4.18	0.0120	1.550	5.90	0.13	6.03
Beef Liver	1.05	1588	3.67×10^{-4}	4.18	0.0147	1.15	7.13	0.10	7.23
Pig Fat	0.93	1440	3.67×10^{-4}	4.18	0.0285	-2.98	11.08	-0.23	10.9

4.3.1. Comparison of Thermodynamic and Finite Amplitude Methods

Results of the thermodynamic and finite amplitude measurements are listed in Table 4.6. The finite amplitude data are averages of cumulated results of measurements. However, when only one or two samples are measured, the results are listed individually. Homogenized and whole beef liver data are averages of three and five samples, respectively. Data in Table 4.6 are cumulated over a two year period and, consequently, may reflect sample differences and slight variations in the technique of sample preparation. Despite such possible effects, the agreement in liquid samples is excellent, viz., $\pm$ 4%. The comparison of the BSA solutions is less clear. The finite amplitude measurements as a function of concentration yield two sets of B/A values, with the more recent lower than the earlier ones. Figure 4.13 shows the thermodynamic measurements and the two sets of finite amplitude measurements. It is to be noted that the more recent finite amplitude measurements reported herein agree well with those of the thermodynamic method. As discussed previously, variations in the transducer calibration and a thermal drifting of the spectrum analzyer calibration are believed to be the difference between the two finite amplitude measurements. However, the possibility of differences between samples cannot be completely ruled out.

In view of the good agreement between the thermodynamic method and the more recent finite amplitude measurements, the present finite amplitude system and its calibration is judged to be satisfactory for measurements of liquid samples.

Table 4.6. Comparison of the thermodynamic measure with cumulated results of finite amplitude measurements.

Material	(B/A) Thermodyanmic	(B/A) Finite Amplitude
Water	5.31	5.5 ± 0.5*
Dextrose (25%)	5.96	----
Dextrose (28.9%)	---	6.04
Dextran T150 (24%)	6.05	5.94
Dextran T2000 (26.4%)	6.03	6.2
Beef Liver	7.23, 7.0	7.7 ± 0.9**
Beef Liver Homogenate	7.0, 6.53	6.8 ± 0.4***
Pig Fat	10.9	11.0 11.3

* Average of seven samples.

** Average of five samples.

*** Average of three samples.

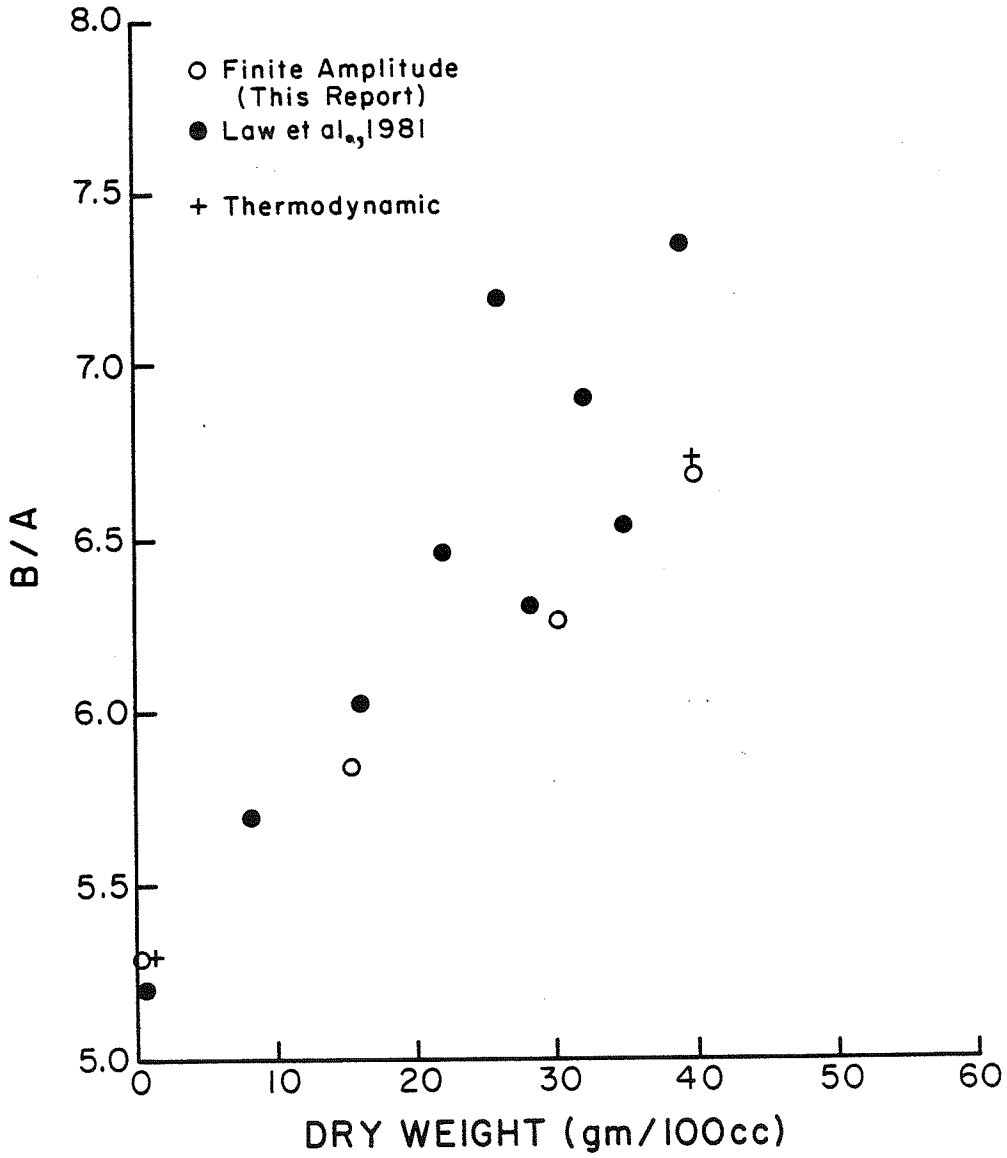

Figure 4.13. Composite plot of the value of B/A in BSA solutions measured by various researchers using the finite amplitude and thermodynamic methods.

The agreement in tissue samples appears to be affected by the nature of the sample. The averaged values of B/A measured by the two methods differs by 9% for liver samples, 2% for pig fat and 1% for liver homogenate. The discrepancies appear to increase with the degree of tissue inhomogeniety. The liver homogenate is the most homogeneous among the three, followed by pig fat, which contains few blood vessels, and whole liver which contains blood and biliary vessels of various sizes and orientations. The standard deviation of the values of B/A of whole liver measured by the finite amplitude method is $\pm$ 12%, perhaps an indication of the significance of tissue structure and inhomogeneity.

In order to determine the importance of sample differences, direct comparison was made using both the thermodynamic method and the finite amplitude method with the same sample of a BSA solution and of samples of beef liver obtained from the same animal. The results are shown in Table 4.7. The two methods agree well with each other for liquid samples, but a 7% discrepancy is observed with one of the beef liver samples. Both tissue inhomogeneity and the presence of air bubbles from autolysis may have contributed to the discrepancy. Due to the substantial size of the tissue sample, an attempt to degas the sample using a gentle vacuum was not successful. Air bubbles collected inside the tissue samples to form cavities, instead of rising to the surface of the samples.

The thermodynamic measurements of dextran solutions and of beef liver homogenate have confirmed the usefulness of the finite amplitude method. The B/A value of dextrose and dextran solutions is relatively insensitive to the molecular weight of the solutes, over the range of molecular weights 10^1 to 10^6, although a very

Table 4.7 Direct comparison of the two methods using the same sample or samples from the same animal.

Material	(B/A) Thermodynamic	(B/A) Finite Amplitude
Water	5.31	5.3
BSA (39%)	6.68	6.64
Beef Liver #1	7.0	6.5
Beef Liver #2	6.88	7.15

slight increase with molecular weight may be present, as shown in a plot of B/A versus molecular weight of the solute, Fig. 4.14.

A decrease in the value of B/A for homogenized liver as compared to whole liver is also confirmed by the thermodynamic method. It seems possible that the process of homogenization destroys some nonlinearity producing structures in the liver.

4.4. Errors in the Thermodynamic Method

The value of B/A is computed from Eq. (2.12)

$$B/A = B/A' + B/A'' = \rho_o c_o \left(\frac{\partial c}{\partial p}\right)_T + \frac{c_o \beta' T}{c_p} \left(\frac{\partial c}{\partial T}\right)_p \qquad (4.2)$$

The second term of the equation requires the knowledge of the specific heat (c_p) and the thermal coefficient of expansion (β') of the materials measured, which are not available in the literature for the materials of interest in the present study. However, the value of c_p for rabbit liver has been reported [Bowman et al., 1975] to be about 20% less than that of water, and the value of β' for a 30% BSA solution has been measured in this labroatory to be 13% greater than water, by using a calibrated capillary to determine the volume change of a sample inside a volumetric flask as a function of temperature (with correction for the thermal expansion of the flask). Based on these observations, it is assumed that the values of β' and c_p for the biological materials measured are not significantly different from water for the purpose of computation of B/A since β' and c_p are involved only in the B/A" term which contributes only about 3% to the B/A values. The substitution should introduce approximately a 1%

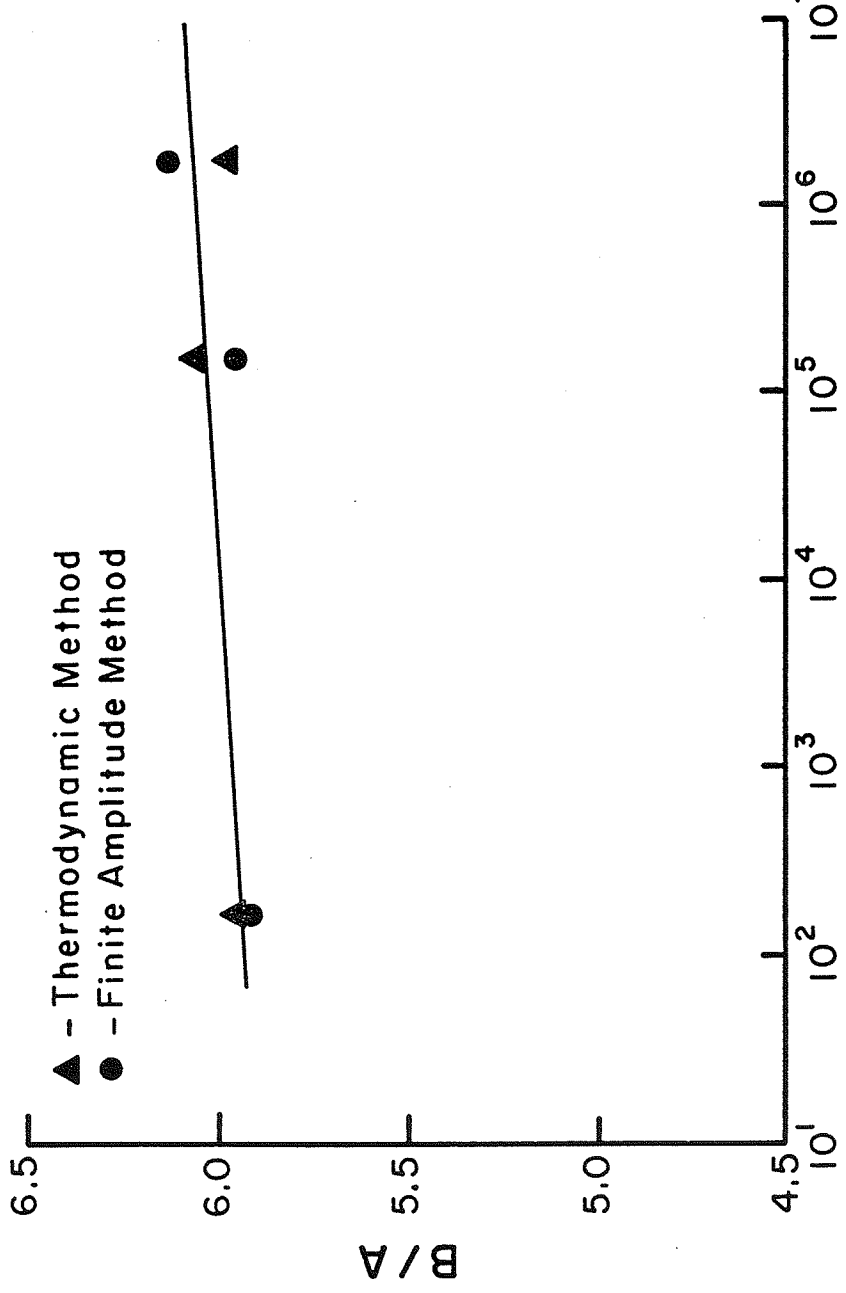

Figure 4.14. B/A as a function of solute molecular weight in dextran solutions.

error to the computed B/A value. The errors in the other parameters in the B/A" terms are much smaller than those of β' and c_p and are therefore negligible. The error in determining the values of B/A" is set at $\pm$ 2% to allow for variations of β' and c_p more drastic than that observed for rabbit liver and BSA.

The more significant contribution of errors comes from the first term, viz., in the measurement of sound velocity, density, and $(\partial c/\partial p)_T$. The error in the velocity at a fixed temperature-pressure point is determined by (1) the errors in measuring the time-of-flight, (2) the error in determining the length of the sample chamber, and (3) the effect of random temperature fluctuation of the temperature controlled bath on the sound velocity. The error in $(\partial c/\partial p)_T$ can be considered as the combination of the errors in two velocity measurements, divided by the difference in hydrostatic pressure between the two measurements. For the purpose of making this computation, the uncertainty in temperature and pressure should be expressed as equivalent speed errors in the analysis. The amount of errors and their analysis are itemized as follows:

1. Error in density:

   $\pm$ 1/2% for liquids

   $\pm$ 1% for tissues.

2. Errors in velocity measurements:

   For the solutions and tissues measured,

   $c_o \cong 1600$ m/s

   $(\partial c/\partial T)p \cong 1.5$ m/(s-^oC)

   $(\partial c/\partial p)_T \cong 0.012$ m/(s-psi).

a. The random error in the temperature, which is $\pm$ 0.02°C, can be expressed as an equivalent speed error of (1.5 x $\pm$ 0.02) = $\pm$ 0.03 m/s.

b. The random error in hydrostatic pressure, which is $\pm$ 5 psi, can be expressed as an equivalent speed error of (0.012 x $\pm$ 5) = $\pm$ 0.06 m/s.

c. For the time of-flight-measurement there is a $\pm$ 0.008% random error in aligning the time mark to a fixed reference point in the wave packet, and a $\pm$ 0.001% random error in the accuracy of the frequency counter. The RMS error in the time-of-flight is therefore $\pm$ 0.008%, or $\pm$ 0.13 m/s when expressed as an equivalent speed error.

d. There is a $\pm$ 0.03% systematic error in determining the length of the sample chamber. However, the error is cancelled out in the measurement of $(\partial c/\partial p)_T$ and is significant only in the measurement of the absolute velocity. One may consider the $\pm$ 0.03% error to be much smaller than the other errors and is negligible.

3. Computed indeterminacy in $(\partial c/\partial p)_T$:

The RMS error in the measurement of sound velocity is the combination of items a, b, and c, viz., $\pm(0.03^2 + 0.06^2 + 0.13^2)^{1/2} = \pm 0.16$ m/s. The RMS error in $(\partial c/\partial p)_T$ is the combination of errors in two velocity measurements, divided by the interval, viz., $\pm [(0.16)^2 + (0.16)^2]^{1/2}/2000 = \pm 0.0011$ m/(s-psi) = $\pm$ 0.9%.

The random error in determining the parameter B/A' is the combination of errors in density and $(\partial c/\partial p)$, viz., $(0.5^2 + 0.9^2)^{1/2} = \pm 1\%$ for liquids, and $(1^2 + 0.9^2)^{1/2} = \pm 1.4\%$ for tissues. Adding the $\pm$ 2% uncertainty in estimating the value of B/A", the error in B/A is $\pm$ 3% for liquids, and $\pm$ 3.4% for tissues.

There are other possible sources of error in the thermodynamic measurements of tissue. First, due to the semi-solid, deformable nature of the tissue, the length of the sample could not be measured accurately. The length of the sample was not precisely 3" long but was usually longer by about 0.04". The extra length was provided deliberately so that the sample could be compressed slightly by the two transducers at the two ends to provide an intimate surface contact between the sample and the transducer elements. It is difficult to estimate the error caused by this compression, since the amount of compression itself was not unique. However, since there was space in the sample chamber to allow the tissue to extend laterally when compressed longitudinally, it is felt that the compression did not change the acoustic properties of the tissue sample significantly.

The second source of error comes from the inhomogeneity of the tissue. Gross inhomogeneity, most notably the presence of blood vessels (and biliary vessels in the case of liver, ventricles in brain, etc.), can cause an acoustic pulse to arrive at the receiver at slightly different times, either due to a difference in velocity in parts of the tissue, or due to an alteration of the sound path through scattering and diffraction. Again, the amount of uncertainty is difficult to specify because

the extent and location inhomgenieties are generally unknown. One general indication of gross inhomogeneity is the presence of a detected acoustic signal outside the packet of received waves, indicating arrivals of sound sooner or later than the main packet. Throughout the measurements, no such occurrence has been detected. It is therefore concluded that either the inhomogeneity affects only a small portion of the arriving acoustic energy, so that the effect is not detectable, or that the time difference between different arrivals is smaller than one wave period so that the arriving waves are not distinguishable from each other. In the first case, inhomogeneity can be confidently neglected. In the second case, the uncertainty in the time-of-flight is less than one wave period, or equivalent to less than $\pm$ 1% in the sound velocity.

In view of the uncertainty in sample length and in the effect of inhomogeneity on velocity, the error estimate in the thermodynamic determination of B/A in tissue is increased from the original estimate of 3.4% to 5%.

CHAPTER 5

SUMMARY AND CONCLUDING REMARKS

The nonlinearity parameter B/A has been determined for tissue models (aqueous solutions of biological macromolecules) and for excised tissues using finite amplitude and thermodynamic methods. The two methods yielded excellent agreement for the liquid samples and clearly acceptable agreement for the soft tissues (± 10%). The discrepancy between the two methods for tissues is most probably due to the combined effects of tissue inhomogeneity and the flexible and deformable nature of tissue which made the measurement of the sample thicknesses less accurate, as compared to the liquids. The formation of air bubbles, as a result of autolysis, may also contribute to the discrepancy.

The general demeanor of the tissue model results is that B/A increases nearly linearly with solute concentration but, for a fixed concentration, is relatively insensitive to the molecular weight of the solute molecules. Whole mammalian blood, whose dry weight consists largely of protein, exhibits a B/A value essentially equal to that of protein solutions of the same dry weight concentration. Excised mammalian liver yields a B/A value significantly greater than blood or protein solutions of the same dry weight content, but homogenization of the tissue reduces this B/A value. Among the soft tissues measured, fat has the highest B/A value.

It is of interest to compare these experimental findings with the theory of intermolecular potential proposed by some researchers as a physical basis for the nonlinearity in a medium

[Hartman, 1979]. In the model, it is assumed that each of the molecules is a rigid sphere which moves under the force of an acoustic wave, against the forces which hold the molecules together. It is further assumed that the intermolecular potential is at a minimum at the equilibrium molecular separation, and it is more difficult to force the molecules together than it is to pull them apart. As a result, when a liquid is compressed to a smaller volume, it becomes more difficult to compress. One of the simplest potentials with the proper qualitative feature that satisfies the assumption is the Mie potential

$$U = ar^{-n} - br^{-m} \tag{5.1}$$

where $n > m$ and a and b are constants, spherical symmetry is assumed, and r is the average distance between molecules.

When applied to a solution, this model implies that three kinds of interactions between molecules are possible, namely, solute-solvent, solute-solute, and solvent-solvent. The solvent-solvent interaction accounts for the baseline value of B/A at 0% concentrations. The lack of dependence of the B/A value on solute moleuclar weight suggests that the interaction between molecular subunits within a solute macromolecule does not contribute significantly to the nonlinearity of the solution. This observation is consistent with the assumption of rigid molecules in the theory of intermolecular potential. The solute-solute interaction also appears to contribute insignificantly to the nonlinearity of the medium, since the amount of interaction between solute molecules should increase more than linearly with the number of solute molecules present,

thus resulting in a nonlinear increase of B/A with concentration, which contradicts the experimental observations. However, the observed linear increase of B/A value with concentration is consistent with the theory of solute-solvent interaction. Each interaction between a solute molecule and the solvent can be viewed as a "nonlinear spring." The number of such "nonlinear springs," and hence the overall nonlinearity of the medium, increases linearly with the amount of solute, viz., the concentration of the solution.

The greater value of B/A for tissue as compared with protein solutions of the same dry weight content, together with the decrease of B/A value with homogenization, suggest that the tissue structure plays an important role in determining its B/A value. One may speculate that the nonlinear interaction exists on two levels: an intermolecular level and an inter-cellular, or macrostructural, level. The binding or interaction between macrostructures again acts as "nonlinear springs," increasing the B/A value of a tissue above that of the constituent protein solutions. When such structures are destroyed by homogenization, the value of B/A then decreases. This dependence of the B/A value on structure is illustrated in a schematic diagram of B/A versus structural hierarchy in Fig. 5.1. The values of B/A are seen to increase progressively with increased structures.

It is felt that the knowledge of the nonlinearity parameter of tissues, presented herein, will lead to a better understanding of the interaction of ultrasound and biological media and to possible improvement of clinical diagnostic and therapeutic applications of ultrasound. It is also felt that these new data

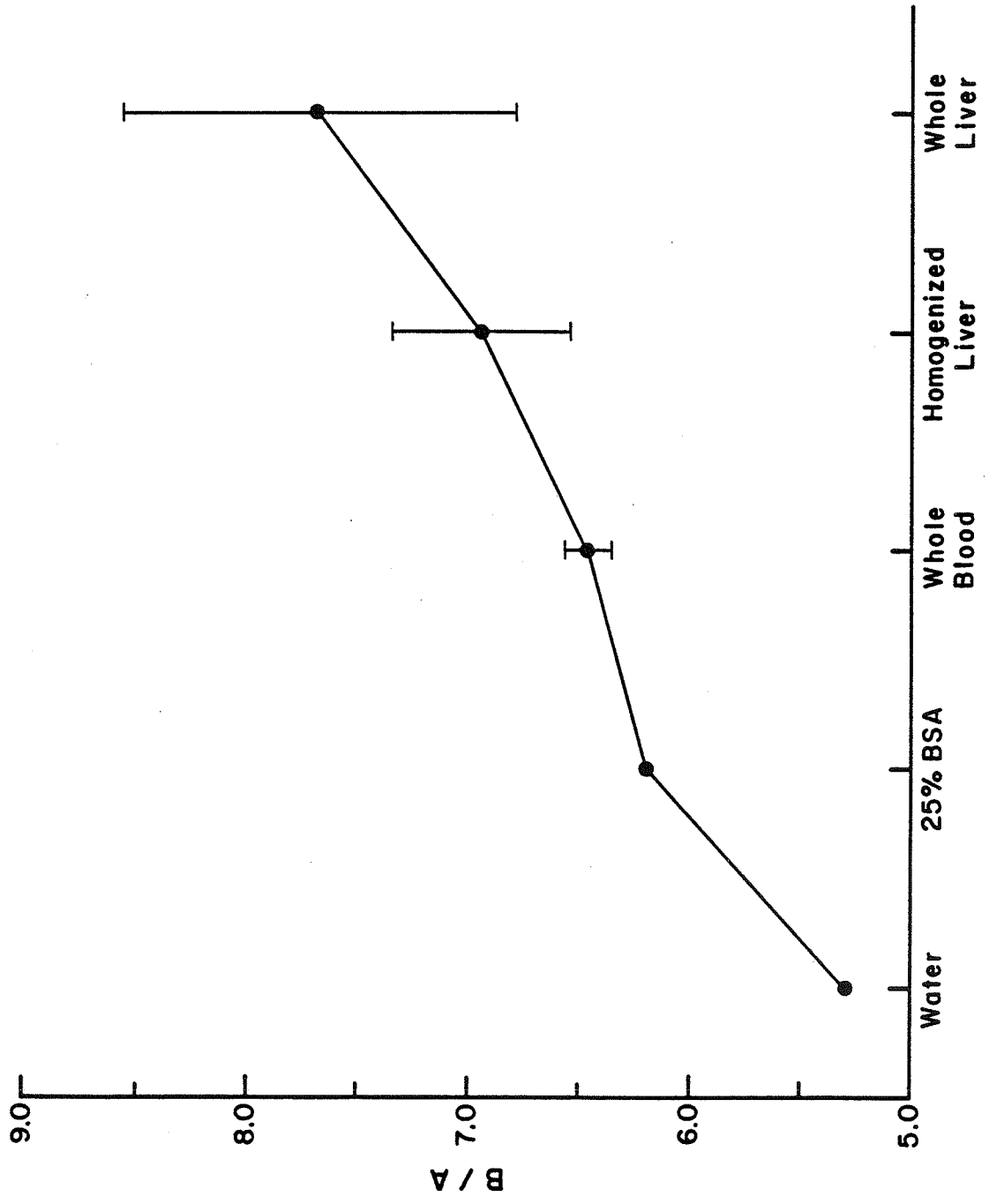

Figure 5.1. Schematic diagram of B/A vs. structural hierarchy.

will provide information about the mechanical structure of the biological media not obtainable through conventional means of tissue characterization.

REFERENCES

1. L. Adler and E. A. Hiedemann, "Determination of the Nonlinearity Parameter B/A for water and m-xylene," J. Acoust. Soc. Am. 34, 410-412 (1962).

2. E. O. Attinger and D. D. Michie, "The Body Fluids," in Biological Foundations of Biomedical Engineering, edited by J. Kline (Little, Brown and Co., Boston, 1948), p.141.

3. R. Bass, "Diffraction effects in ultrasonic field of a piston source," J. Acoust. Soc. Am. 30, 602-605 (1958).

4. R. T. Beyer, "Parameter of nonlinearity in fluids," J. Acoust. Soc. Am. 32, 719-721 (1960).

5. R. T. Beyer, Nonlinear Acoustics (Naval Ship Systems Command, Dept. of the Navy, 1974), pp.91-164.

6. D. T. Blackstock, "Thermoviscous attenuation of plane, periodic finite amplitude sound waves," J. Acoust. Soc. Am. 36, 534 (1964).

7. D. T. Blackstock, "Connection between the Fay and Fubini solutions for plane sound waves of finite amplitude," J. Acoust. Soc. Am. 39, 1020-1026 (1966).

8. D. T. Blackstock, Nonlinear Acoustics, in American Institute of Physics Handbook, edited by D. E. Gray (McGraw-Hill, New York, 1972), pp. 3-205 - 3-205.

9. H. F. Bowman, E. G. Cravalho, and M. Woods, Annual Review of Biophysics and Bioengineering 4, 43-80 (1975).

10. E. L. Carstensen, K. Li, and H. P. Schwan, "Determination of the acoustic properties of blood and its components," J. Acoust. Soc. Am. 25, 286-289 (1953).

11. E. L. Carstensen, W. K. Law, N. D. McKay, and T. G. Muir, "Demonstration of nonlinear acoustical effects at biomedical frequencies and intensities," Ultrasound Med. Biol. 6, 359-368 (1980).

12. E. L. Carstensen, S. A. Becroft, W. K. Law, and D. B. Barbee, "Finite amplitude effects on the thresholds for lesion production in tissue by unfocused ultrasound," J. Acoust. Soc. Am. 70, 302-309 (1981).

13. P. L. Carson, P. R. Fischella, and T. V. Oughton, "Ultrasonic power and intensities produced by diagnostic ultrasound equipment," Ultrasound Med. Biol. 3, 341-350 (1978).

14. W. N. Cobb, "Measurement of the Acoustic Nonlinearity Parameter for Biological Media," Ph.D. Thesis, Yale University, New Haven, CT (1982).

15. Cobb, W. N., "Finite amplitude method for the determinaton of the acoustic nonlinearity parameter B/A," J. Acoust. Soc. Am. 73, 1525-1532 (1983).

16. A. B. Coppens, R. T. Beyer, M. B. Reider, J. Donohue, F. Guepin, R. H. Hodson, and C. Townsend, "Parameter of nonlinearity in fluids II," J. Acoust. Soc. Am. 38, 797-804 (1965).

17. F. Dunn, "Temperature and amplitude dependence of acoustic absorption in tissue." J. Acoust. Soc. Am. 34, 1545-1547 (1962).

18. F. Dunn and W. D. O'Brien, Jr., "Ultrasonic absorption and dispersion," in Ultrasound: Its Applications in Medicine and Biology, edited by F. J. Fry (Elsevier, Amsterdam, 1978),

pp. 393-439.

19. F. Dunn, W. K. Law, and L. A. Frizzell, "Nonlinear ultrasonic wave propagation in biological materials," IEEE Ultrasonics Symp., pp. 527-532 (1981).
20. F. Dunn, W. K. Law, and L. A. Frizzell, "Nonlinear ultrasonic propagation in biological media," Br. J. Cancer, 45, Suppl. V, 55-58 (1982).
21. J. Emery, S. Gasse, and C. Dugue, "Coefficient de non linearite acoustique dans les melanges eau-methanol et eau-ethanol," J. Phys., Colloque C8, Supplement au N 11, Tome 40, page C8-231, Nov. (1979).
22. W. J. Fry and F. Dunn, "Ultrasound: Analysis and Experimental Methods in Biological Research," in Physical Techniques in Biological Research, edited by W. L. Nastuk, (Adademic Press, New York, 1962), Vol. IV, Chap. 6, pp. 261-394.
23. S. A. Goss and F. Dunn, "Concentration Dependence of Ultrasonic Absorption in Aqueous Solutions of Bovine Serum Albumin," Proc. IEEE Symp., 65-68 (1974).
24. S. A. Goss, R. L. Johnston, and F. Dunn, "Comprehensive compilation of empirical ultrasonic properties of mammalian tissues," J. Acoust. Soc. Am. 64, 423-457 (1978).
25. S. A. Goss, and F. J. Fry, "Nonlinear acoustic behavior in focused ultrasonic fields: Observations of intensity dependent absorption in biological tissue," IEEE Trans. Sonics Ultrason. SU-28 (1981).
26. R. K. Gould, C. W. Smith, A. O. Williams, Jr., and R. P. Ryan, "Measured structure of harmonics self-generated in

an acoustic beam," J. Acoust. Soc. Am. 40, 421-427 (1966).

27. M. Greenspan, and C. E. Tschiegg, "Tables of the speed of sound in water," J. Acoust. Soc. Am. 31, 75-76 (1959).

28. M. P. Hagelberg, , G. Holton, and S. Kao, "Calculation of B/A for water from measurements of ultrasonic velocity versus temperature and pressure to 10,000 kg/cm ," J. Acoust. Soc. Am. 41, 564-568 (1967).

29. M. E. Haran, Priviate Communication (1980).

30. M. E. Haran, and B. D. Cook, "Distortion of finite amplitude ultrasound in lossy media," J. Acoust. Soc. Am. 73, 774-780 (1983).

31. B. Hartman, "Potential energy effects on the sound speed in liquids," J. Acous. Soc. Am. 65, 1392-1396 (1979).

32. E. A. Hiedemann and K. L. Zankel, "The study of ultrasonic waveform by optical methods," Acoustica 11, 213-233 (1961).

33. F. Ingenito and A. O. Williams, Jr., "Calculation of second-harmonic generation in a piston beam," J. Acoust. Soc. Am. 49, 319-328 (1971).

34. C. Kammoun, J. Emery, and P. Alias, "Determination of the acoustic parameter of nonlinearity in liquids at very low pressure," in Seventh International Symposium on Nonlinear Acoustics, Virginia Polytechnic Institute and State University, pp. 146-149, August (1976).

35. A. S. Khimunin, "Ultrasonic propagation parameter measurements incorporating exact diffraction corrections," Acoustica 39, 87-95 (1978).

36. L. E. Kinsler, R. F. Austin, A. B. Coppens, and J. V. Sanders, Fundamentals of Acoustics (John Wiley and Sons, New York, 1982).

37. R. Kompfner, and R. A. Lemons, "Nonlinear acoustic microscopy," Appl. Phys. Lett. 28, No. 6, 295-287 (1976).

38. V. E. Kunitsyn, and O. V. Rudenco, "Second harmonic generation in the field of a piston radiator," Sov. Phys. Acoust. 24, 310-313 (1978).

39. W. K. Law, "Harmonic Generation in the Sound Field of A 3 MHz, 1/2" Diameter Plane Piston Source," M. S. thesis, University of Illinois, Urbana, Illinois (1978).

40. W. K. Law, L. A. Frizzell, and F. Dunn, "Ultrasonic determination of the nonlinearity parameter B/A for biological media," J. Acoust. Soc. Am. 69, 1210-1212 (1981).

41. P. W. Marcus and E. L. Carstensen, "Problems with absorption measurements of inhomogeneous solids," J. Acoust. Soc. Am. 58, 1334-1335 (1975).

42. H. J. McSkimin, "Ultrasonic methods for measuring the mechanical properties of liquids and solids," in Physical Acoustics, edited by W. P. Mason, (Academic Press, New York, 1964) 1, Part A, Ch. 4, pp. 272-330.

43. J. S. Mendousse, "Nonlinear dissipative distortion of progressive and sound waves at moderate amplitudes," J. Acoust. Soc. Am. 25, 51 (1953).

44. P. M. Morse and K. V. Ingand, Theoretical Acoustics, (McGraw Hill, New York, 1968), pp. 59.

45. T. G. Muir and E. L. Carstensen, "Prediction of nonlinear

acoustical effects at biomedical frequencies and intensities," Ultrasound Med. Biol. 6, 345-357 (1980).

46. W. D. O'Brien, Jr., "The absorption of ultrasound in aqueous solutions of polyethylene glycol," M. S. thesis, University of Illinois, Urbana, Illinois (1968).

47. W. D. O'Brien, Jr., "The absorption of ultrsound in aqueous solutions of biologica polymers," Ph.D. thesis, University of Illinois, Urbana, Illinois (1970).

48. J. D. Pandey, H. C. Pandey, and P. Dubey, "Thermodynamic nonlinearity parameter of castor oil," Acoust. Lett., 3, No. 1, 28-31 (1979).

49. H. Pauly and H. P. Schwan, "Mechanism of absorption of ultrasound in liver tissue," J. Acoust. Soc. Am. 50, 692-699 (1971).

50. P. H. Rogers, "A Theoretical Study of Second Harmonic Generation in the Acoustic Beam of a Circular Plane Piston," Ph.D. thesis, Brown University, Providence, RI (1970).

51. O. V. Rudenko and S. I. Solugan, Theoretical Foundations of Nonlinear Acoustics (Plenum, New York,1977).

52. R. P. Ryan, A. Lutsch, and R. T. Beyer, "Measurement of the distortion of finite ultrasonic waves in liquids by a pulse method", J. Acoust. Soc. Am 34, 31-35, (1962).

53. J. A. Shooter, T. G. Muir, and D. T. Blackstock, "Acoustic saturation of spherical waves in water", J. Acoust. Soc. Am. 55, 54-62 (1974).

54. A. L. Thuras, K. T. Jenkins, and H. T. O'Neil, "Extraneous frequencies generated in air carrying intense sound waves," J. Acoust. Soc. Am. 6, 173-180 (1935).

55. P. N. T. Wells, Biomedical Ultrasonics (Academic Press, London, 1977), p. 121.

56. T. Yasunaga, "Effects of pressure on the structure of and sound velocity in water," J. Acoust. Soc. Am. 32, 713-715 (1960).

57. K. L. Zankel and E. A. Hiedemann, "Diffraction of light by ultrasonic wave progressing with finite but moderate amplitude in liquids," J. Acoust. Soc. Am. 31, 44-54 (1959).

58. J. Zemanek, "Beam behavior within the nearfield of a vibrating piston," J. Acoust. Soc. Am. 49, 181-191 (1971).

VITA

Wing K. Law was born in Hong Kong in 1954. He was an amateur electronics enthusiast in high school and obtained an engineering scholarship to attend the University of Rochester in Rochester, New York in 1974. While at Rochester, he was a part-time student worker in the Bioultrasonics Laboratory, working on problems of acoustic cavitation, bioeffects, and finite amplitude wave propagation, which subsequently led to the publication of five papers in scientific journals. He obtained the B.S. degree in Electrical Engineering in June 1978 and was awarded the Daniel Ward Healy, Jr. prize for the most promising student in Bioengineering in the same year.

Mr. Law then attended graduate school at the University of Illinois under the supervision of Professors Floyd Dunn and Leon A. Frizzell and obtained his M.S. degree in Electrical Engineering in January 1980. His M.S. thesis was titled Harmonic Generation in the Sound Field of a 3 MHz, 1/2 Inch Diameter Plane Piston Source. Appointments at the University of Illinois included teaching assistantships in courses of electronics, electromagnetics, and fundamental acoustics. He was also a research assistant in the Bioacoustics Research Laboratory, working on problems of nonlinear ultrasonic propagation in biological materials.